Massive Galaxies at High Redshift:

Rare...? Or Impossible?!

Martin Stringer

l'Observatoire de Paris

LERMA

Laboratoire d'Étude du Rayonnement et de la Matière en Astrophysique

Massive Galaxies at High Redshift:

Early Semi-Analytic Model
(~12,000yr)

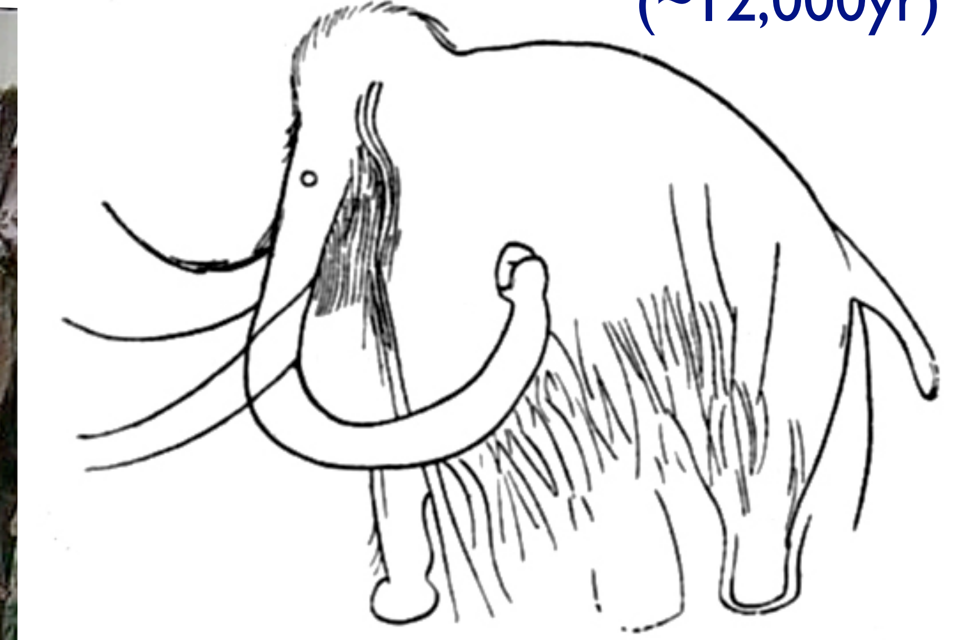

Martin Stringer

l'Observatoire de Paris

LERMA

Laboratoire d'Étude du Rayonnement et de la Matière en Astrophysique

Massive Galaxies at High Redshift:

Early Semi-Analytic Model
(~12,000yr)

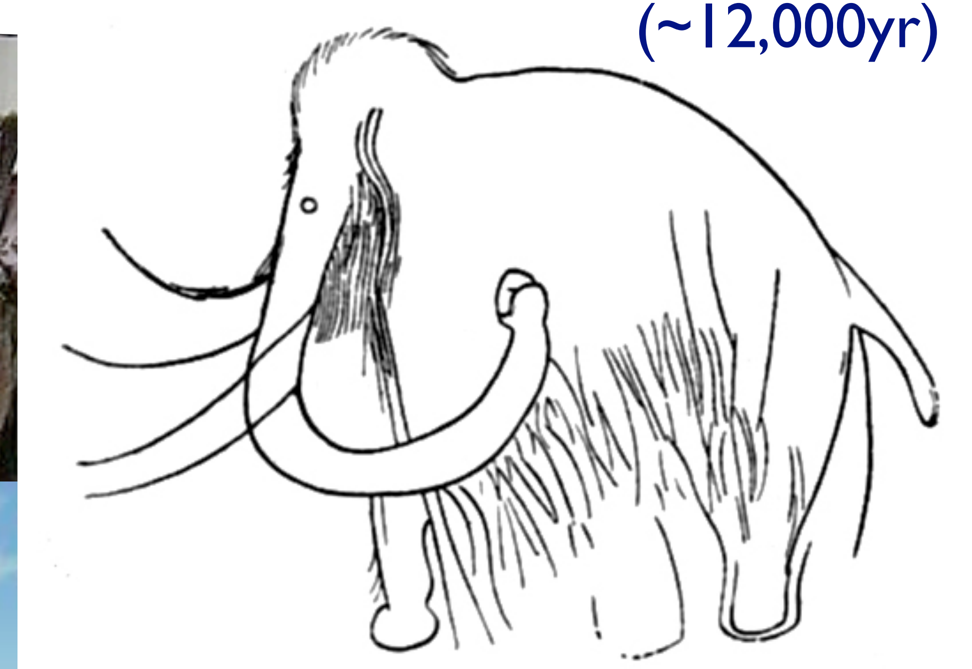

Recent Simulation

Martin Stringer

l'Observatoire de Paris

Laboratoire d'Étude du Rayonnement et d

Monthly Notices of the Royal Astronomical Society

Mon. Not. R. Astron. Soc. **414,** 1927–1936 (2011) doi:10.1111/j.1365-2966.2011.18533.x

Star formation trends in high-redshift galaxy surveys: the elephant or the tail?

Martin Stringer,[1★] Shaun Cole,[1] Carlos S. Frenk[1] and Daniel P. Stark[2]

[1] *Institute of Computational Cosmology, Department of Physics, University of Durham, South Road, Durham DH1 3LE*

[2] *Kavli Institute of Cosmology & Institute of Astronomy, University of Cambridge, Madingley Road, Cambridge CB3 0HA*

Accepted 2011 February 8. Received 2011 January 31; in original form 2010 November 12

ABSTRACT

Star formation rate and accumulated stellar mass are two fundamental physical quantities that describe the evolutionary state of a forming galaxy. Two recent attempts to determine the relationship between these quantities, by interpreting a sample of star-forming galaxies at redshift of $z \sim 4$, have led to opposite conclusions. Using a model galaxy population, we investigate possible causes for this discrepancy and conclude that minor errors in the conversion from observables to physical quantities can lead to a major misrepresentation when applied without awareness of sample selection. We also investigate, in a general way, the physical origin of the correlation between star formation rate and stellar mass within the hierarchical galaxy formation theory.

Key words: galaxies: evolution – galaxies: formation – galaxies: high redshift.

1 INTRODUCTION

As more distant galaxy populations become accessible to modern surveys, astronomers are striving to estimate their physical properties, despite the challenges inherent in such pioneering tasks. Even light that barely registers on our instruments is analysed to infer the stellar mass and star formation activity of its source, providing valuable stepping stones on which our physical picture of structure formation can progress.

For example, Stark et al. (2009) produced estimates of stellar mass for 1038 galaxies from the GOODS survey, grouped into three populations by redshift: $z \approx 4$, 5 and 6. These stellar masses were estimated using a population synthesis model (Bruzual & Charlot 2003; Bruzual 2007) which searches for the stellar population which best fits the observed spectral energy distribution of each galaxy (see Section 3.4).

Star formation rates were specifically not derived for this sample, because of uncertainties in the extinction correction. In lieu of this, the galaxies' 'emerging' UV luminosities were computed (the luminosity at 1550 Å without any dust correction). However, fig. 9 of Stark et al. (2009) does include the star formation rates that would be inferred if a standard proportionality between UV luminosity and star formation rate is assumed (Madau, Pozzetti & Dickinson 1998):

$$\log\left(\frac{\dot{M}_\star}{\mathrm{M}_\odot\,\mathrm{yr}^{-1}}\right) = -\frac{M_{150}+18.45}{2.5}. \qquad (1)$$

The resulting figure, for the galaxies in the nearest of those three samples, is reproduced for reference in the upper panel of our Fig. 1.

Despite only a fleeting appearance in the observational paper, these star formation rate estimates have since been the subject of a quite detailed theoretical analysis. Dutton et al. (2010) summarize the trend given by the sample in Fig. 1 as

$$\frac{\dot{M}_\star}{M_\star} \approx \frac{1}{0.62\,\mathrm{Gyr}}\left(\frac{M_\star}{10^{10}\,\mathrm{M}_\odot}\right)^{-0.2}, \qquad (2)$$

which implies that the *specific star formation rate* ($\dot{M}_\star/M_\star$) is only weakly dependent on the stellar mass.

Meanwhile, the same sample of observational estimates has been subject to analysis by Khochfar & Silk (2011). Having chosen to plot the information on different axes, with a derived quantity, the specific star formation rate (SSFR), on the y-axis (as in the lower panel of Fig. 1) these authors perceive there to be a 'strong observed mass-dependence' with stellar mass.

So the same sample has been interpreted, on the one hand, as having a strong correlation with stellar mass and, on the other hand, a weak correlation.[1] What is the reader to conclude from this literature?

The confusion can be appreciated by comparing the two panels in Fig. 1. The trend (2) does not seem unreasonable when looking at the top panel, but the problem is that the observational limit in

[1] Both groups of authors agree on the relative evolution in specific star formation rate implied by the data when compared with equivalent relationships at low redshifts, and that this evolution seems to cease (appear constant) for $z \gtrsim 4$. Dutton et al. (2010) explain this in terms of high gas densities, and thus higher star formation rates, for a galaxy of a given mass at higher redshift. Khochfar & Silk (2011) look for modulated models of accretion-driven star formation. In this paper, we focus on the extent to which the data may or may not reveal the true underlying evolution (Section 4).

★E-mail: martin.stringer@durham.ac.uk

Monthly Notices of the ROYAL ASTRONOMICAL SOCIETY

Mon. Not. R. Astron. Soc. **414,** 1927–1936 (2011) doi:10.1111/j.1365-2966.2011.18533.x

Star formation trends in high-redshift galaxy surveys: the elephant or the tail?

Martin Stringer,[1★] Shaun Cole,[1] Carlos S. Frenk[1] and Daniel P. Stark[2]

[1]*Institute of Computational Cosmology, Department of Physics, University of Durham, South Road, Durham DH1 3LE*

[2]*Kavli Institute of Cosmology & Institute of Astronomy, University of Cambridge, Madingley Road, Cambridge CB3 0HA*

Accepted 2011 February 8. Received 2011 January 31; in original form 2010 November 12

ABSTRACT

Star formation rate and accumulated stellar mass are two fundamental physical quantities that describe the evolutionary state of a forming galaxy. Two recent attempts to determine the relationship between these quantities, by interpreting a sample of star-forming galaxies at redshift of $z \sim 4$, have led to opposite conclusions. Using a model galaxy population, we investigate possible causes for this discrepancy and conclude that minor errors in the conversion from observables to physical quantities can lead to a major misrepresentation when applied without awareness of sample selection. We also investigate, in a general way, the physical origin of the correlation between star formation rate and stellar mass within the hierarchical galaxy formation theory.

Key words: galaxies: evolution – galaxies: formation – galaxies: high redshift.

1 INTRODUCTION

As more distant galaxy populations become accessible to modern surveys, astronomers are striving to estimate their physical properties, despite the challenges inherent in such pioneering tasks. Even light that barely registers on our instruments is analysed to infer the stellar mass and star formation activity of its source, providing valuable stepping stones on which our physical picture of structure formation can progress.

For example, Stark et al. (2009) produced estimates of stellar mass for 1038 galaxies from the GOODS survey, grouped into three populations by redshift: $z \approx 4$, 5 and 6. These stellar masses were estimated using a population synthesis model (Bruzual & Charlot 2003; Bruzual 2007) which searches for the stellar population which best fits the observed spectral energy distribution of each galaxy (see Section 3.4).

Star formation rates were specifically not derived for this sample, because of uncertainties in the extinction correction. In lieu of this, the galaxies' 'emerging' UV luminosities were computed (the luminosity at 1550 Å without any dust correction). However, fig. 9 of Stark et al. (2009) does include the star formation rates that would be inferred if a standard proportionality between UV luminosity and star formation rate is assumed (Madau, Pozzetti & Dickinson 1998):

$$\log\left(\frac{\dot{M}_\star}{\mathrm{M}_\odot\,\mathrm{yr}^{-1}}\right) = -\frac{M_{150} + 18.45}{2.5}. \qquad (1)$$

The resulting figure, for the galaxies in the nearest of those three samples, is reproduced for reference in the upper panel of our Fig. 1.

Despite only a fleeting appearance in the observational paper, these star formation rate estimates have since been the subject of a quite detailed theoretical analysis. Dutton et al. (2010) summarize the trend given by the sample in Fig. 1 as

$$\frac{\dot{M}_\star}{M_\star} \approx \frac{1}{0.62\,\mathrm{Gyr}}\left(\frac{M_\star}{10^{10}\,\mathrm{M}_\odot}\right)$$

which implies that the *specific s*

weakly dependent on the stellar

Meanwhile, the same sample

subject to analysis by Khochfa

plot the information on differer

specific star formation rate (SS

panel of Fig. 1) these authors pe

mass-dependence' with stellar r

So the same sample has bee

having a strong correlation w

hand, a weak correlation.[1] Wha

literature?

The confusion can be apprec

in Fig. 1. The trend (2) does nc

at the top panel, but the proble

[1] Both groups of authors agree on t

mation rate implied by the data wher

at low redshifts, and that this evolut

$z \gtrsim 4$. Dutton et al. (2010) explain th

higher star formation rates, for a ga

Khochfar & Silk (2011) look for m

formation. In this paper, we focus

may not reveal the true underlying

★E-mail: martin.stringer@durham.ac.uk

The Astrophysical Journal, 697:1493–1511, 2009 June 1 doi:10.1088/0004-637X/697/2/1493

THE EVOLUTIONARY HISTORY OF LYMAN BREAK GALAXIES BETWEEN REDSHIFT 4 AND 6: OBSERVING SUCCESSIVE GENERATIONS OF MASSIVE GALAXIES IN FORMATION

Daniel P. Stark[1,2], Richard S. Ellis[1,3], Andrew Bunker[3], Kevin Bundy[4,5,8], Tom Targett[1,6], Andrew Benson[1], and Mark Lacy[7]

[1] Department of Astrophysics, California Institute of Technology, MS 105-24, Pasadena, CA 91125, USA; dps@astro.caltech.edu
[2] Institute of Astronomy, University of Cambridge, Madingley Road, Cambridge CB3 0HA, USA
[3] Department of Astrophysics, University of Oxford, OX1 3RH, USA
[4] Department of Astronomy, University of California, Berkeley, CA 94720, USA
[5] Department of Astronomy & Astrophysics, University of Toronto, 50 St. George Street, Toronto, ON, M5S 3H4, USA
[6] Department of Physics and Astronomy, University of British Columbia, 6224 Agricultural Rd., Vancouver, B.C., V6T 1Z1, Canada
[7] Spitzer Science Center, California Institute of Technology, MC-220-6, 1200 E. California Blvd, Pasadena, CA 91125, USA
Received 2008 October 13; accepted 2009 March 10; published 2009 May 13

ABSTRACT

We present new measurements of the evolution in the Lyman break galaxy (LBG) population between $z \simeq 4$ and $z \simeq 6$. By utilizing the extensive multiwavelength data sets available in the GOODS fields, we identify 2443 B, 506 V, and 137 i'-band dropout galaxies likely to be at $z \approx 4$, 5, and 6. For the subset of dropouts for which reliable *Spitzer* IRAC photometry is feasible (roughly 35% of the sample), we estimate luminosity-weighted ages and stellar masses. With the goal of understanding the duration of typical star formation episodes in galaxies at $z \gtrsim 4$, we examine the distribution of stellar masses and ages as a function of cosmic time. We find that at a fixed rest-UV luminosity, the average stellar masses and ages of galaxies do not increase significantly between $z \simeq 6$ and 4. In order to maintain this near equilibrium in the average properties of high-redshift LBGs, we argue that there must be a steady flux of young, newly luminous objects at each successive redshift. When considered along with the short duty cycles inferred from clustering measurements, these results may suggest that galaxies are undergoing star formation episodes lasting only several hundred million years. In contrast to the unchanging relationship between the average stellar mass and rest-UV luminosity, we find that the number density of massive galaxies increases considerably with time over $4 \lesssim z \lesssim 6$. Given this rapid increase of UV luminous massive galaxies, we explore the possibility that a significant fraction of massive ($10^{11}\,M_\odot$) $z \simeq 2$–3 distant red galaxies (DRGs) were in part assembled in an LBG phase at earlier times. Integrating the growth in the stellar mass function of actively forming LBGs over $4 \lesssim z \lesssim 6$ down to $z \simeq 2$, we find that $z \gtrsim 3$ LBGs could have contributed significantly to the quiescent DRG population, indicating that the intense star-forming systems probed by submillimeter observations are not the only route toward the assembly of DRGs at $z \simeq 2$.

Key words: galaxies: evolution – galaxies: formation – galaxies: high-redshift – galaxies: starburst – surveys – ultraviolet: galaxies

Online-only material: color figures

1. INTRODUCTION

The detailed study of various classes of distant galaxies has enabled great progress in understanding the star formation and mass assembly history of normal field galaxies (for recent reviews, see Hopkins & Beacom 2006; Ellis 2008; Wilkins et al. 2008). Multiwavelength probes have been particularly effective in revealing the coexistence of diverse categories of galaxies with redshifts $z \simeq 2$–3. These include the relatively unobscured star-forming "Lyman break" galaxies (LBGs, e.g., Steidel et al. 1996; Shapley et al. 2005), the infrared-selected massive "distant red" galaxies (DRGs; e.g., Franx et al. 2003; van Dokkum et al. 2006) and heavily obscured submillimeter galaxies which contain both intensely star-forming and active components (SMGs; e.g., Smail et al. 1998; Chapman et al. 2005). The collective study of these populations has revealed that the redshift range $1 < z < 3$ is a formative one when the bulk of the stars in present-day massive galaxies was produced (Hopkins & Beacom 2006).

Understanding the inter-relationship between these various sources is an important goal and intense efforts are now underway to address this issue (e.g., van Dokkum et al. 2006; Reddy et al. 2008). A relevant aspect of this discussion concerns the assembly history of objects observed during the redshift interval $4 < z < 6$, corresponding to a period only 1 Gyr earlier. Such data may provide valuable insight into the connection between actively star-forming and passive populations as well as define the mode of star formation in typical massive galaxies.

Over the last five years, deep multiwavelength surveys have resulted in the discovery of large samples of LBGs at $z \simeq 4$–6 (Bouwens et al. 2007). Despite early controversies (Bunker et al. 2004; Stanway et al. 2003; Giavalisco et al. 2004a; Beckwith et al. 2006), it now seems clear that the star formation density declines with redshift beyond $z \simeq 3$. Recent evidence also suggests the characteristic luminosity is also fading (Yoshida et al. 2006; Bouwens et al. 2007; McLure et al. 2009). Bouwens et al. (2007) attribute this evolutionary pattern to the simple hierarchical assembly of galaxies. Unfortunately, because of the transient nature of star formation probed by the rest-frame UV luminosity function (LF), these studies alone provide only an approximate measure of the evolutionary processes occurring

[8] Hubble Fellow.

Martin Stringer l'Observatoire de Paris LERMA

The Astrophysical Journal, 697:1493–1511, 2009 June 1

THE EVOLUTIONARY HISTORY OF LYMAN BR
OBSERVING SUCCESSIVE GENERATIONS

Daniel P. Stark[1,2], Richard S. Ellis[1,3], Andrew Bunke
and Ma
[1] Department of Astrophysics, California Institute of Technolog
[2] Institute of Astronomy, University of Cambrid
[3] Department of Astrophysics, Un
[4] Department of Astronomy, University
[5] Department of Astronomy & Astrophysics, University of
[6] Department of Physics and Astronomy, University of British Co
[7] Spitzer Science Center, California Institute of Technology, N
Received 2008 October 13; accepted 2

ABST

We present new measurements of the evolution in the
and $z \simeq 6$. By utilizing the extensive multiwavelengt
2443 *B*, 506 *V*, and 137 i'-band dropout galaxies likel
for which reliable *Spitzer* IRAC photometry is feasible
weighted ages and stellar masses. With the goal of unde
in galaxies at $z \gtrsim 4$, we examine the distribution of stell
that at a fixed rest-UV luminosity, the average stellar r
between $z \simeq 6$ and 4. In order to maintain this near equ
we argue that there must be a steady flux of young, ne
considered along with the short duty cycles inferred fr
that galaxies are undergoing star formation episodes la
the unchanging relationship between the average stella
density of massive galaxies increases considerably with
luminous massive galaxies, we explore the possibility t
distant red galaxies (DRGs) were in part assembled in
the stellar mass function of actively forming LBGs ove
could have contributed significantly to the quiescent D
systems probed by submillimeter observations are not

Key words: galaxies: evolution – galaxies: formation –
ultraviolet: galaxies

Online-only material: color figures

1. INTRODUCTION

The detailed study of various classes of distant galaxies has enabled great progress in understanding the star formation and mass assembly history of normal field galaxies (for recent reviews, see Hopkins & Beacom 2006; Ellis 2008; Wilkins et al. 2008). Multiwavelength probes have been particularly effective in revealing the coexistence of diverse categories of galaxies with redshifts $z \simeq 2$–3. These include the relatively unobscured star-forming "Lyman break" galaxies (LBGs, e.g., Steidel et al. 1996; Shapley et al. 2005), the infrared-selected massive "distant red" galaxies (DRGs; e.g., Franx et al. 2003; van Dokkum et al. 2006) and heavily obscured submillimeter galaxies which contain both intensely star-forming and active components (SMGs; e.g., Smail et al. 1998; Chapman et al. 2005). The collective study of these populations has revealed that the redshift range $1 < z < 3$ is a formative one when the bulk of the stars in present-day massive galaxies was produced (Hopkins & Beacom 2006).

[8] Hubble Fellow.

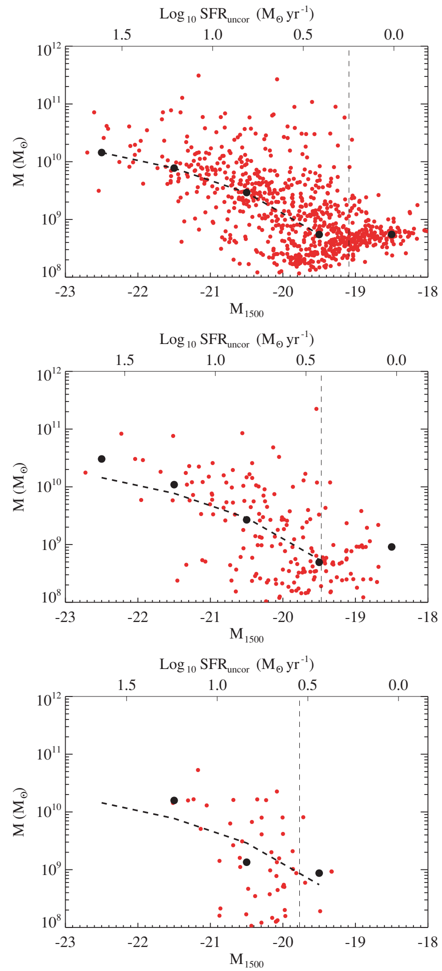

Figure 9. Stellar mass vs. absolute magnitude at 1500 Å (uncorrected for dust extinction) over $z \simeq 4$–6. Small red circles correspond to inferred stellar masses and rest-UV absolute magnitudes for individual *B* drops (top), *V* drops (middle) and i' drops (bottom) assuming a $\tau = 100$ Myr exponential decay model. The dark solid circles are the median stellar mass in each magnitude bin. The relationship at $z \simeq 4$ is overlaid on the $z \simeq 5$ and $z \simeq 6$ panels as a black solid dashed line. The vertical solid lines represent the adopted completeness limits for each sample. The median stellar mass increases monotonically with M_{1500} in each dropout sample; however, at a fixed M_{1500}, the median stellar mass does not decrease significantly with increasing redshift, as may be expected in simple steady growth models.

(A color version of this figure is available in the online journal.)

Table 2
Evolution of Galaxy Properties over $4 \lesssim z \lesssim 6$

M_{UV} (mag)	Num	$M_\star$ ($\tau = 100$) ($10^8\ M_\odot$)	$M_\star$ (CSF) ($10^8\ M_\odot$)	Age (Myr)
		B drops ($z \simeq 4$)		
−22.5	15	144 (31-410)	223	180
−21.5	73	77 (24-380)	114	203
−20.5	227	29 (4.0-130)	38	181
−19.5	370	5.5 (2.0-42)	7.3	143
		V drops ($z \simeq 5$)		
−22.5	3	304 (180-830)	520	286
−21.5	20	109 (5.4-234)	112	227
−20.5	67	27 (2.2-158)	36	181
−19.5	...	...	...	...
		i' drops ($z \simeq 6$)		
−22.5	0	...	...	...
−21.5	8	160 (24-530)	226	286
−20.5	41	13 (1.3-90)	27	102
−19.5	...	...	...	...

Notes. The stellar masses and ages are inferred from models using a Salpeter IMF and solar metallicity. In Column 3, we present the median stellar masses (and the range of masses spanned by the middle 80% of the distribution) determined from an exponentially declining star formation history with $\tau = 100$ Myr. In Column 4, we provide the median stellar masses inferred assuming a constant star formation history. In Column 5, we present the median ages inferred for the $\tau = 100$ Myr models.

shown in Table 2, the absence of a systematic increase in the average stellar masses is not strongly dependent on the chosen star formation history. Overall these results seem to imply that the ratio of median stellar mass to emerging UV luminosity does not evolve significantly for LBGs over $z = 4$–6. A galaxy with a given M_{1500} at $z \simeq 6$ will, on average, have the same assembled mass (to within a factor of $\simeq 2$) as a galaxy seen at $z \simeq 4$ with the same M_{1500}. This suggests that the specific SFR evolves weakly over $4 \lesssim z \lesssim 6$, indicating that the typical duration of past star formation for a galaxy of a given luminosity does not vary significantly between $z \simeq 6$ and 4.

While the inclusion of a dust correction would shift the $M_\star$–M_{1500} relation brightward (i.e., to the left in Figure 9), it would likely not lead to an increase in the normalization of the $M_\star$–M_{1500} relation over time. As has been shown elsewhere (e.g., Stanway et al. 2005; Bouwens et al. 2007) galaxies at $M_{1500} < -19.8$ do potentially become marginally dustier between $z \simeq 6$ and 4 which would cause the $z \simeq 4$ $M_\star$–M_{1500} relation to shift slightly more than the $z \simeq 5$ and 6 relations. Since a relative shift brightward is roughly the same as a shift toward lower stellar masses at fixed M_{1500}, this would actually have the effect of slightly decreasing the normalization of the $M_\star$–M_{1500} relation over the $4 \lesssim z \lesssim 6$ redshift range.

6.1. Testing the Steady Growth Scenario

We now attempt to place the $M_\star$–M_{1500} relation presented in Figure 9 in the context of the steady growth scenario discussed at the outset of this section. To approximate this scenario, we assume that galaxies follow a constant SFR. Using solar metallicity templates and allowing the dust content to freely vary, we find that the typical implied star formation lifetimes of the *B* drops are in excess of 700 Myr in the two brightest bins (Figure 10), implying that the precursors of the majority of *B* drops would have been equally luminous in *V*- and

Martin Stringer

The Astrophysical Journal, 697:1493–1511, 2009 June 1

THE EVOLUTIONARY HISTORY OF LYMAN BR
OBSERVING SUCCESSIVE GENERATIONS

Daniel P. Stark[1,2], Richard S. Ellis[1,3], Andrew Bunke
and Ma
[1] Department of Astrophysics, California Institute of Technolog
[2] Institute of Astronomy, University of Cambrid
[3] Department of Astrophysics, Un
[4] Department of Astronomy, University
[5] Department of Astronomy & Astrophysics, University of
[6] Department of Physics and Astronomy, University of British Co
[7] Spitzer Science Center, California Institute of Technology, N
Received 2008 October 13; accepted 2

ABST

We present new measurements of the evolution in the
and $z \simeq 6$. By utilizing the extensive multiwavelengt
2443 *B*, 506 *V*, and 137 *i*′-band dropout galaxies likel
for which reliable *Spitzer* IRAC photometry is feasible
weighted ages and stellar masses. With the goal of unde
in galaxies at $z \gtrsim 4$, we examine the distribution of stell
that at a fixed rest-UV luminosity, the average stellar r
between $z \simeq 6$ and 4. In order to maintain this near equ
we argue that there must be a steady flux of young, ne
considered along with the short duty cycles inferred fi
that galaxies are undergoing star formation episodes la
the unchanging relationship between the average stella
density of massive galaxies increases considerably with
luminous massive galaxies, we explore the possibility t
distant red galaxies (DRGs) were in part assembled in
the stellar mass function of actively forming LBGs ove
could have contributed significantly to the quiescent D
systems probed by submillimeter observations are not

Key words: galaxies: evolution – galaxies: formation –
ultraviolet: galaxies

Online-only material: color figures

1. INTRODUCTION

The detailed study of various classes of distant galaxies has enabled great progress in understanding the star formation and mass assembly history of normal field galaxies (for recent reviews, see Hopkins & Beacom 2006; Ellis 2008; Wilkins et al. 2008). Multiwavelength probes have been particularly effective in revealing the coexistence of diverse categories of galaxies with redshifts $z \simeq 2$–3. These include the relatively unobscured star-forming "Lyman break" galaxies (LBGs, e.g., Steidel et al. 1996; Shapley et al. 2005), the infrared-selected massive "distant red" galaxies (DRGs; e.g., Franx et al. 2003; van Dokkum et al. 2006) and heavily obscured submillimeter galaxies which contain both intensely star-forming and active components (SMGs; e.g., Smail et al. 1998; Chapman et al. 2005). The collective study of these populations has revealed that the redshift range $1 < z < 3$ is a formative one when the bulk of the stars in present-day massive galaxies was produced (Hopkins & Beacom 2006).

[8] Hubble Fellow.

Redshift

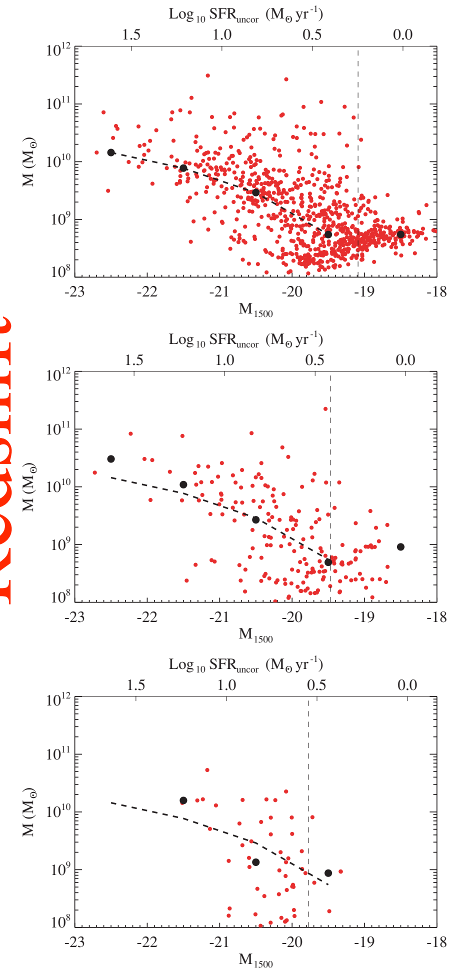

Figure 9. Stellar mass vs. absolute magnitude at 1500 Å (uncorrected for dust extinction) over $z \simeq 4$–6. Small red circles correspond to inferred stellar masses and rest-UV absolute magnitudes for individual *B* drops (top), *V* drops (middle) and *i*′ drops (bottom) assuming a $\tau = 100$ Myr exponential decay model. The dark solid circles are the median stellar mass in each magnitude bin. The relationship at $z \simeq 4$ is overlaid on the $z \simeq 5$ and $z \simeq 6$ panels as a black solid dashed line. The vertical solid lines represent the adopted completeness limits for each sample. The median stellar mass increases monotonically with M_{1500} in each dropout sample; however, at a fixed M_{1500}, the median stellar mass does not decrease significantly with increasing redshift, as may be expected in simple steady growth models.

(A color version of this figure is available in the online journal.)

Table 2
Evolution of Galaxy Properties over $4 \lesssim z \lesssim 6$

M_{UV} (mag)	Num	$M_\star$ ($\tau = 100$) ($10^8\ M_\odot$)	$M_\star$ (CSF) ($10^8\ M_\odot$)	Age (Myr)
		B drops ($z \simeq 4$)		
−22.5	15	144 (31-410)	223	180
−21.5	73	77 (24-380)	114	203
−20.5	227	29 (4.0-130)	38	181
−19.5	370	5.5 (2.0-42)	7.3	143
		V drops ($z \simeq 5$)		
−22.5	3	304 (180-830)	520	286
−21.5	20	109 (5.4-234)	112	227
−20.5	67	27 (2.2-158)	36	181
−19.5	. . .	. . .	. . .	. . .
		i′ drops ($z \simeq 6$)		
−22.5	0	. . .	. . .	. . .
−21.5	8	160 (24-530)	226	286
−20.5	41	13 (1.3-90)	27	102
−19.5	. . .	. . .	. . .	. . .

Notes. The stellar masses and ages are inferred from models using a Salpeter IMF and solar metallicity. In Column 3, we present the median stellar masses (and the range of masses spanned by the middle 80% of the distribution) determined from an exponentially declining star formation history with $\tau = 100$ Myr. In Column 4, we provide the median stellar masses inferred assuming a constant star formation history. In Column 5, we present the median ages inferred for the $\tau = 100$ Myr models.

shown in Table 2, the absence of a systematic increase in the average stellar masses is not strongly dependent on the chosen star formation history. Overall these results seem to imply that the ratio of median stellar mass to emerging UV luminosity does not evolve significantly for LBGs over $z = 4$–6. A galaxy with a given M_{1500} at $z \simeq 6$ will, on average, have the same assembled mass (to within a factor of $\simeq 2$) as a galaxy seen at $z \simeq 4$ with the same M_{1500}. This suggests that the specific SFR evolves weakly over $4 \lesssim z \lesssim 6$, indicating that the typical duration of past star formation for a galaxy of a given luminosity does not vary significantly between $z \simeq 6$ and 4.

While the inclusion of a dust correction would shift the $M_\star$–M_{1500} relation brightward (i.e., to the left in Figure 9), it would likely not lead to an increase in the normalization of the $M_\star$–M_{1500} relation over time. As has been shown elsewhere (e.g., Stanway et al. 2005; Bouwens et al. 2007) galaxies at $M_{1500} < -19.8$ do potentially become marginally dustier between $z \simeq 6$ and 4 which would cause the $z \simeq 4$ $M_\star$–M_{1500} relation to shift slightly more than the $z \simeq 5$ and 6 relations. Since a relative shift brightward is roughly the same as a shift toward lower stellar masses at fixed M_{1500}, this would actually have the effect of slightly decreasing the normalization of the $M_\star$–M_{1500} relation over the $4 \lesssim z \lesssim 6$ redshift range.

6.1. Testing the Steady Growth Scenario

We now attempt to place the $M_\star$–M_{1500} relation presented in Figure 9 in the context of the steady growth scenario discussed at the outset of this section. To approximate this scenario, we assume that galaxies follow a constant SFR. Using solar metallicity templates and allowing the dust content to freely vary, we find that the typical implied star formation lifetimes of the *B* drops are in excess of 700 Myr in the two brightest bins (Figure 10), implying that the precursors of the majority of *B* drops would have been equally luminous in *V*- and

Martin Stringer

l'Observatoire de Paris LERMA

THE ASTROPHYSICAL JOURNAL, 697:1493–1511, 2009 June 1

THE EVOLUTIONARY HISTORY OF LYMAN BR
OBSERVING SUCCESSIVE GENERATIONS

DANIEL P. STARK[1,2], RICHARD S. ELLIS[1,3], ANDREW BUNKE
AND MA
[1] Department of Astrophysics, California Institute of Technolog
[2] Institute of Astronomy, University of Cambrid
[3] Department of Astrophysics, Un
[4] Department of Astronomy, University
[5] Department of Astronomy & Astrophysics, University of
[6] Department of Physics and Astronomy, University of British Co
[7] Spitzer Science Center, California Institute of Technology, M
Received 2008 October 13; accepted 2

ABST

We present new measurements of the evolution in the
and $z \simeq 6$. By utilizing the extensive multiwavelengt
2443 *B*, 506 *V*, and 137 *i'*-band dropout galaxies likel
for which reliable *Spitzer* IRAC photometry is feasible
weighted ages and stellar masses. With the goal of unde
in galaxies at $z \gtrsim 4$, we examine the distribution of stell
that at a fixed rest-UV luminosity, the average stellar r
between $z \simeq 6$ and 4. In order to maintain this near equ
we argue that there must be a steady flux of young, ne
considered along with the short duty cycles inferred fr
that galaxies are undergoing star formation episodes la
the unchanging relationship between the average stella
density of massive galaxies increases considerably with
luminous massive galaxies, we explore the possibility t
distant red galaxies (DRGs) were in part assembled in
the stellar mass function of actively forming LBGs ove
could have contributed significantly to the quiescent D
systems probed by submillimeter observations are not

Key words: galaxies: evolution – galaxies: formation –
ultraviolet: galaxies

Online-only material: color figures

1. INTRODUCTION

The detailed study of various classes of distant galaxies has enabled great progress in understanding the star formation and mass assembly history of normal field galaxies (for recent reviews, see Hopkins & Beacom 2006; Ellis 2008; Wilkins et al. 2008). Multiwavelength probes have been particularly effective in revealing the coexistence of diverse categories of galaxies with redshifts $z \simeq 2$–3. These include the relatively unobscured star-forming "Lyman break" galaxies (LBGs, e.g., Steidel et al. 1996; Shapley et al. 2005), the infrared-selected massive "distant red" galaxies (DRGs; e.g., Franx et al. 2003; van Dokkum et al. 2006) and heavily obscured submillimeter galaxies which contain both intensely star-forming and active components (SMGs; e.g., Smail et al. 1998; Chapman et al. 2005). The collective study of these populations has revealed that the redshift range $1 < z < 3$ is a formative one when the bulk of the stars in present-day massive galaxies was produced (Hopkins & Beacom 2006).

[8] Hubble Fellow.

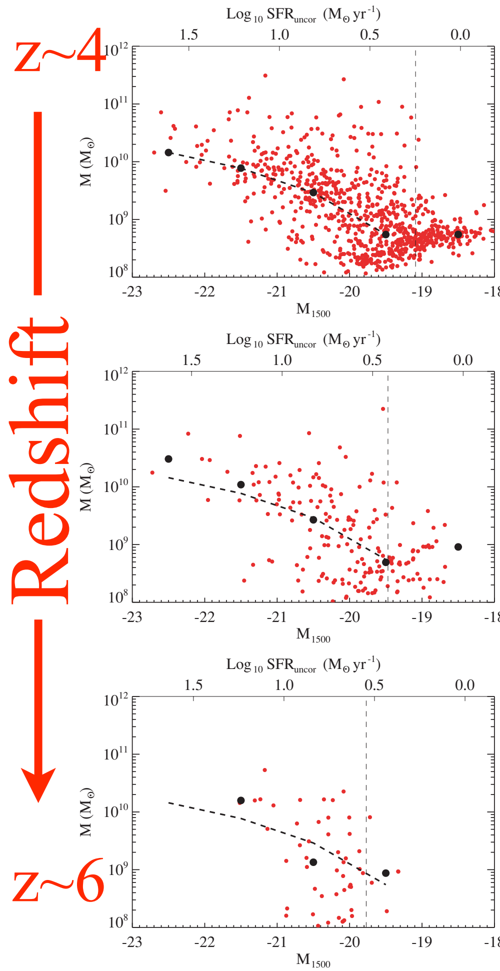

Figure 9. Stellar mass vs. absolute magnitude at 1500 Å (uncorrected for dust extinction) over $z \simeq 4$–6. Small red circles correspond to inferred stellar masses and rest-UV absolute magnitudes for individual *B* drops (top), *V* drops (middle) and *i'* drops (bottom) assuming a $\tau = 100$ Myr exponential decay model. The dark solid circles are the median stellar mass in each magnitude bin. The relationship at $z \simeq 4$ is overlaid on the $z \simeq 5$ and $z \simeq 6$ panels as a black solid dashed line. The vertical solid lines represent the adopted completeness limits for each sample. The median stellar mass increases monotonically with M_{1500} in each dropout sample; however, at a fixed M_{1500}, the median stellar mass does not decrease significantly with increasing redshift, as may be expected in simple steady growth models.

(A color version of this figure is available in the online journal.)

Table 2
Evolution of Galaxy Properties over $4 \lesssim z \lesssim 6$

M_{UV} (mag)	Num	$M_\star$ ($\tau = 100$) ($10^8\ M_\odot$)	$M_\star$ (CSF) ($10^8\ M_\odot$)	Age (Myr)
		B drops ($z \simeq 4$)		
−22.5	15	144 (31-410)	223	180
−21.5	73	77 (24-380)	114	203
−20.5	227	29 (4.0-130)	38	181
−19.5	370	5.5 (2.0-42)	7.3	143
		V drops ($z \simeq 5$)		
−22.5	3	304 (180-830)	520	286
−21.5	20	109 (5.4-234)	112	227
−20.5	67	27 (2.2-158)	36	181
−19.5	…	…	…	…
		i' drops ($z \simeq 6$)		
−22.5	0	…	…	…
−21.5	8	160 (24-530)	226	286
−20.5	41	13 (1.3-90)	27	102
−19.5	…	…	…	…

Notes. The stellar masses and ages are inferred from models using a Salpeter IMF and solar metallicity. In Column 3, we present the median stellar masses (and the range of masses spanned by the middle 80% of the distribution) determined from an exponentially declining star formation history with $\tau = 100$ Myr. In Column 4, we provide the median stellar masses inferred assuming a constant star formation history. In Column 5, we present the median ages inferred for the $\tau = 100$ Myr models.

shown in Table 2, the absence of a systematic increase in the average stellar masses is not strongly dependent on the chosen star formation history. Overall these results seem to imply that the ratio of median stellar mass to emerging UV luminosity does not evolve significantly for LBGs over $z = 4$–6. A galaxy with a given M_{1500} at $z \simeq 6$ will, on average, have the same assembled mass (to within a factor of $\simeq 2$) as a galaxy seen at $z \simeq 4$ with the same M_{1500}. This suggests that the specific SFR evolves weakly over $4 \lesssim z \lesssim 6$, indicating that the typical duration of past star formation for a galaxy of a given luminosity does not vary significantly between $z \simeq 6$ and 4.

While the inclusion of a dust correction would shift the $M_\star$–M_{1500} relation brightward (i.e., to the left in Figure 9), it would likely not lead to an increase in the normalization of the $M_\star$–M_{1500} relation over time. As has been shown elsewhere (e.g., Stanway et al. 2005; Bouwens et al. 2007) galaxies at $M_{1500} < -19.8$ do potentially become marginally dustier between $z \simeq 6$ and 4 which would cause the $z \simeq 4$ $M_\star$–M_{1500} relation to shift slightly more than the $z \simeq 5$ and 6 relations. Since a relative shift brightward is roughly the same as a shift toward lower stellar masses at fixed M_{1500}, this would actually have the effect of slightly decreasing the normalization of the $M_\star$–M_{1500} relation over the $4 \lesssim z \lesssim 6$ redshift range.

6.1. Testing the Steady Growth Scenario

We now attempt to place the $M_\star$–M_{1500} relation presented in Figure 9 in the context of the steady growth scenario discussed at the outset of this section. To approximate this scenario, we assume that galaxies follow a constant SFR. Using solar metallicity templates and allowing the dust content to freely vary, we find that the typical implied star formation lifetimes of the *B* drops are in excess of 700 Myr in the two brightest bins (Figure 10), implying that the precursors of the majority of *B* drops would have been equally luminous in *V*- and

Martin Stringer

The Astrophysical Journal, 697:1493–1511, 2009 June 1

THE EVOLUTIONARY HISTORY OF LYMAN BR
OBSERVING SUCCESSIVE GENERATIONS

Daniel P. Stark[1,2], Richard S. Ellis[1,3], Andrew Bunke
and Ma
[1] Department of Astrophysics, California Institute of Technolog
[2] Institute of Astronomy, University of Cambrid
[3] Department of Astrophysics, Un
[4] Department of Astronomy, University
[5] Department of Astronomy & Astrophysics, University of
[6] Department of Physics and Astronomy, University of British Co
[7] Spitzer Science Center, California Institute of Technology, N
Received 2008 October 13; accepted 2

ABST

We present new measurements of the evolution in the
and $z \simeq 6$. By utilizing the extensive multiwavelengt
2443 B, 506 V, and 137 i'-band dropout galaxies likel
for which reliable *Spitzer* IRAC photometry is feasible
weighted ages and stellar masses. With the goal of und
in galaxies at $z \gtrsim 4$, we examine the distribution of stell
that at a fixed rest-UV luminosity, the average stellar r
between $z \simeq 6$ and 4. In order to maintain this near equ
we argue that there must be a steady flux of young, ne
considered along with the short duty cycles inferred fr
that galaxies are undergoing star formation episodes la
the unchanging relationship between the average stella
density of massive galaxies increases considerably with
luminous massive galaxies, we explore the possibility t
distant red galaxies (DRGs) were in part assembled in
the stellar mass function of actively forming LBGs ove
could have contributed significantly to the quiescent D
systems probed by submillimeter observations are not

Key words: galaxies: evolution – galaxies: formation –
ultraviolet: galaxies

Online-only material: color figures

1. INTRODUCTION

The detailed study of various classes of distant galaxies has enabled great progress in understanding the star formation and mass assembly history of normal field galaxies (for recent reviews, see Hopkins & Beacom 2006; Ellis 2008; Wilkins et al. 2008). Multiwavelength probes have been particularly effective in revealing the coexistence of diverse categories of galaxies with redshifts $z \simeq 2$–3. These include the relatively unobscured star-forming "Lyman break" galaxies (LBGs, e.g., Steidel et al. 1996; Shapley et al. 2005), the infrared-selected massive "distant red" galaxies (DRGs; e.g., Franx et al. 2003; van Dokkum et al. 2006) and heavily obscured submillimeter galaxies which contain both intensely star-forming and active components (SMGs; e.g., Smail et al. 1998; Chapman et al. 2005). The collective study of these populations has revealed that the redshift range $1 < z < 3$ is a formative one when the bulk of the stars in present-day massive galaxies was produced (Hopkins & Beacom 2006).

[8] Hubble Fellow.

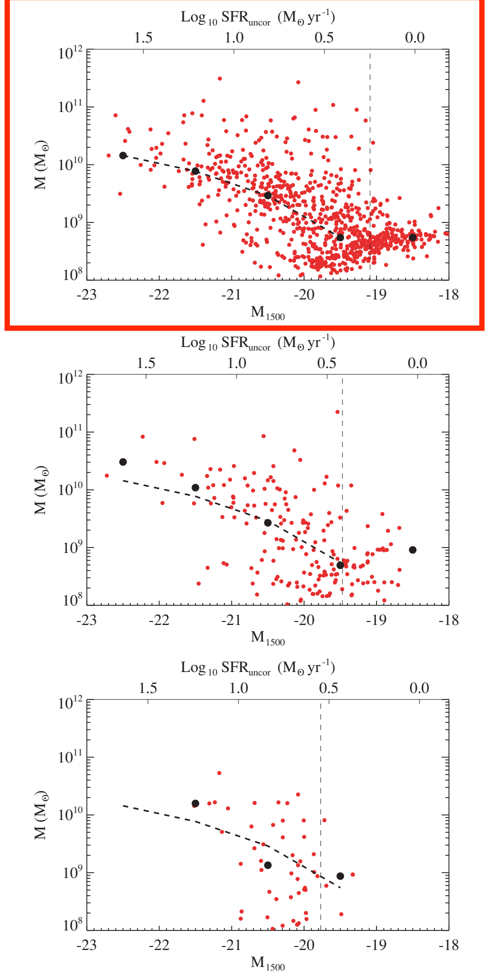

Figure 9. Stellar mass vs. absolute magnitude at 1500 Å (uncorrected for dust extinction) over $z \simeq 4$–6. Small red circles correspond to inferred stellar masses and rest-UV absolute magnitudes for individual B drops (top), V drops (middle) and i' drops (bottom) assuming a $\tau = 100$ Myr exponential decay model. The dark solid circles are the median stellar mass in each magnitude bin. The relationship at $z \simeq 4$ is overlaid on the $z \simeq 5$ and $z \simeq 6$ panels as a black solid dashed line. The vertical solid lines represent the adopted completeness limits for each sample. The median stellar mass increases monotonically with M_{1500} in each dropout sample; however, at a fixed M_{1500}, the median stellar mass does not decrease significantly with increasing redshift, as may be expected in simple steady growth models.

(A color version of this figure is available in the online journal.)

Table 2
Evolution of Galaxy Properties over $4 \lesssim z \lesssim 6$

M_{UV} (mag)	Num	$M_\star$ ($\tau = 100$) ($10^8\ M_\odot$)	$M_\star$ (CSF) ($10^8\ M_\odot$)	Age (Myr)
		B drops ($z \simeq 4$)		
−22.5	15	144 (31-410)	223	180
−21.5	73	77 (24-380)	114	203
−20.5	227	29 (4.0-130)	38	181
−19.5	370	5.5 (2.0-42)	7.3	143
		V drops ($z \simeq 5$)		
−22.5	3	304 (180-830)	520	286
−21.5	20	109 (5.4-234)	112	227
−20.5	67	27 (2.2-158)	36	181
−19.5	...	...	...	...
		i' drops ($z \simeq 6$)		
−22.5	0	...	...	...
−21.5	8	160 (24-530)	226	286
−20.5	41	13 (1.3-90)	27	102
−19.5	...	...	...	...

Notes. The stellar masses and ages are inferred from models using a Salpeter IMF and solar metallicity. In Column 3, we present the median stellar masses (and the range of masses spanned by the middle 80% of the distribution) determined from an exponentially declining star formation history with $\tau = 100$ Myr. In Column 4, we provide the median stellar masses inferred assuming a constant star formation history. In Column 5, we present the median ages inferred for the $\tau = 100$ Myr models.

shown in Table 2, the absence of a systematic increase in the average stellar masses is not strongly dependent on the chosen star formation history. Overall these results seem to imply that the ratio of median stellar mass to emerging UV luminosity does not evolve significantly for LBGs over $z = 4$–6. A galaxy with a given M_{1500} at $z \simeq 6$ will, on average, have the same assembled mass (to within a factor of $\simeq 2$) as a galaxy seen at $z \simeq 4$ with the same M_{1500}. This suggests that the specific SFR evolves weakly over $4 \lesssim z \lesssim 6$, indicating that the typical duration of past star formation for a galaxy of a given luminosity does not vary significantly between $z \simeq 6$ and 4.

While the inclusion of a dust correction would shift the $M_\star$–M_{1500} relation brightward (i.e., to the left in Figure 9), it would likely not lead to an increase in the normalization of the $M_\star$–M_{1500} relation over time. As has been shown elsewhere (e.g., Stanway et al. 2005; Bouwens et al. 2007) galaxies at $M_{1500} < -19.8$ do potentially become marginally dustier between $z \simeq 6$ and 4 which would cause the $z \simeq 4$ $M_\star$–M_{1500} relation to shift slightly more than the $z \simeq 5$ and 6 relations. Since a relative shift brightward is roughly the same as a shift toward lower stellar masses at fixed M_{1500}, this would actually have the effect of slightly decreasing the normalization of the $M_\star$–M_{1500} relation over the $4 \lesssim z \lesssim 6$ redshift range.

6.1. Testing the Steady Growth Scenario

We now attempt to place the $M_\star$–M_{1500} relation presented in Figure 9 in the context of the steady growth scenario discussed at the outset of this section. To approximate this scenario, we assume that galaxies follow a constant SFR. Using solar metallicity templates and allowing the dust content to freely vary, we find that the typical implied star formation lifetimes of the B drops are in excess of 700 Myr in the two brightest bins (Figure 10), implying that the precursors of the majority of B drops would have been equally luminous in V- and

Martin Stringer

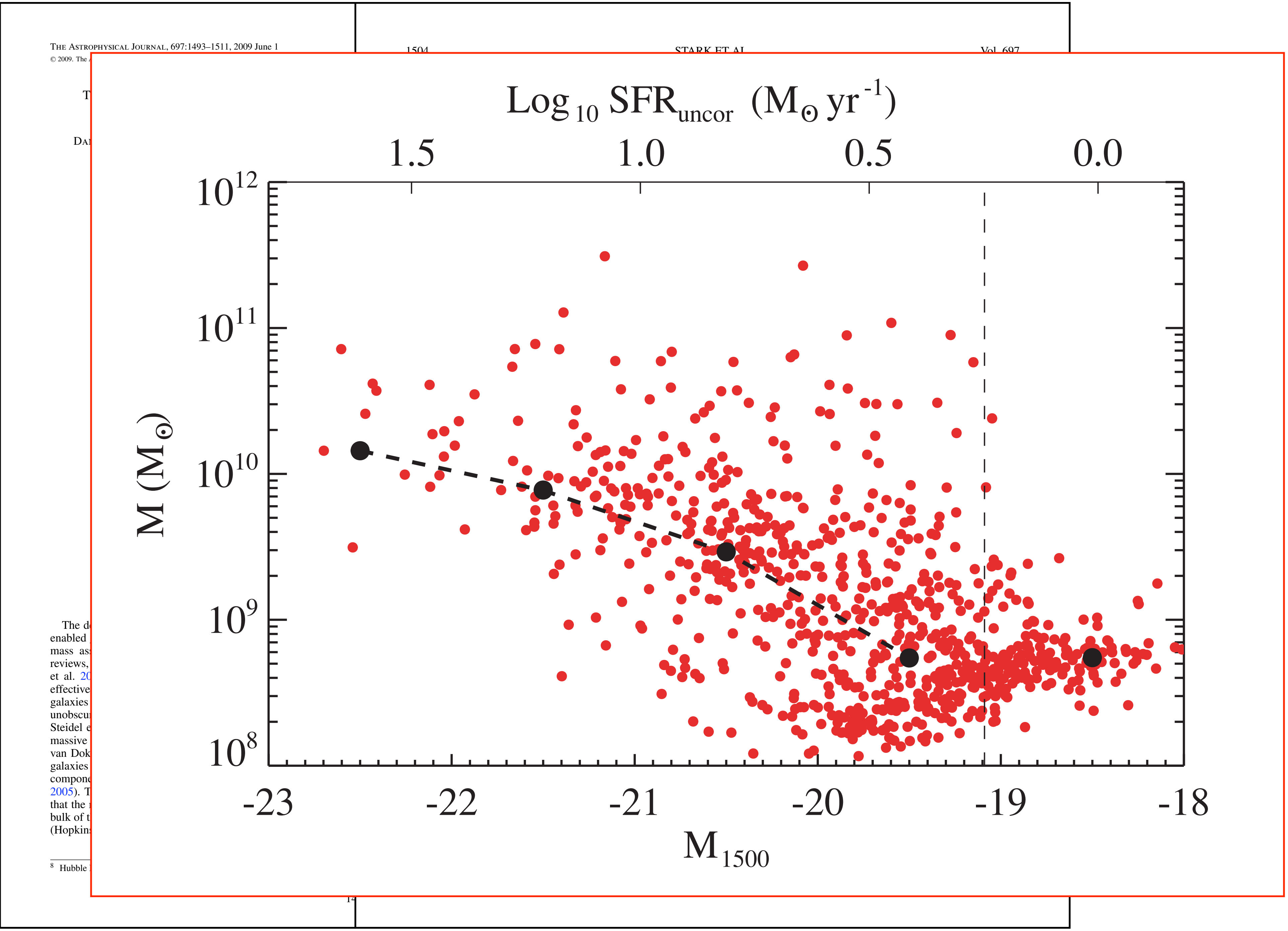

Martin Stringer

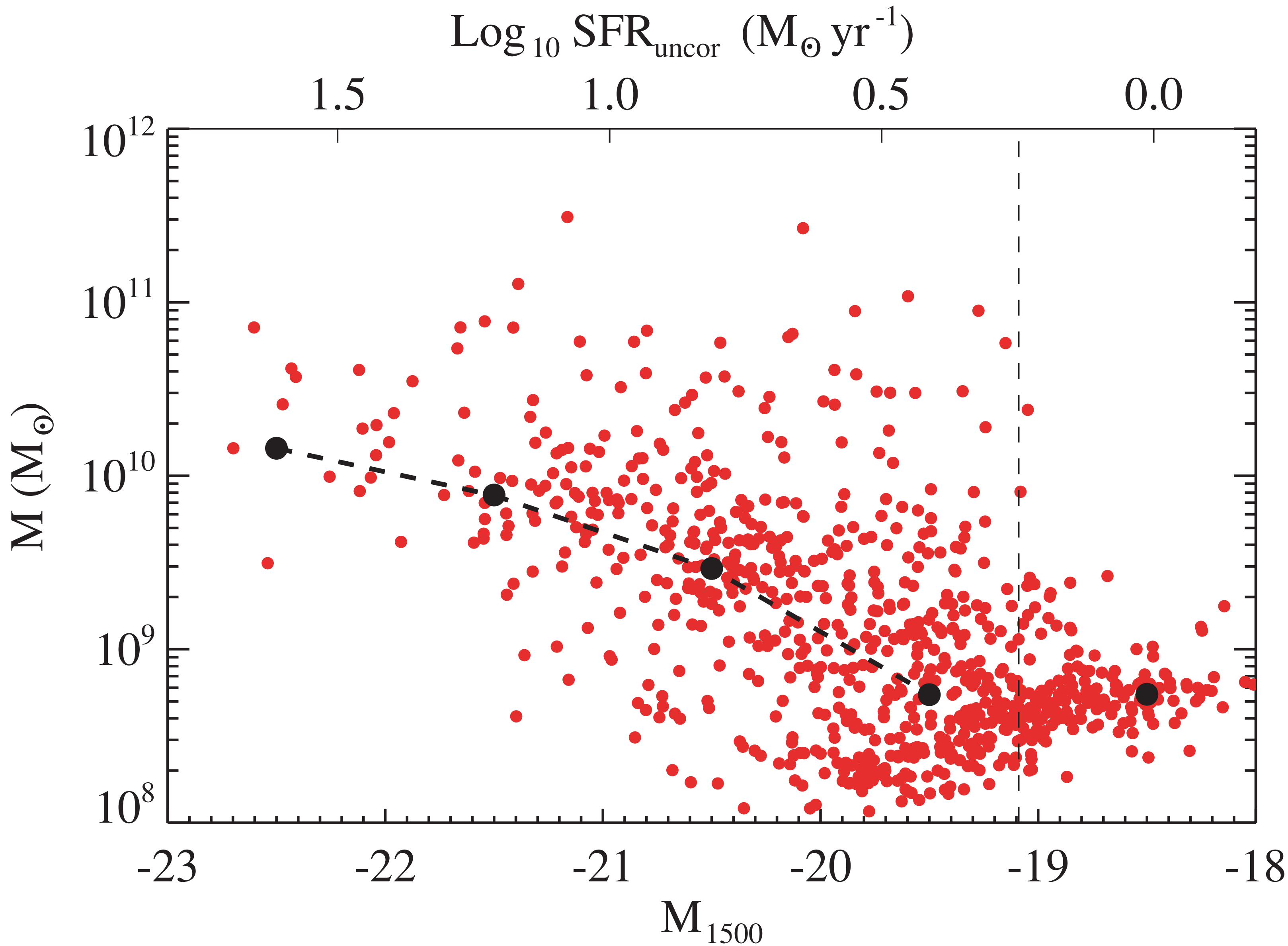

Martin Stringer l'Observatoire de Paris LERMA

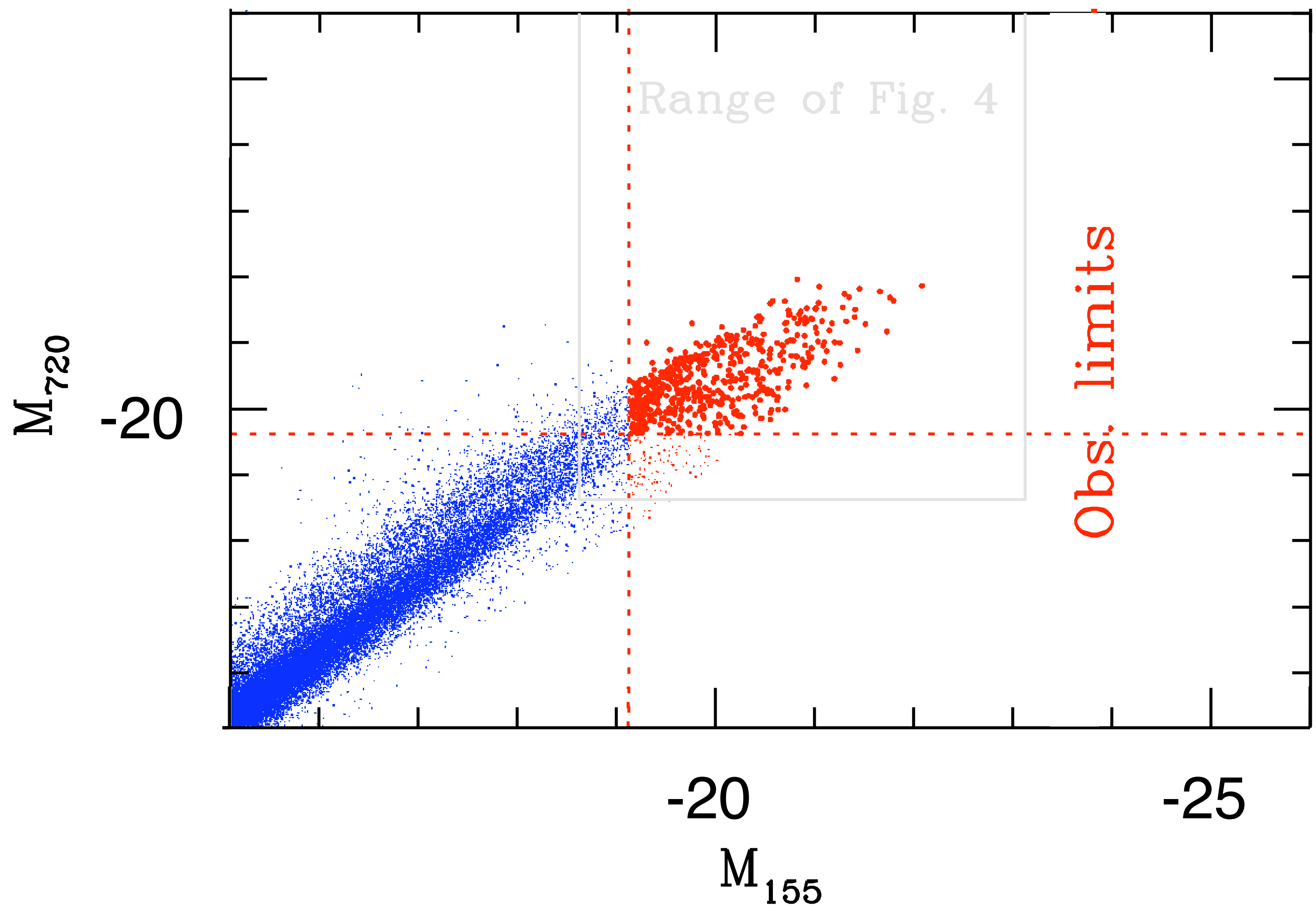

Range of Fig. 4
Obs. limits
M720
-20
-20
-25
M155

Mock Galaxy Samples

$z \approx 4$ $\dashrightarrow$ $z \approx 6$

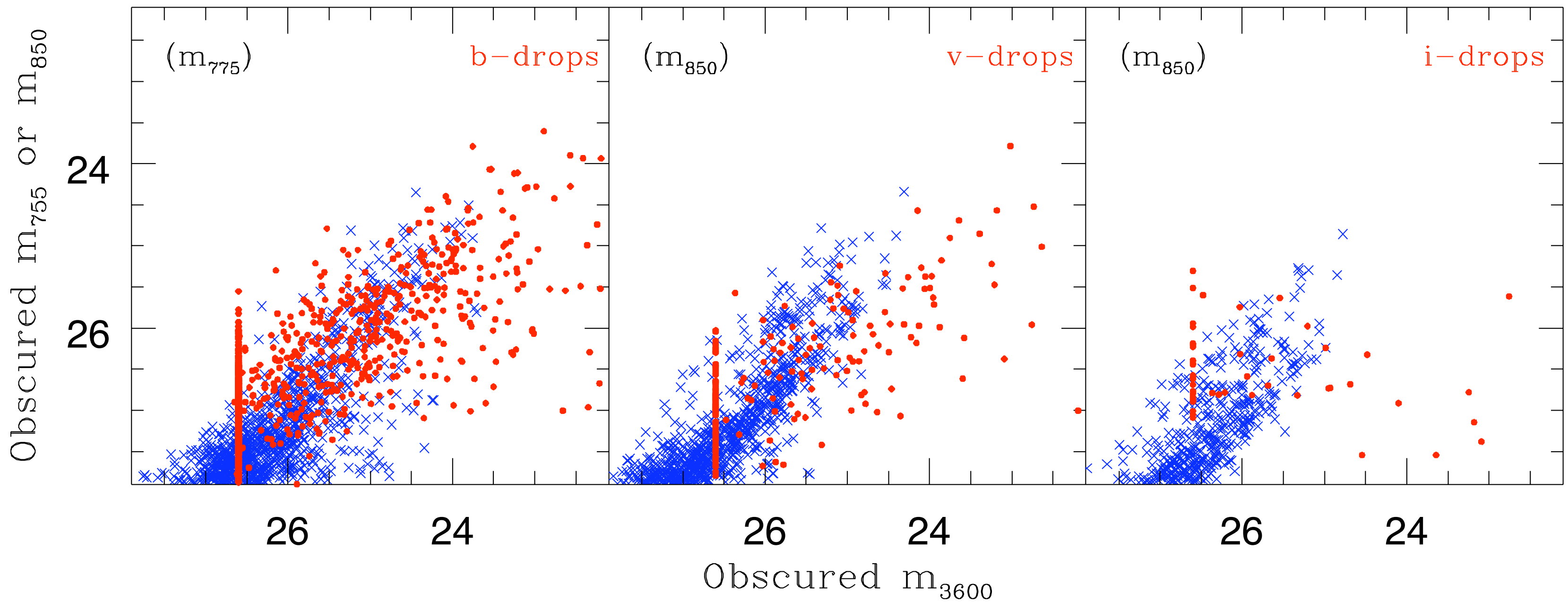

x Mock Sample

● Observational Sample

Martin Stringer

The Astrophysical Journal, 697:1493–1511, 2009 June 1

THE EVOLUTIONARY HISTORY OF LYMAN BR
OBSERVING SUCCESSIVE GENERATIONS

Daniel P. Stark[1,2], Richard S. Ellis[1,3], Andrew Bunke
and Ma
[1] Department of Astrophysics, California Institute of Technolog
[2] Institute of Astronomy, University of Cambrid
[3] Department of Astrophysics, Un
[4] Department of Astronomy, University
[5] Department of Astronomy & Astrophysics, University of
[6] Department of Physics and Astronomy, University of British Co
[7] Spitzer Science Center, California Institute of Technology, M
Received 2008 October 13; accepted 2

ABST

We present new measurements of the evolution in the
and $z \simeq 6$. By utilizing the extensive multiwavelengt
2443 B, 506 V, and 137 i'-band dropout galaxies likel
for which reliable *Spitzer* IRAC photometry is feasible
weighted ages and stellar masses. With the goal of unde
in galaxies at $z \gtrsim 4$, we examine the distribution of stell
that at a fixed rest-UV luminosity, the average stellar m
between $z \simeq 6$ and 4. In order to maintain this near equ
we argue that there must be a steady flux of young, ne
considered along with the short duty cycles inferred fr
that galaxies are undergoing star formation episodes la
the unchanging relationship between the average stella
density of massive galaxies increases considerably with
luminous massive galaxies, we explore the possibility t
distant red galaxies (DRGs) were in part assembled in
the stellar mass function of actively forming LBGs ove
could have contributed significantly to the quiescent D
systems probed by submillimeter observations are not

Key words: galaxies: evolution – galaxies: formation –
ultraviolet: galaxies

Online-only material: color figures

1. INTRODUCTION

The detailed study of various classes of distant galaxies has enabled great progress in understanding the star formation and mass assembly history of normal field galaxies (for recent reviews, see Hopkins & Beacom 2006; Ellis 2008; Wilkins et al. 2008). Multiwavelength probes have been particularly effective in revealing the coexistence of diverse categories of galaxies with redshifts $z \simeq 2$–3. These include the relatively unobscured star-forming "Lyman break" galaxies (LBGs, e.g., Steidel et al. 1996; Shapley et al. 2005), the infrared-selected massive "distant red" galaxies (DRGs; e.g., Franx et al. 2003; van Dokkum et al. 2006) and heavily obscured submillimeter galaxies which contain both intensely star-forming and active components (SMGs; e.g., Smail et al. 1998; Chapman et al. 2005). The collective study of these populations has revealed that the redshift range $1 < z < 3$ is a formative one when the bulk of the stars in present-day massive galaxies was produced (Hopkins & Beacom 2006).

[8] Hubble Fellow.

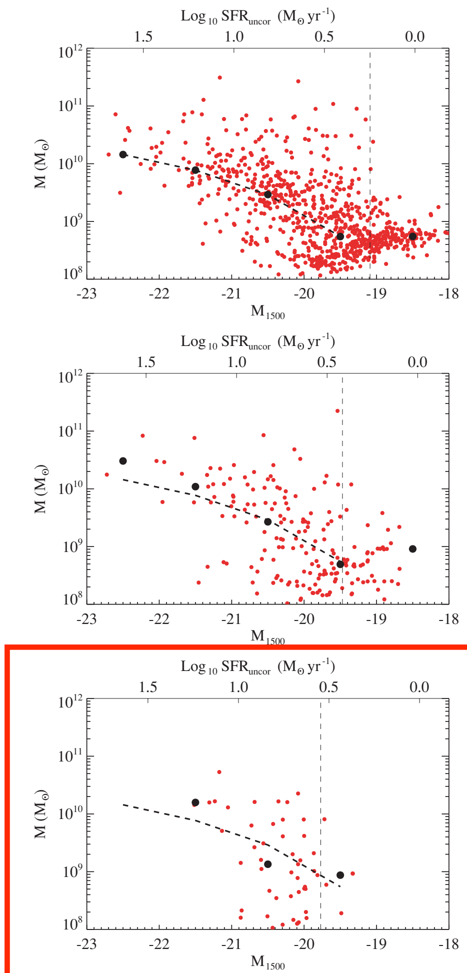

Figure 9. Stellar mass vs. absolute magnitude at 1500 Å (uncorrected for dust extinction) over $z \simeq 4$–6. Small red circles correspond to inferred stellar masses and rest-UV absolute magnitudes for individual B drops (top), V drops (middle) and i' drops (bottom) assuming a $\tau = 100$ Myr exponential decay model. The dark solid circles are the median stellar mass in each magnitude bin. The relationship at $z \simeq 4$ is overlaid on the $z \simeq 5$ and $z \simeq 6$ panels as a black solid dashed line. The vertical solid lines represent the adopted completeness limits for each sample. The median stellar mass increases monotonically with M_{1500} in each dropout sample; however, at a fixed M_{1500}, the median stellar mass does not decrease significantly with increasing redshift, as may be expected in simple steady growth models.

(A color version of this figure is available in the online journal.)

Table 2
Evolution of Galaxy Properties over $4 \lesssim z \lesssim 6$

M_{UV} (mag)	Num	$M_\star$ ($\tau = 100$) ($10^8\ M_\odot$)	$M_\star$ (CSF) ($10^8\ M_\odot$)	Age (Myr)
		B drops ($z \simeq 4$)		
−22.5	15	144 (31-410)	223	180
−21.5	73	77 (24-380)	114	203
−20.5	227	29 (4.0-130)	38	181
−19.5	370	5.5 (2.0-42)	7.3	143
		V drops ($z \simeq 5$)		
−22.5	3	304 (180-830)	520	286
−21.5	20	109 (5.4-234)	112	227
−20.5	67	27 (2.2-158)	36	181
−19.5	…	…	…	…
		i' drops ($z \simeq 6$)		
−22.5	0	…	…	…
−21.5	8	160 (24-530)	226	286
−20.5	41	13 (1.3-90)	27	102
−19.5	…	…	…	…

Notes. The stellar masses and ages are inferred from models using a Salpeter IMF and solar metallicity. In Column 3, we present the median stellar masses (and the range of masses spanned by the middle 80% of the distribution) determined from an exponentially declining star formation history with $\tau = 100$ Myr. In Column 4, we provide the median stellar masses inferred assuming a constant star formation history. In Column 5, we present the median ages inferred for the $\tau = 100$ Myr models.

shown in Table 2, the absence of a systematic increase in the average stellar masses is not strongly dependent on the chosen star formation history. Overall these results seem to imply that the ratio of median stellar mass to emerging UV luminosity does not evolve significantly for LBGs over $z = 4$–6. A galaxy with a given M_{1500} at $z \simeq 6$ will, on average, have the same assembled mass (to within a factor of $\simeq 2$) as a galaxy seen at $z \simeq 4$ with the same M_{1500}. This suggests that the specific SFR evolves weakly over $4 \lesssim z \lesssim 6$, indicating that the typical duration of past star formation for a galaxy of a given luminosity does not vary significantly between $z \simeq 6$ and 4.

While the inclusion of a dust correction would shift the $M_\star$–M_{1500} relation brightward (i.e., to the left in Figure 9), it would likely not lead to an increase in the normalization of the $M_\star$–M_{1500} relation over time. As has been shown elsewhere (e.g., Stanway et al. 2005; Bouwens et al. 2007) galaxies at $M_{1500} < -19.8$ do potentially become marginally dustier between $z \simeq 6$ and 4 which would cause the $z \simeq 4$ $M_\star$–M_{1500} relation to shift slightly more than the $z \simeq 5$ and 6 relations. Since a relative shift brightward is roughly the same as a shift toward lower stellar masses at fixed M_{1500}, this would actually have the effect of slightly decreasing the normalization of the $M_\star$–M_{1500} relation over the $4 \lesssim z \lesssim 6$ redshift range.

6.1. Testing the Steady Growth Scenario

We now attempt to place the $M_\star$–M_{1500} relation presented in Figure 9 in the context of the steady growth scenario discussed at the outset of this section. To approximate this scenario, we assume that galaxies follow a constant SFR. Using solar metallicity templates and allowing the dust content to freely vary, we find that the typical inferred star formation lifetimes of the B drops are in excess of 700 Myr in the two brightest bins (Figure 10), implying that the precursors of the majority of B drops would have been equally luminous in V- and

extinction). It is not necessarily obvious that the ongoing star formation in any galaxy should bear any relation to the past star formation history, yet immediately apparent is a correlation between the average optical and mid-infrared flux: sources that are brighter in the ACS bandpasses are, on average, brighter in IRAC. Also noticeable is that the median IRAC flux for a given i_{775} or z_{850} flux does not change significantly over the redshift range probed by the three dropout samples. We discuss the implications of these trends in more detail in Section 6.

4.2. MIPS Detections

We have put considerable effort into removing low-redshift contaminants from our data set. However, as is evident from Figure 4, the dropout samples still contain red objects, some of which are among the brightest sources detected in IRAC. Considering the fact that very massive sources (with bright IRAC fluxes) are likely much more common at $z \simeq 2$ than at $z \gtrsim 4$, it is clear that these sources require more scrutiny before proceeding.

We can gain some insight into the likely redshifts of this population from 24 μm imaging with the Multiband Imaging Photometer for *Spitzer* (MIPS) camera (Dickinson et al., in preparation; Chary et al., in preparation). At $z \simeq 2$, the MIPS imaging passband probes the bright rest-frame 7.7 μm feature from polycyclic aromatic hydrocarbons (PAHs). As a result, dusty star-forming galaxies at $z \simeq 2$ are commonly detected with the MIPS (e.g., Reddy et al. 2006). Such PAH features would not be detected in sources over the redshift range our dropouts sample ($4 \lesssim z \lesssim 6$); hence if any of our sources are detected with MIPS, it very well may indicate that they lie at $z \simeq 2$.

In order to determine what fraction of our catalog is detected at 24 μm, we visually examine the MIPS data of each dropout in the *Spitzer*-isolated sample. While the total number of dropouts with MIPS detections is small (12/800 B drops, 3/186 V drops, and none of the i' drops), it is not negligible. As expected, each of the sources detected with MIPS is quite red ($z'_{850} - m_{3.6} \gtrsim 2$) in addition to being bright in the IRAC bandpasses. These sources thus make up a significant fraction of the subset of our dropout samples with bright IRAC fluxes (10/25, 2/4 of those with $m_{3.6} < 23$ for the B and V drops, respectively) and are hence sure to strongly affect attempts to derive the number density of massive galaxies.

While we consider these sources as prime low-redshift candidates, it is possible that some of these lie at $z \gtrsim 4$. Cross-correlating the 24 μm detected subset with our spectroscopic sample, we find that one of the three MIPS-detected V drops has a spectroscopically confirmed redshift of $z = 4.76$. Since there are few strong PAH features that fall into the 24 μm filter at this redshift, we propose that the 24 μm emission most likely comes from a dusty active galactic nuclei, a conclusion consistent with the point-like morphology in the observed optical-frame. Importantly, this establishes that not all 24 μm detected dropouts are foreground objects. The MIPS-detected subsample thus places an upper limit (1.5% for the B drops and 1.1% for the V drops) on the number of dusty low-z interlopers remaining in our samples. In subsequent sections, we will derive the evolving stellar populations of our dropout sample both with and without the 24 μm detected sources.

5. DERIVATION OF PHYSICAL PROPERTIES

We infer stellar masses for the dropout sample by fitting the latest CB07 stellar population synthesis models to the

Martin Stringer

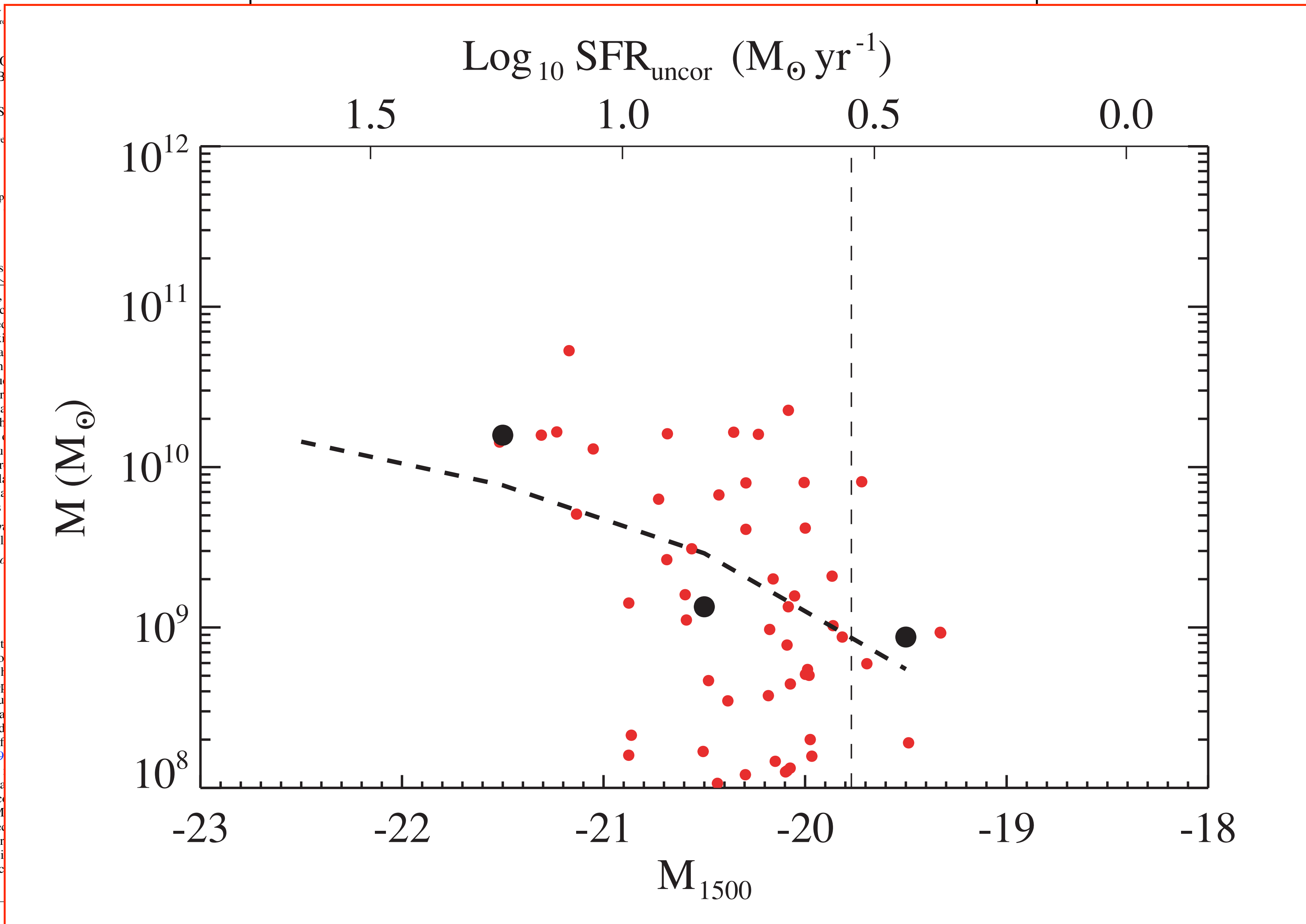

Martin Stringer

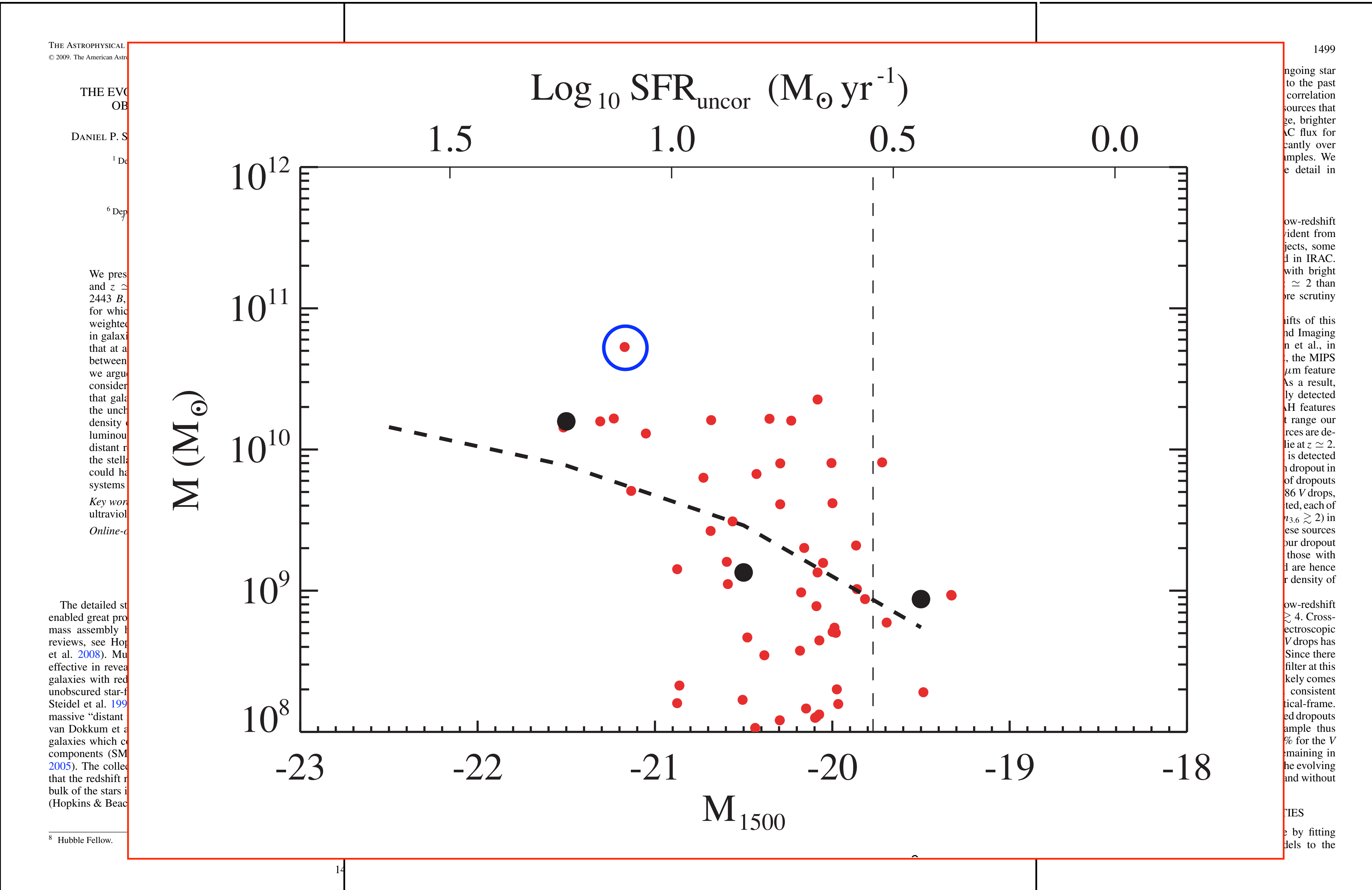

Martin Stringer l'Observatoire de Paris LERMA

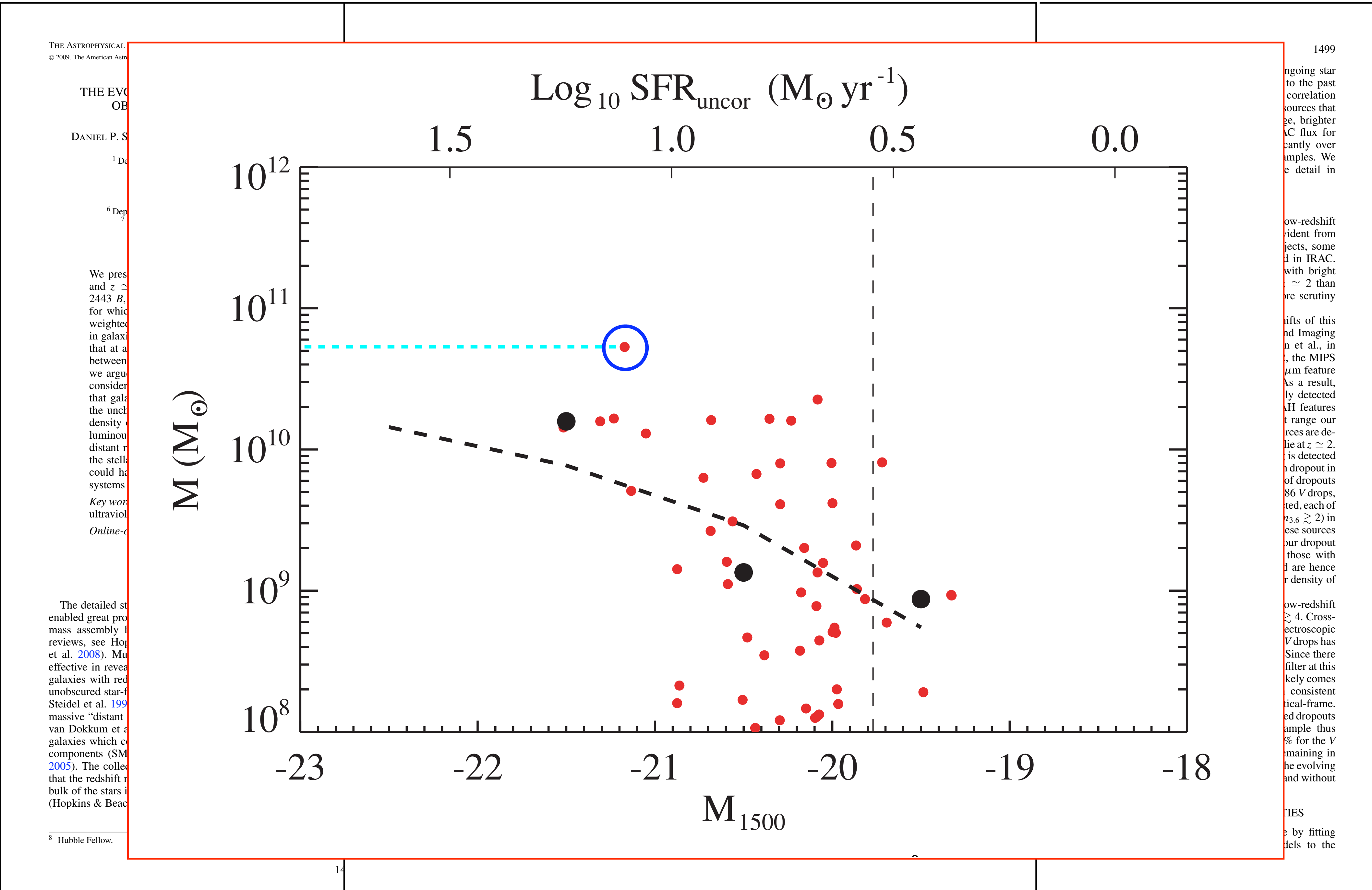

Martin Stringer l'Observatoire de Paris LERMA

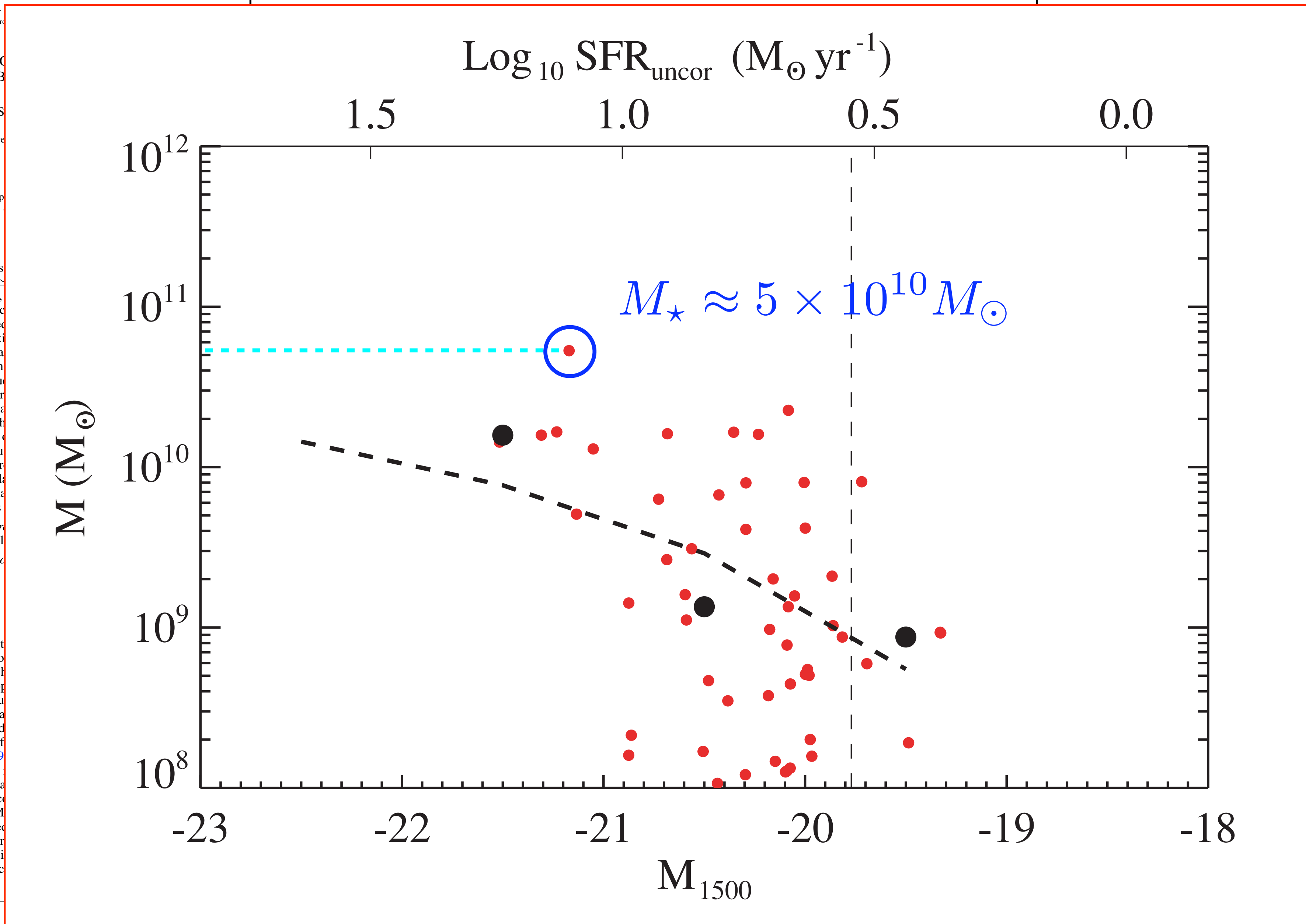

$\mathrm{Log}_{10}\ \mathrm{SFR}_{\mathrm{uncor}}\ (\mathrm{M}_{\odot}\ \mathrm{yr}^{-1})$
1.5
1.0
0.5
0.0
$M_{\star} \approx 5 \times 10^{10} M_{\odot}$
$\mathrm{M}\ (\mathrm{M}_{\odot})$
10^{12}
10^{11}
10^{10}
10^{9}
10^{8}
-23
-22
-21
-20
-19
-18
M_{1500}

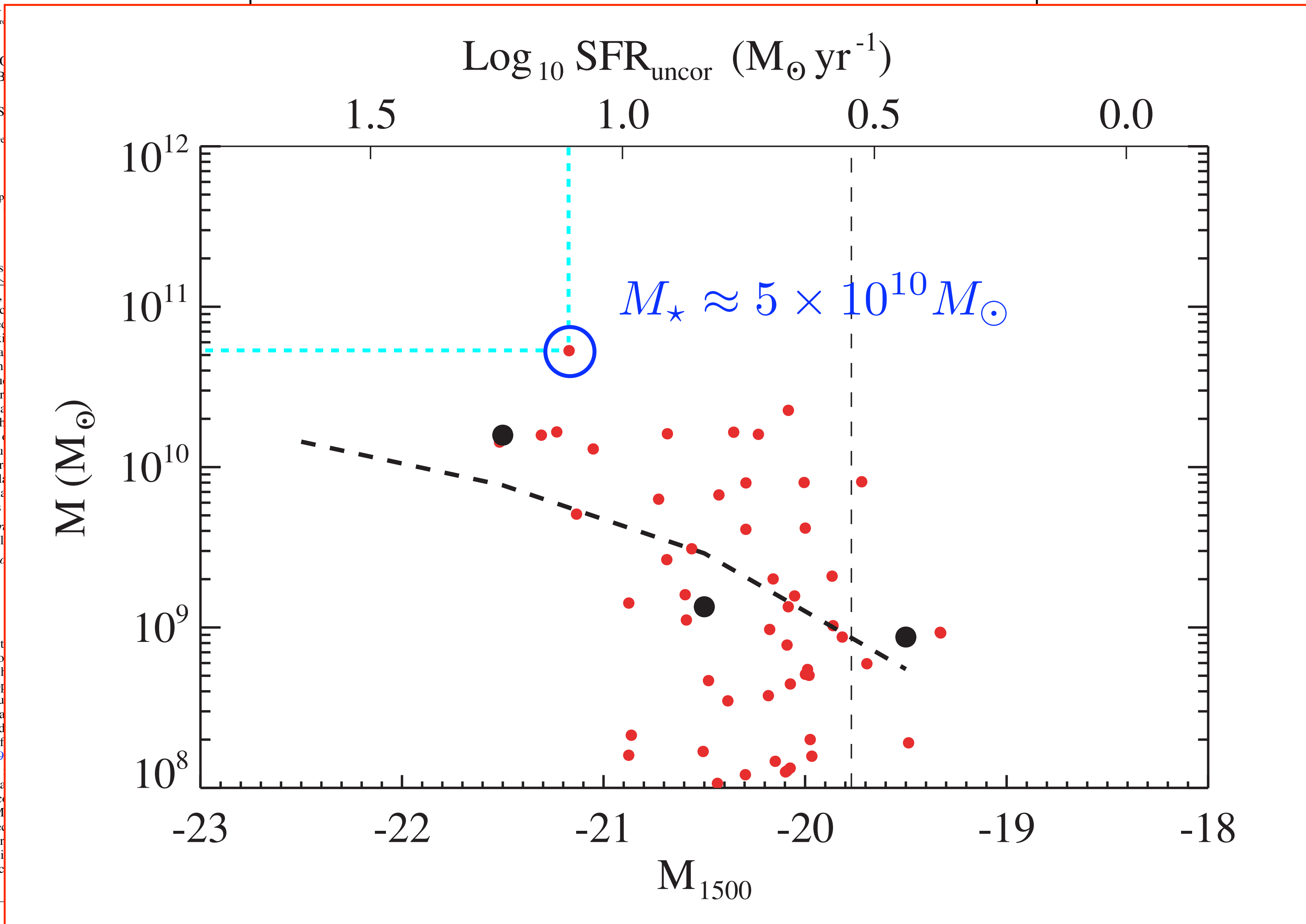

Martin Stringer

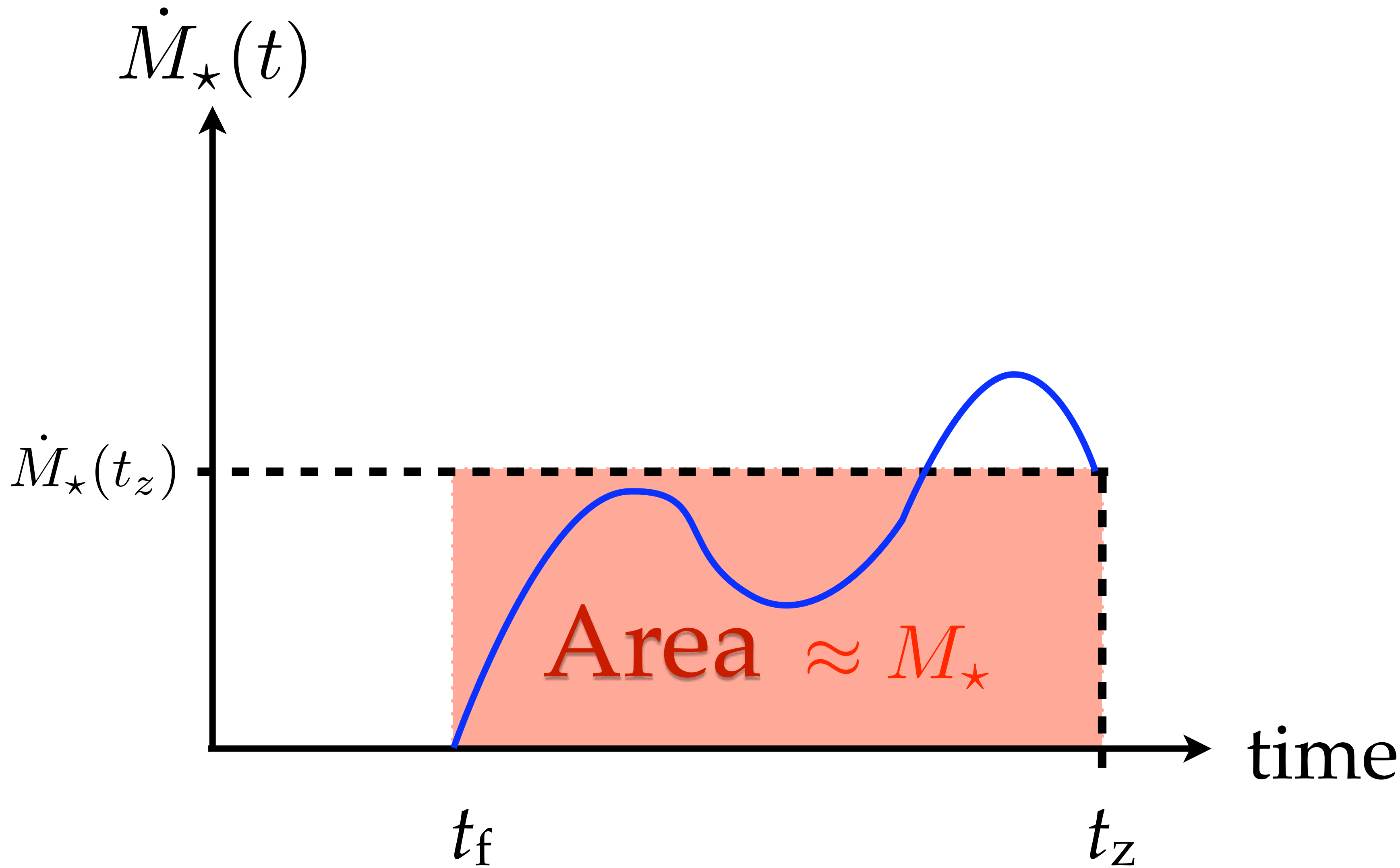
$\dot{M}_\star(t)$
$\dot{M}_\star(t_z)$
Area $\approx M_\star$
time
t_f
t_z

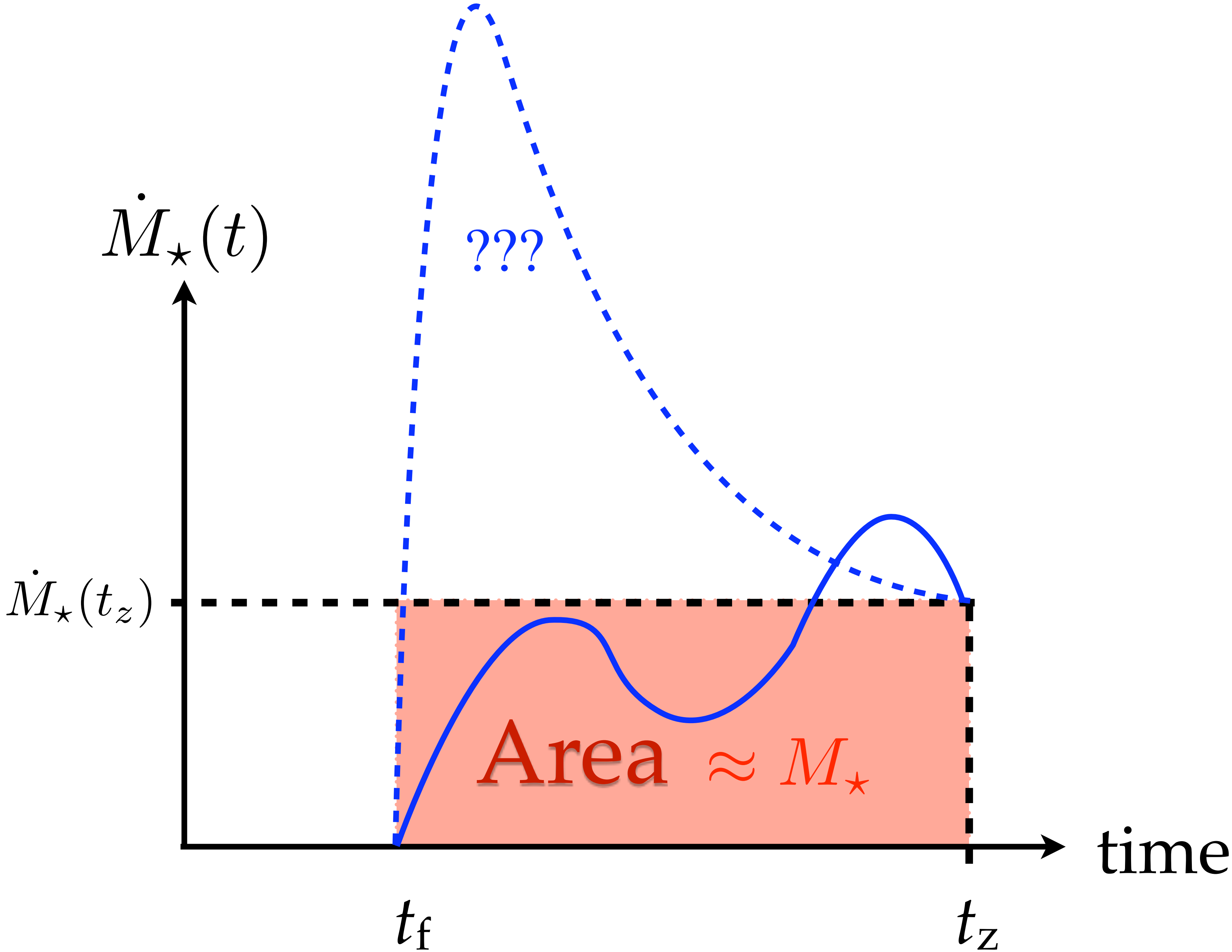

$\dot{M}_\star(t)$
???
$\dot{M}_\star(t_z)$
Area $\approx M_\star$
time
t_f
t_z

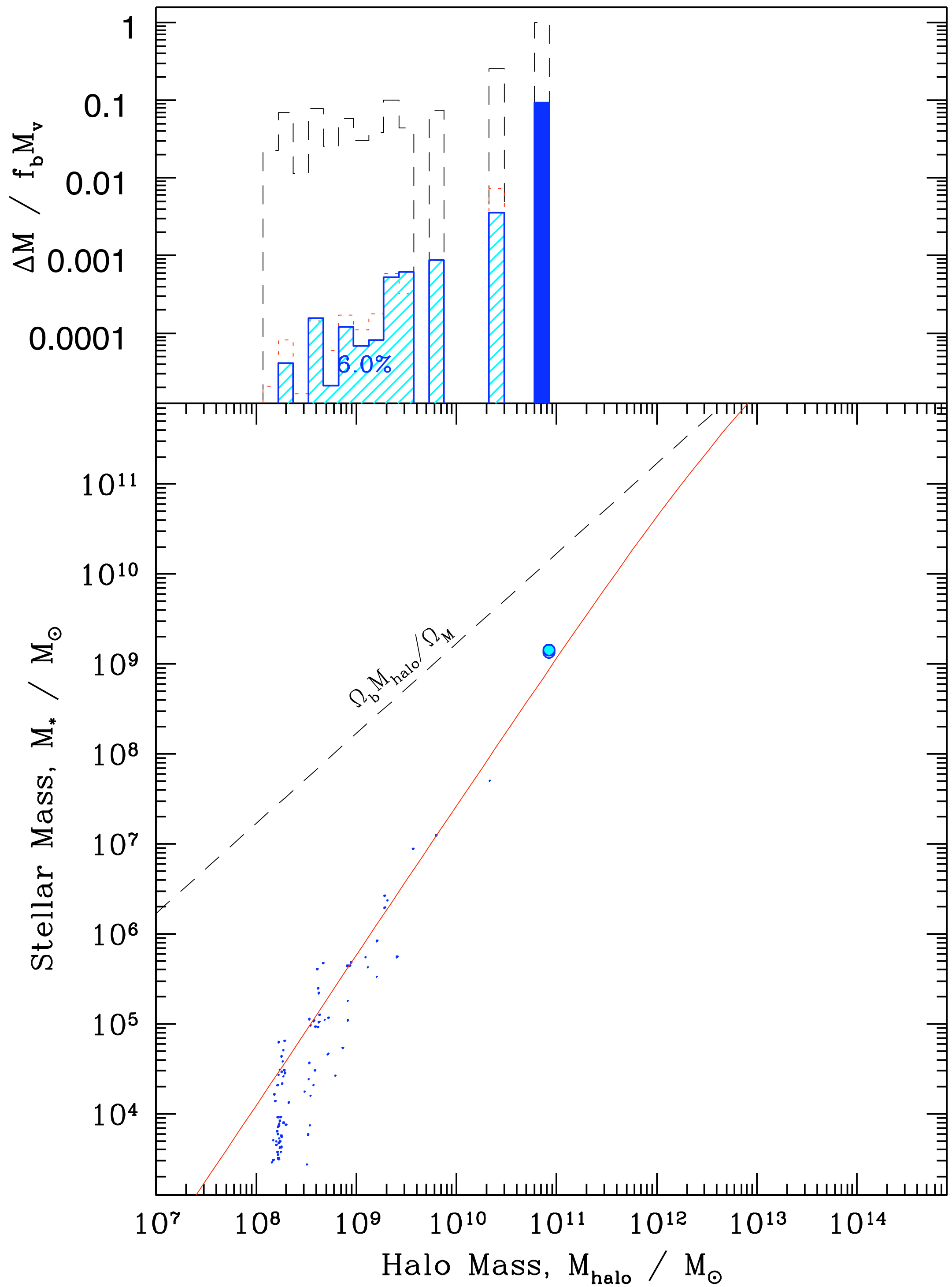

1
0.1
0.01
0.001
0.0001
ΔM / f_b M_v
6.0%
10^{11}
10^{10}
10^{9}
10^{8}
10^{7}
10^{6}
10^{5}
10^{4}
$\Omega_b M_{halo}/\Omega_M$
Stellar Mass, M_* / $M_\odot$
10^{7}
10^{8}
10^{9}
10^{10}
10^{11}
10^{12}
10^{13}
10^{14}
Halo Mass, M_{halo} / $M_\odot$

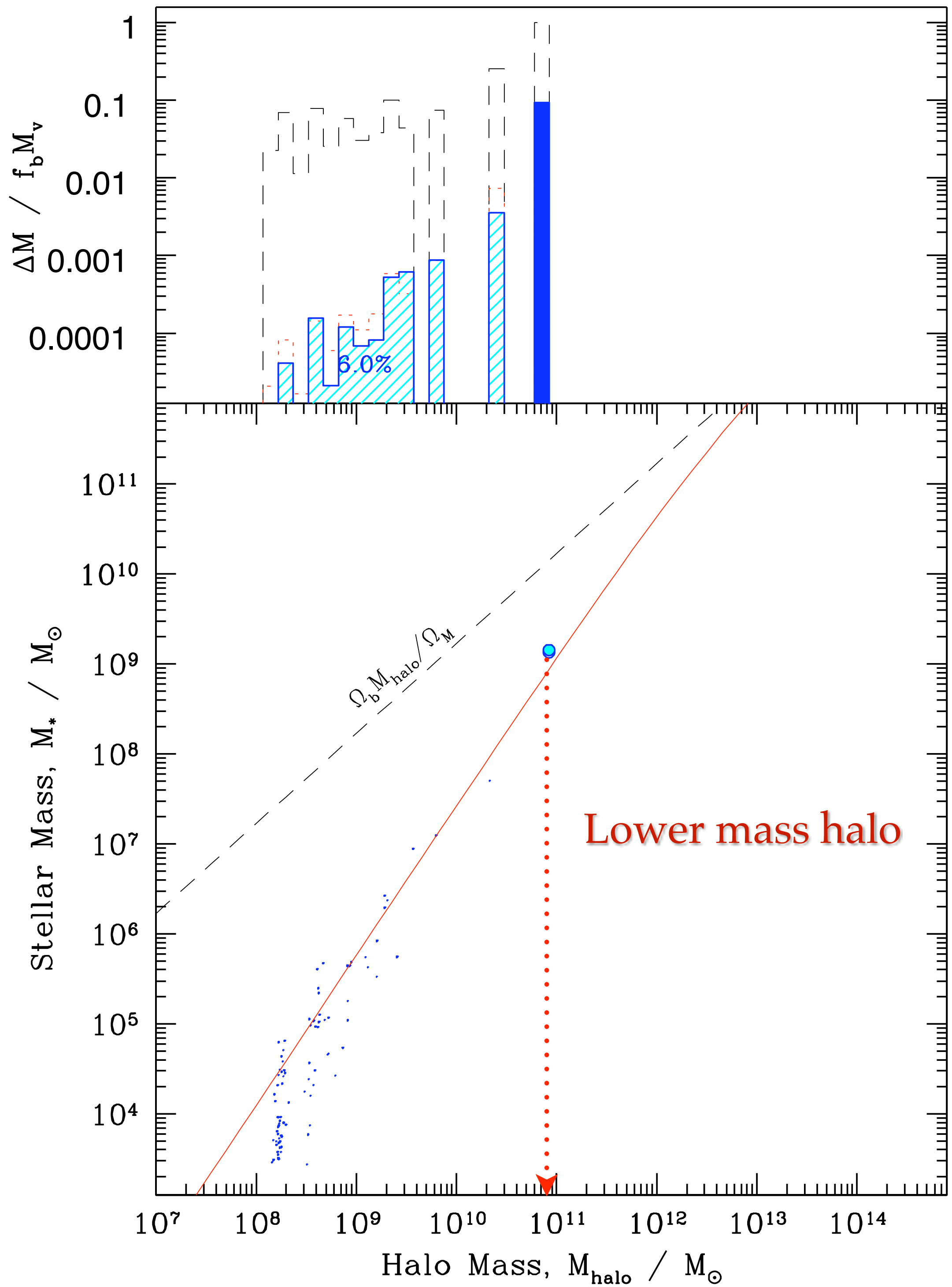

1
0.1
0.01
0.001
0.0001
$\Delta M \;/\; f_b M_v$
6.0%
10^{11}
10^{10}
10^{9}
10^{8}
10^{7}
10^{6}
10^{5}
10^{4}
Stellar Mass, $M_* \;/\; M_\odot$
$\Omega_b M_{halo}/\Omega_M$
Lower mass halo
10^{7}
10^{8}
10^{9}
10^{10}
10^{11}
10^{12}
10^{13}
10^{14}
Halo Mass, $M_{halo} \;/\; M_\odot$

Gas doesn’t cool effectively into satellites

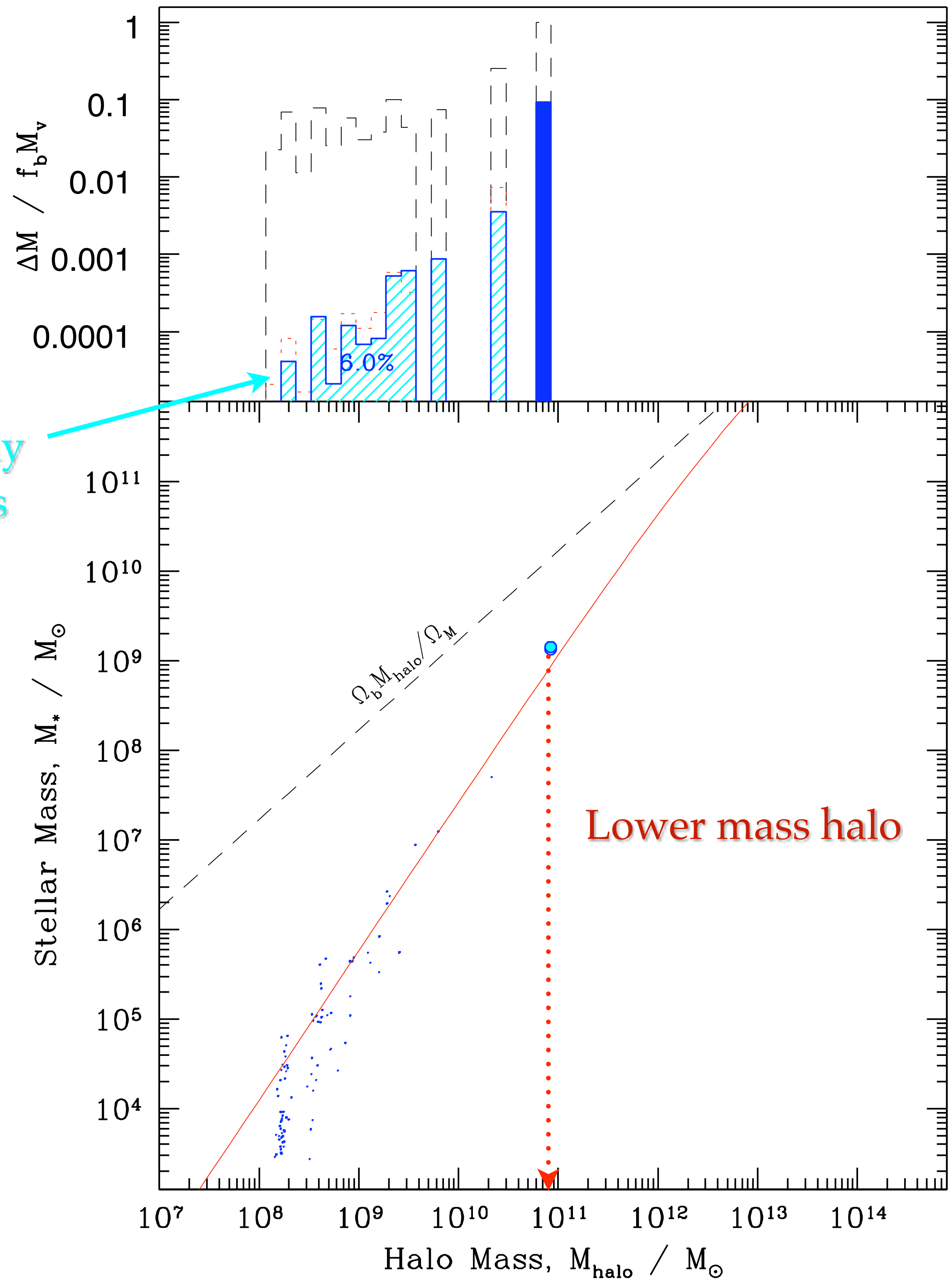

Lower mass halo

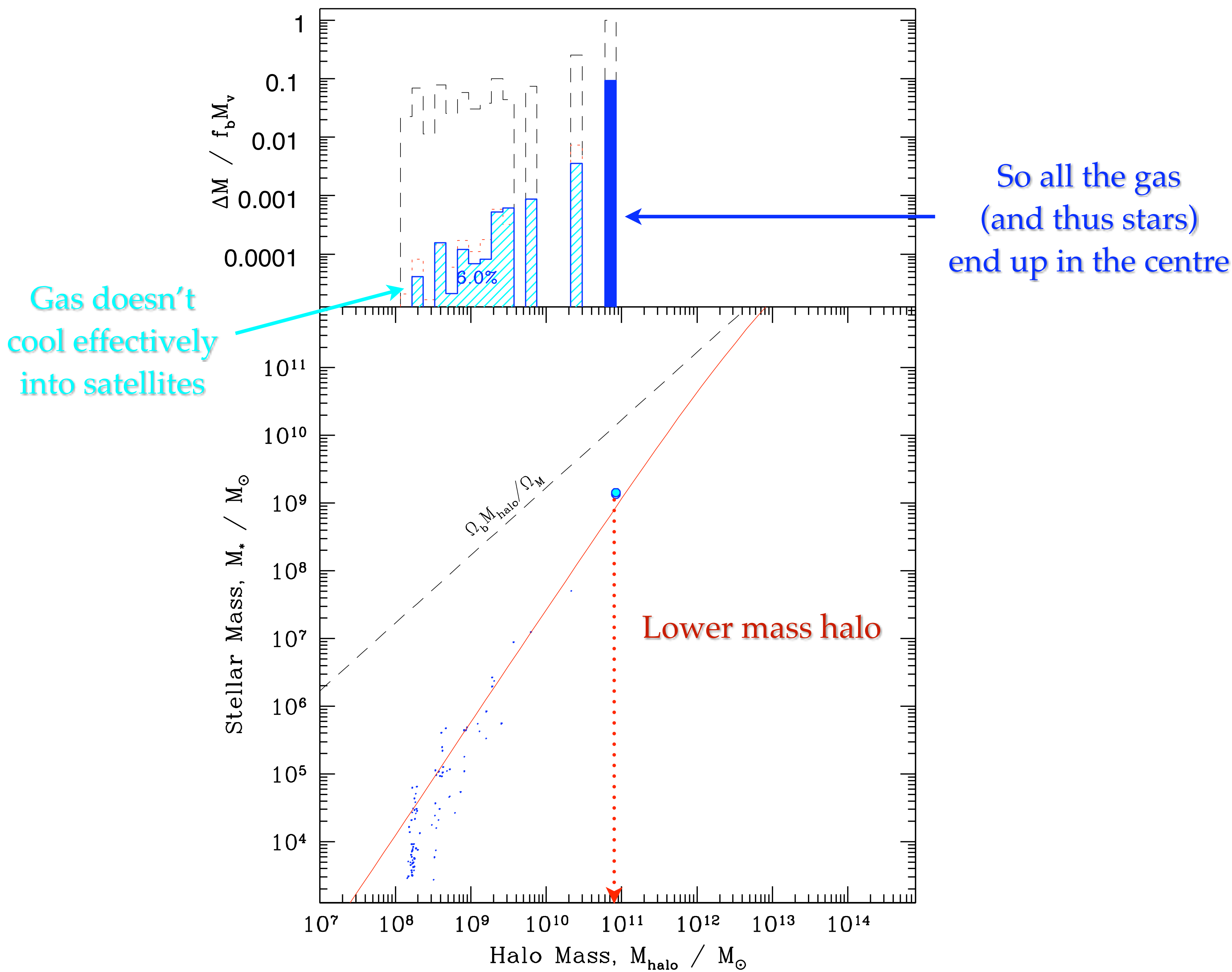

So all the gas
(and thus stars)
end up in the centre
Gas doesn't
cool effectively
into satellites
Lower mass halo
6.0%
ΔM / f_b M_v
1
0.1
0.01
0.001
0.0001
Stellar Mass, M_* / M_⊙
10^11
10^10
10^9
10^8
10^7
10^6
10^5
10^4
Ω_b M_halo / Ω_M
10^7
10^8
10^9
10^10
10^11
10^12
10^13
10^14
Halo Mass, M_halo / M_⊙

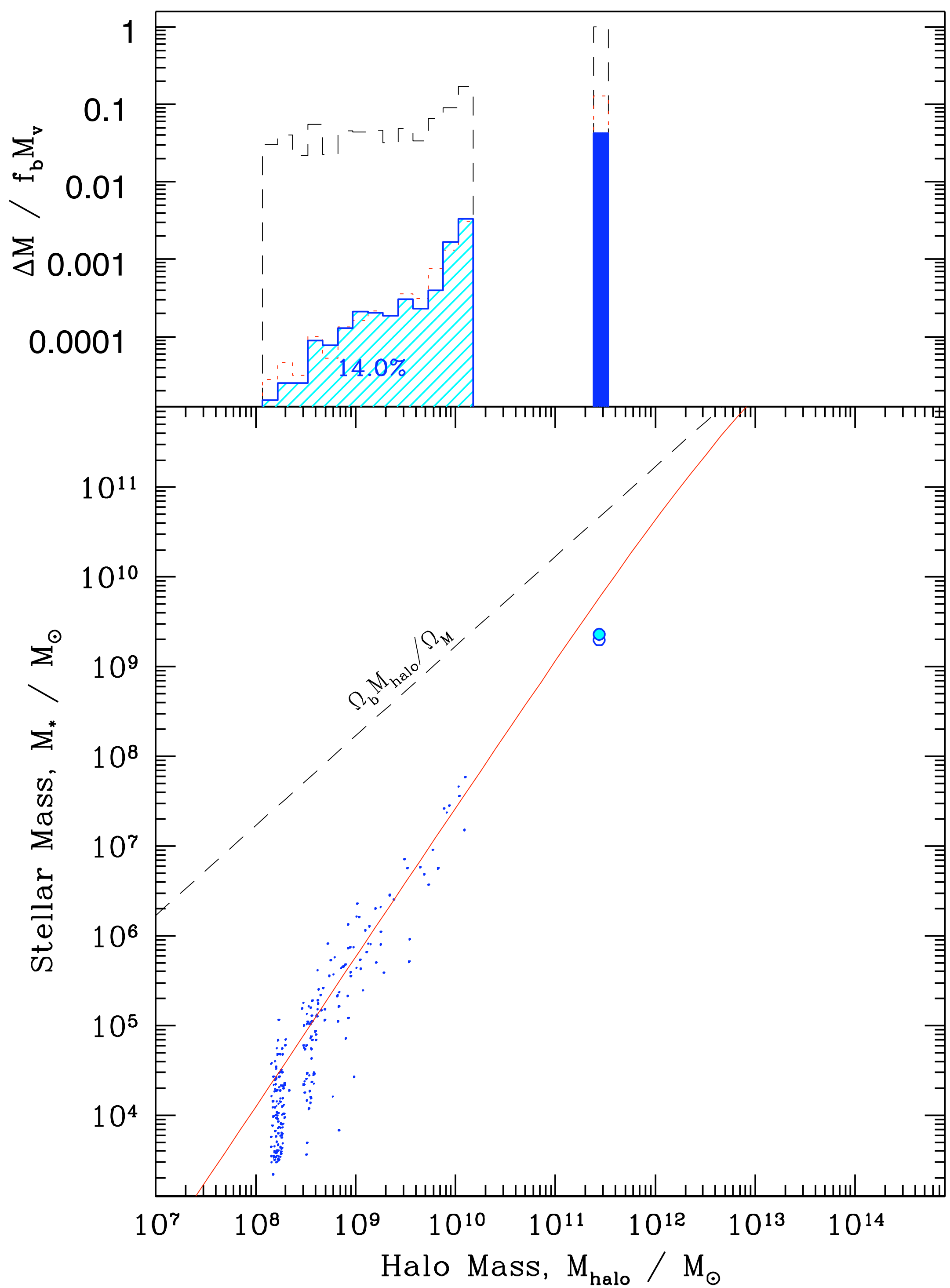

1
0.1
0.01
0.001
0.0001
ΔM / f_b M_v
14.0%
10^11
10^10
10^9
10^8
10^7
10^6
10^5
10^4
Ω_b M_halo/Ω_M
Stellar Mass, M_* / M_⊙
10^7
10^8
10^9
10^10
10^11
10^12
10^13
10^14
Halo Mass, M_halo / M_⊙

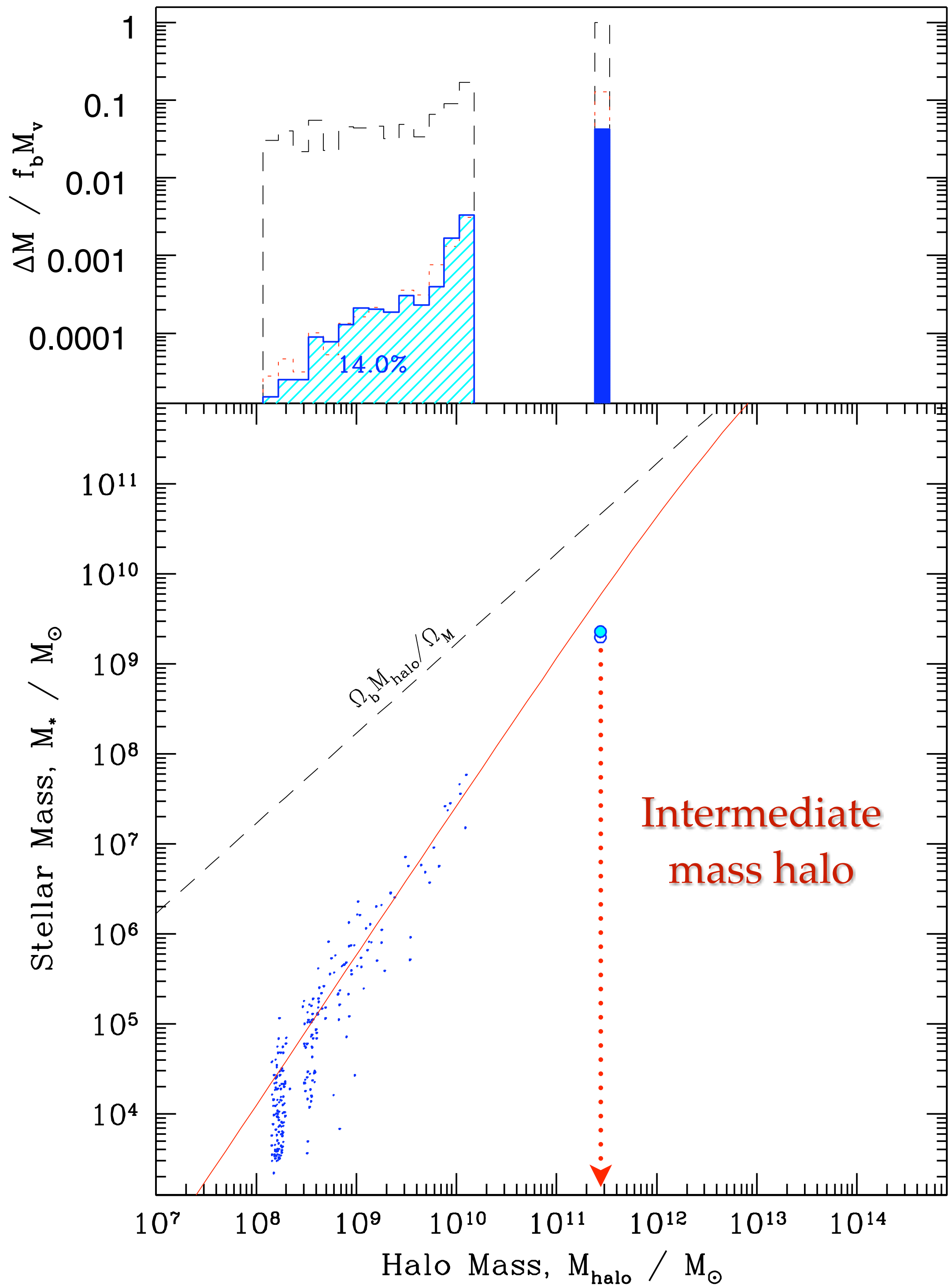

1
0.1
0.01
0.001
0.0001
ΔM / f_b M_v
14.0%
10^{11}
10^{10}
10^{9}
10^{8}
10^{7}
10^{6}
10^{5}
10^{4}
Stellar Mass, M_* / $M_\odot$
$\Omega_b M_{halo}/\Omega_M$
Intermediate mass halo
10^{7} 10^{8} 10^{9} 10^{10} 10^{11} 10^{12} 10^{13} 10^{14}
Halo Mass, M_{halo} / $M_\odot$

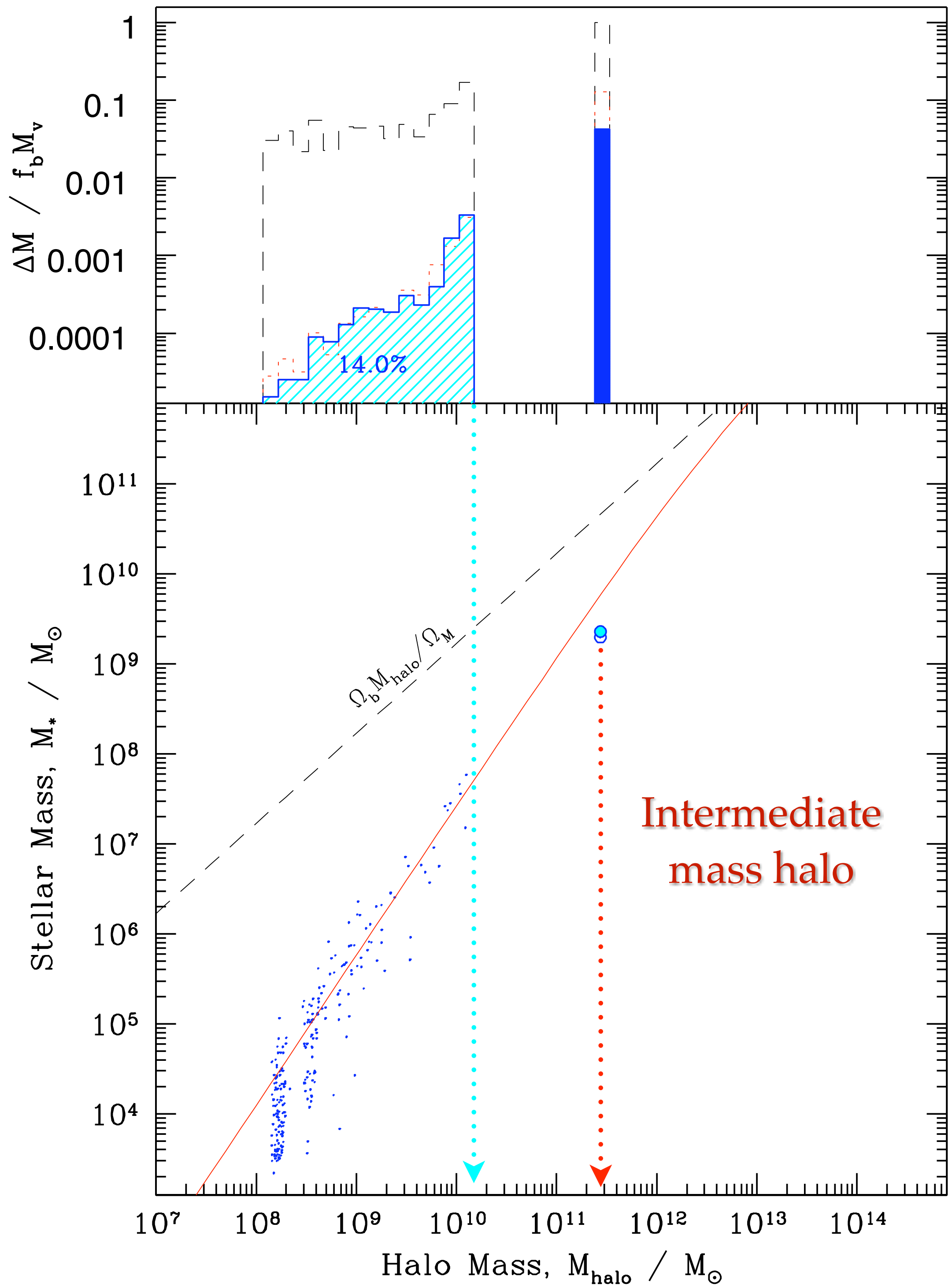

1
0.1
0.01
0.001
0.0001
ΔM / f_b M_v
14.0%
Ω_b M_halo / Ω_M
Intermediate
mass halo
10^11
10^10
10^9
10^8
10^7
10^6
10^5
10^4
Stellar Mass, M_* / M_⊙
10^7
10^8
10^9
10^10
10^11
10^12
10^13
10^14
Halo Mass, M_halo / M_⊙

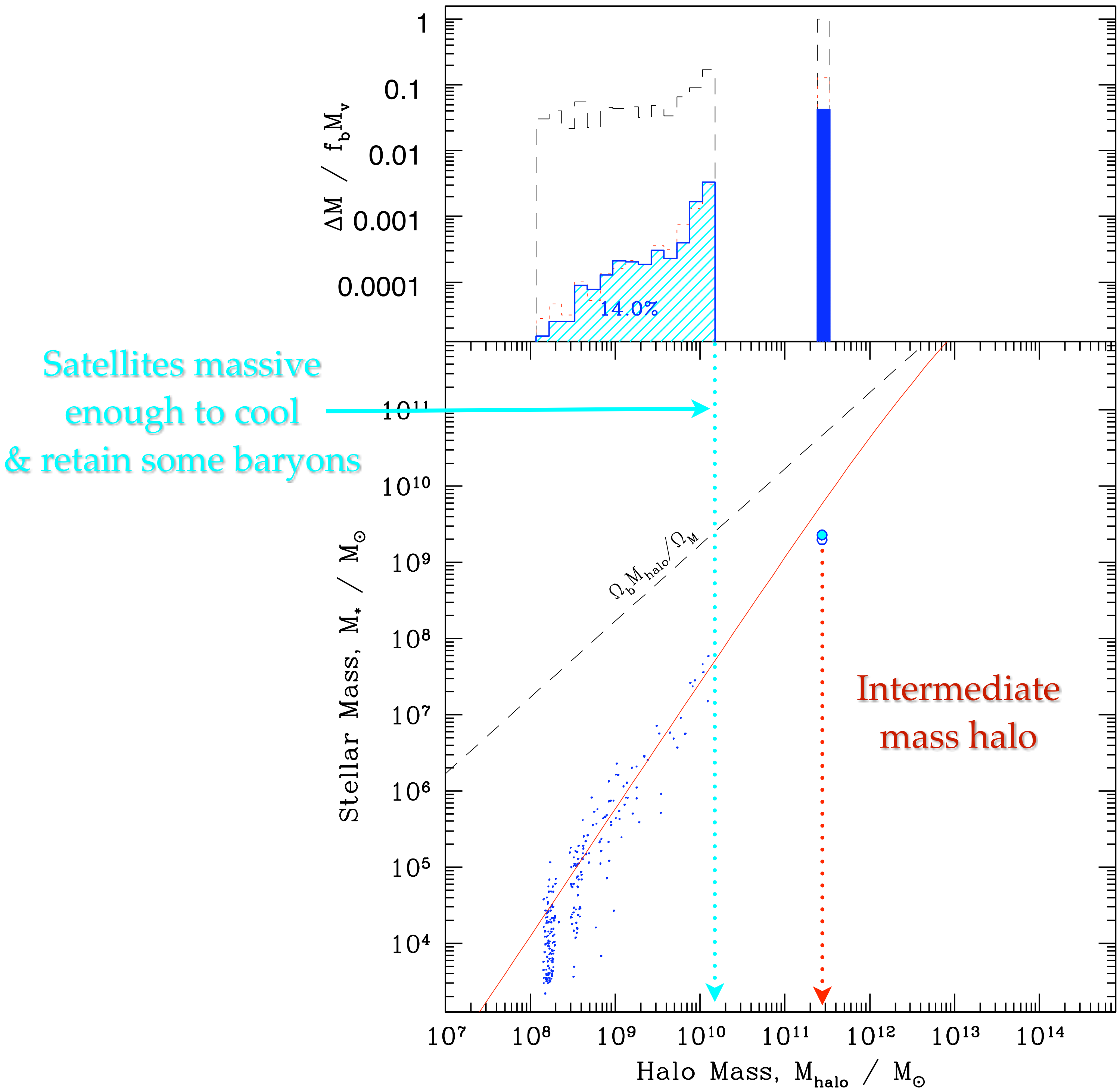

1
0.1
0.01
0.001
0.0001
ΔM / f_b M_v
14.0%
Satellites massive
enough to cool
& retain some baryons
10^{11}
10^{10}
10^{9}
10^{8}
10^{7}
10^{6}
10^{5}
10^{4}
Stellar Mass, M_* / $M_\odot$
$\Omega_b M_{halo}/\Omega_M$
Intermediate
mass halo
10^{7} 10^{8} 10^{9} 10^{10} 10^{11} 10^{12} 10^{13} 10^{14}
Halo Mass, M_{halo} / $M_\odot$

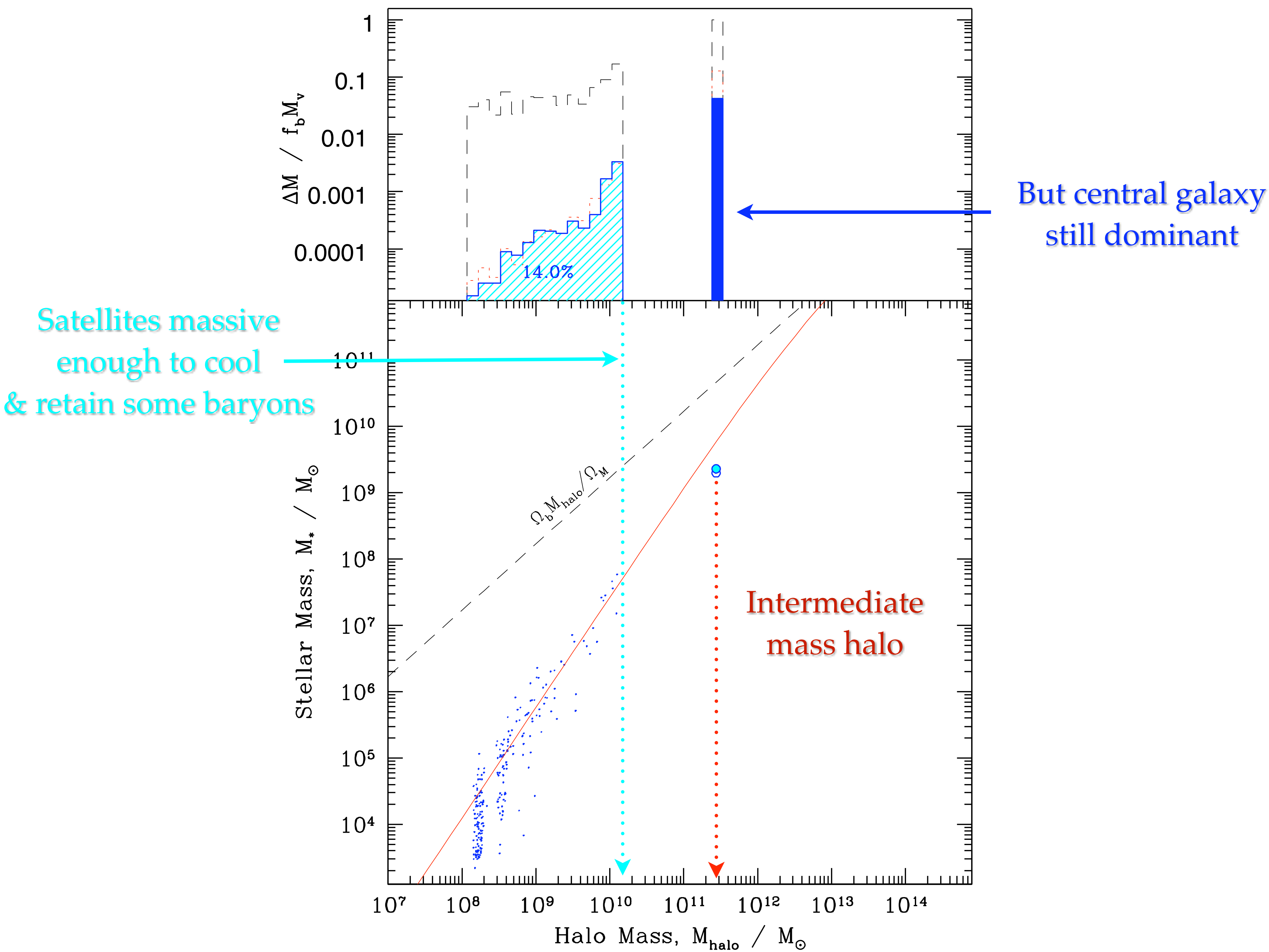

But central galaxy still dominant
Satellites massive enough to cool & retain some baryons
Intermediate mass halo
14.0%
$\Omega_b M_{halo}/\Omega_M$
ΔM / $f_b M_v$
Stellar Mass, M_* / $M_\odot$
Halo Mass, M_{halo} / $M_\odot$
1
0.1
0.01
0.001
0.0001
10^{11}
10^{10}
10^9
10^8
10^7
10^6
10^5
10^4
10^7 10^8 10^9 10^{10} 10^{11} 10^{12} 10^{13} 10^{14}

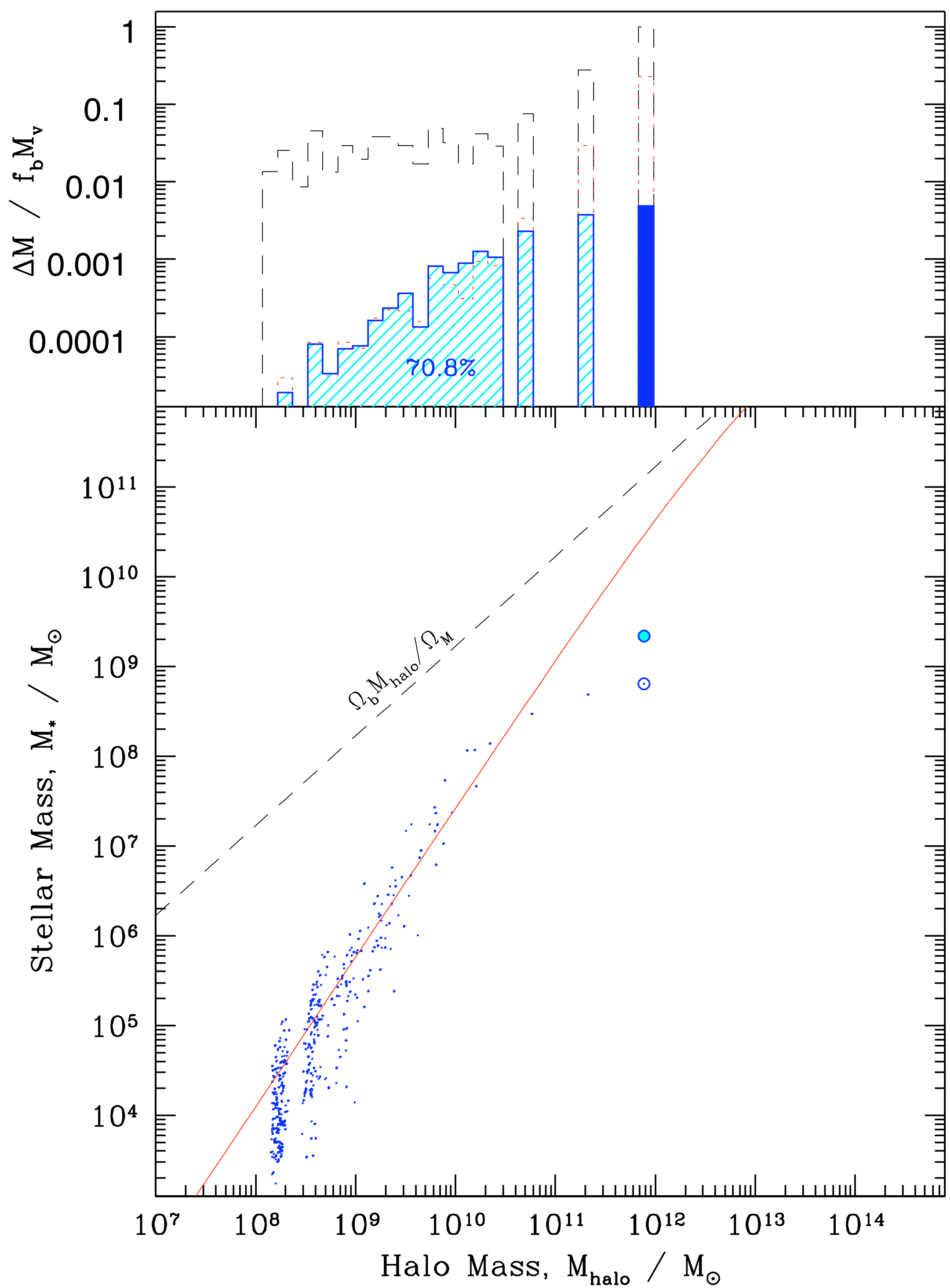

1
0.1
0.01
0.001
0.0001
ΔM / f_b M_v
70.8%
10^11
10^10
10^9
10^8
10^7
10^6
10^5
10^4
Ω_b M_halo/Ω_M
Stellar Mass, M_* / M_⊙
10^7
10^8
10^9
10^10
10^11
10^12
10^13
10^14
Halo Mass, M_halo / M_⊙

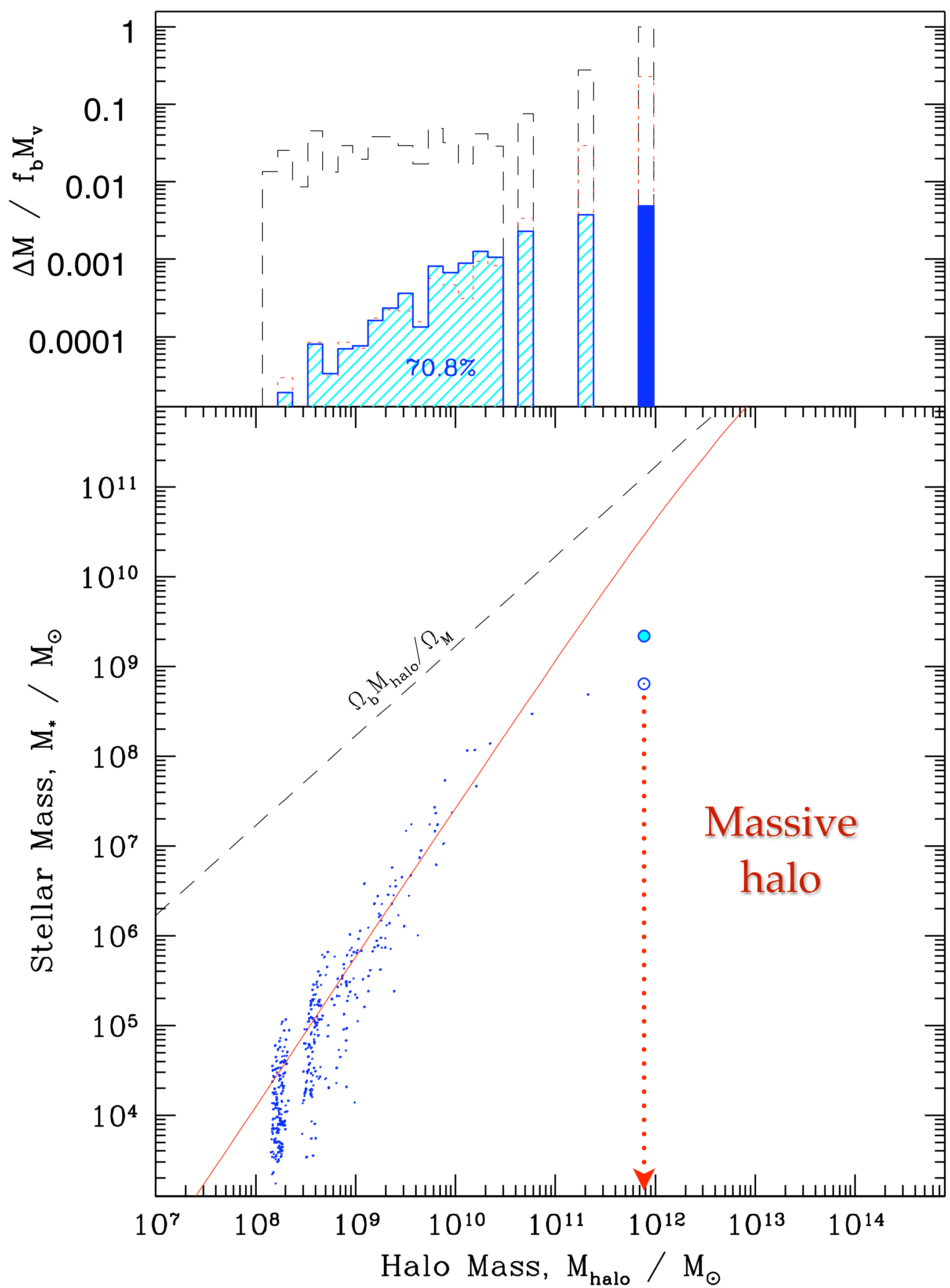

1
0.1
0.01
0.001
0.0001
ΔM / f_b M_v
70.8%
Stellar Mass, M_* / M_⊙
Ω_b M_halo / Ω_M
Massive halo
Halo Mass, M_halo / M_⊙

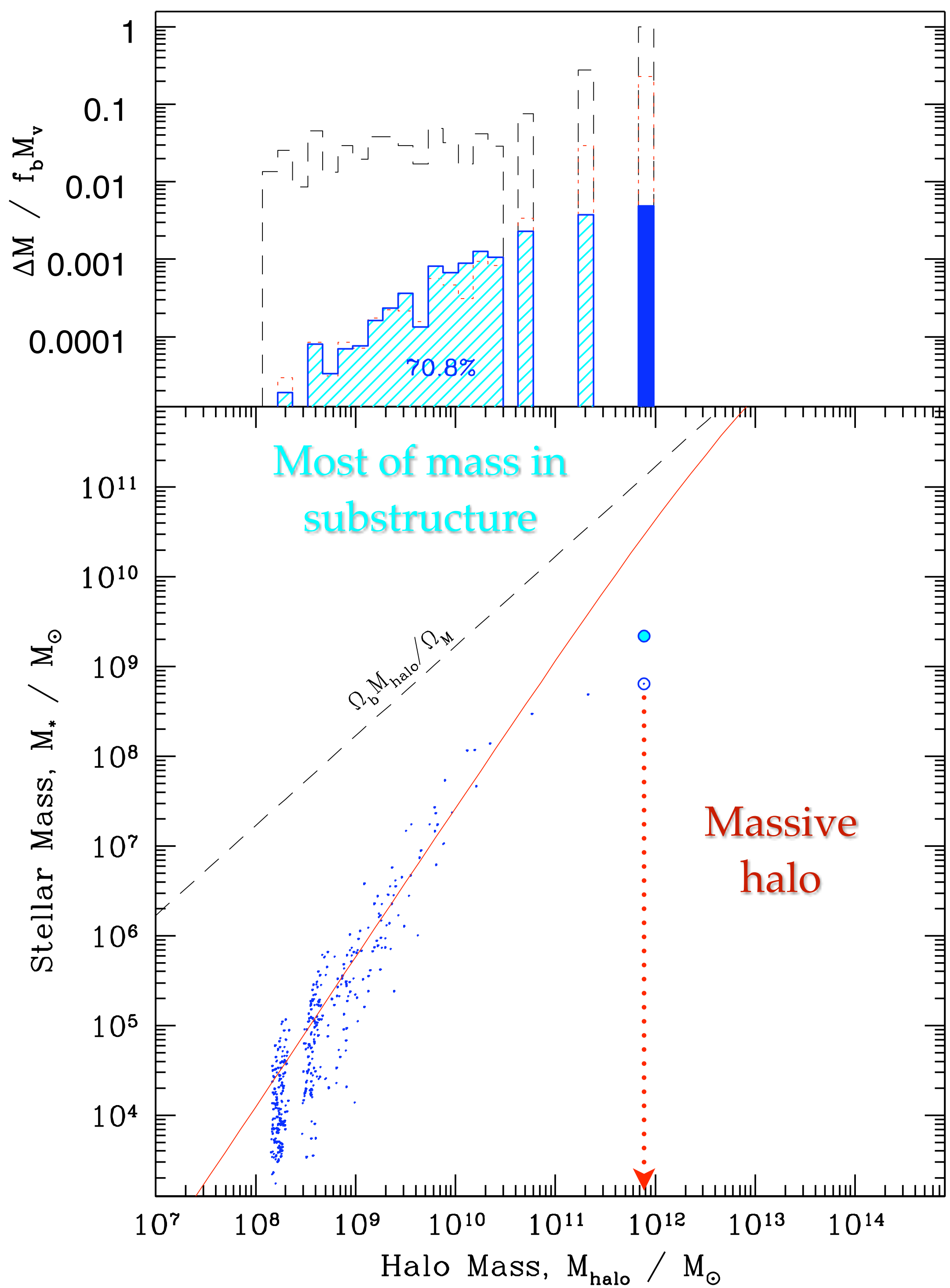

1
0.1
0.01
0.001
0.0001
ΔM / f_b M_v
70.8%
Most of mass in substructure
Massive halo
$\Omega_b M_{halo}/\Omega_M$
10^{11}
10^{10}
10^{9}
10^{8}
10^{7}
10^{6}
10^{5}
10^{4}
Stellar Mass, M_* / $M_\odot$
10^{7}
10^{8}
10^{9}
10^{10}
10^{11}
10^{12}
10^{13}
10^{14}
Halo Mass, M_{halo} / $M_\odot$

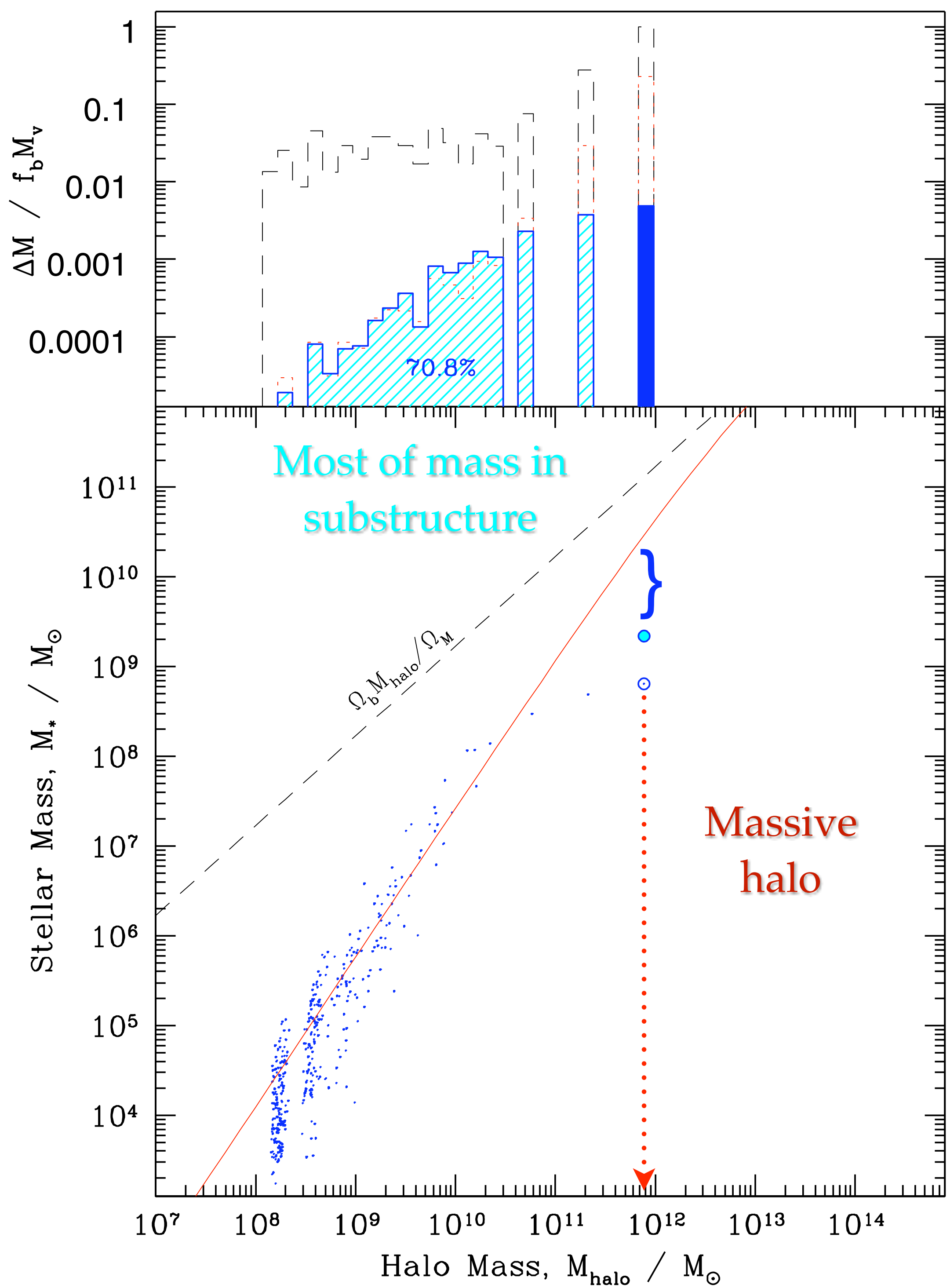

1
0.1
0.01
0.001
0.0001
ΔM / f_b M_v
70.8%
Most of mass in substructure
Massive halo
Ω_b M_halo/Ω_M
Stellar Mass, M_* / M_⊙
Halo Mass, M_halo / M_⊙

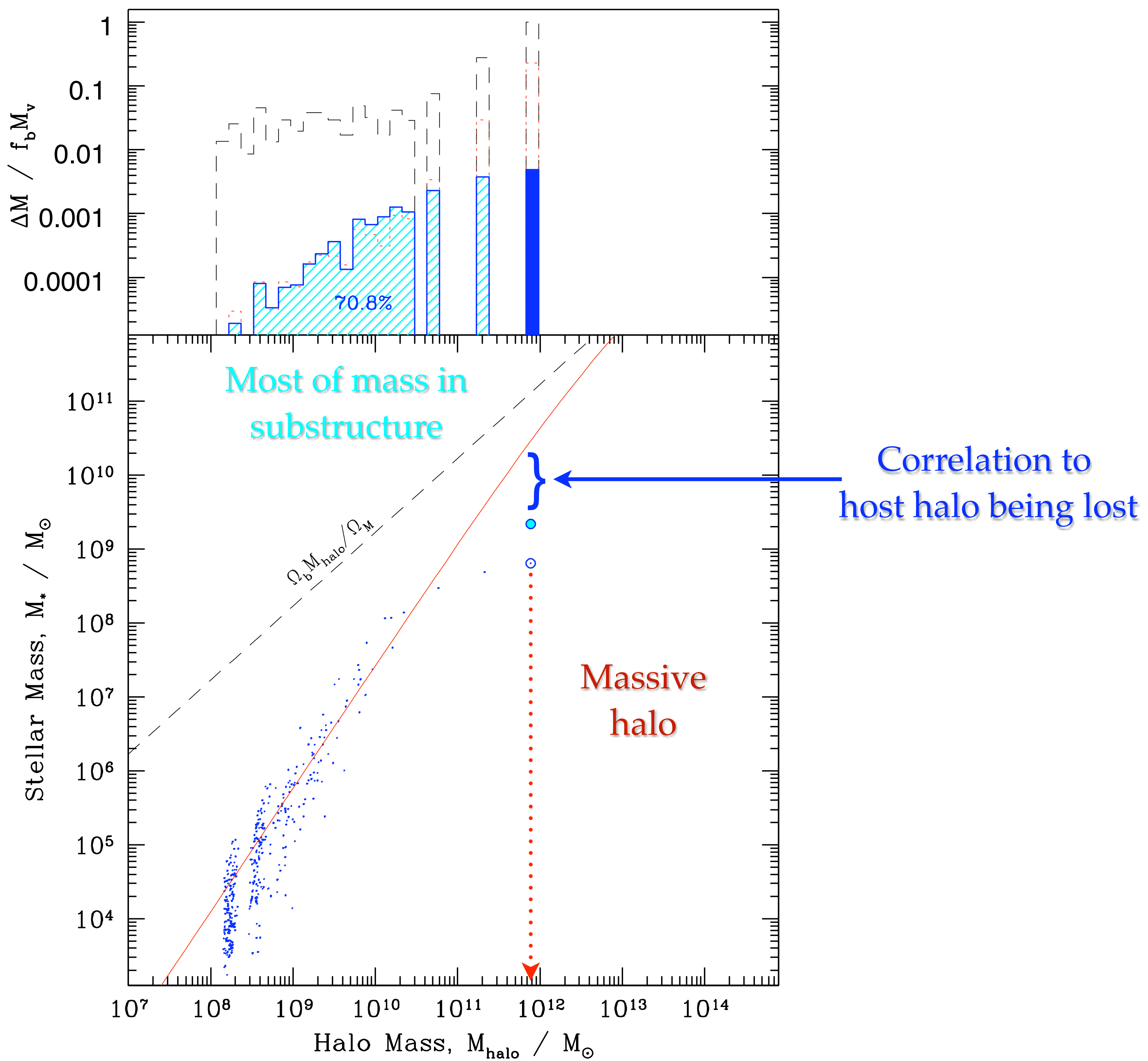
1
0.1
0.01
0.001
0.0001
ΔM / f_b M_v
70.8%
Most of mass in
substructure
Correlation to
host halo being lost
Massive
halo
Ω_b M_halo / Ω_M
Stellar Mass, M_* / M_⊙
10^11
10^10
10^9
10^8
10^7
10^6
10^5
10^4
10^7 10^8 10^9 10^10 10^11 10^12 10^13 10^14
Halo Mass, M_halo / M_⊙

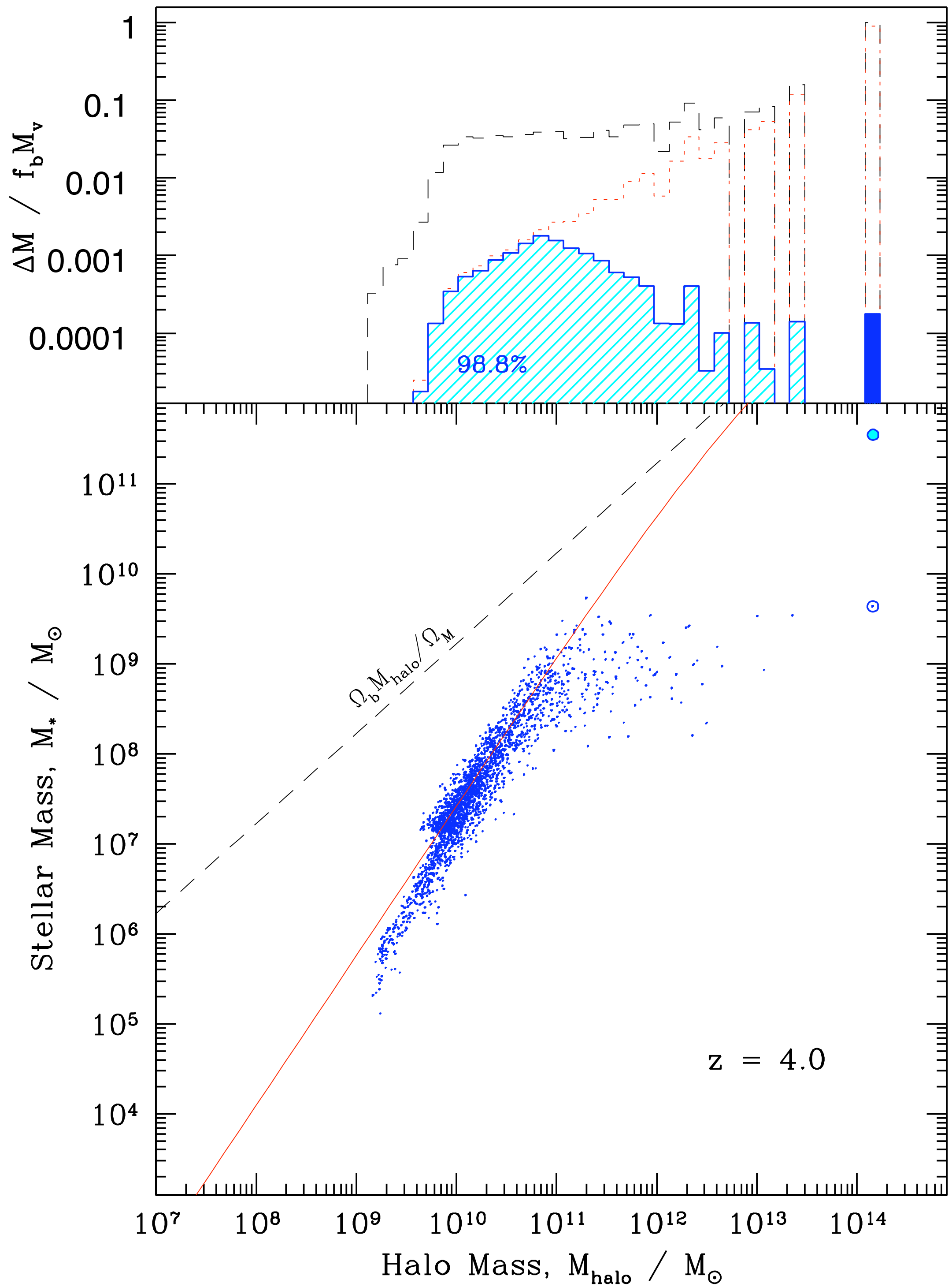

1
0.1
0.01
0.001
0.0001
$\Delta M / f_b M_v$
98.8%
10^{11}
10^{10}
10^9
10^8
10^7
10^6
10^5
10^4
Stellar Mass, M_* / $M_\odot$
$\Omega_b M_{halo} / \Omega_M$
z = 4.0
10^7 10^8 10^9 10^{10} 10^{11} 10^{12} 10^{13} 10^{14}
Halo Mass, M_{halo} / $M_\odot$

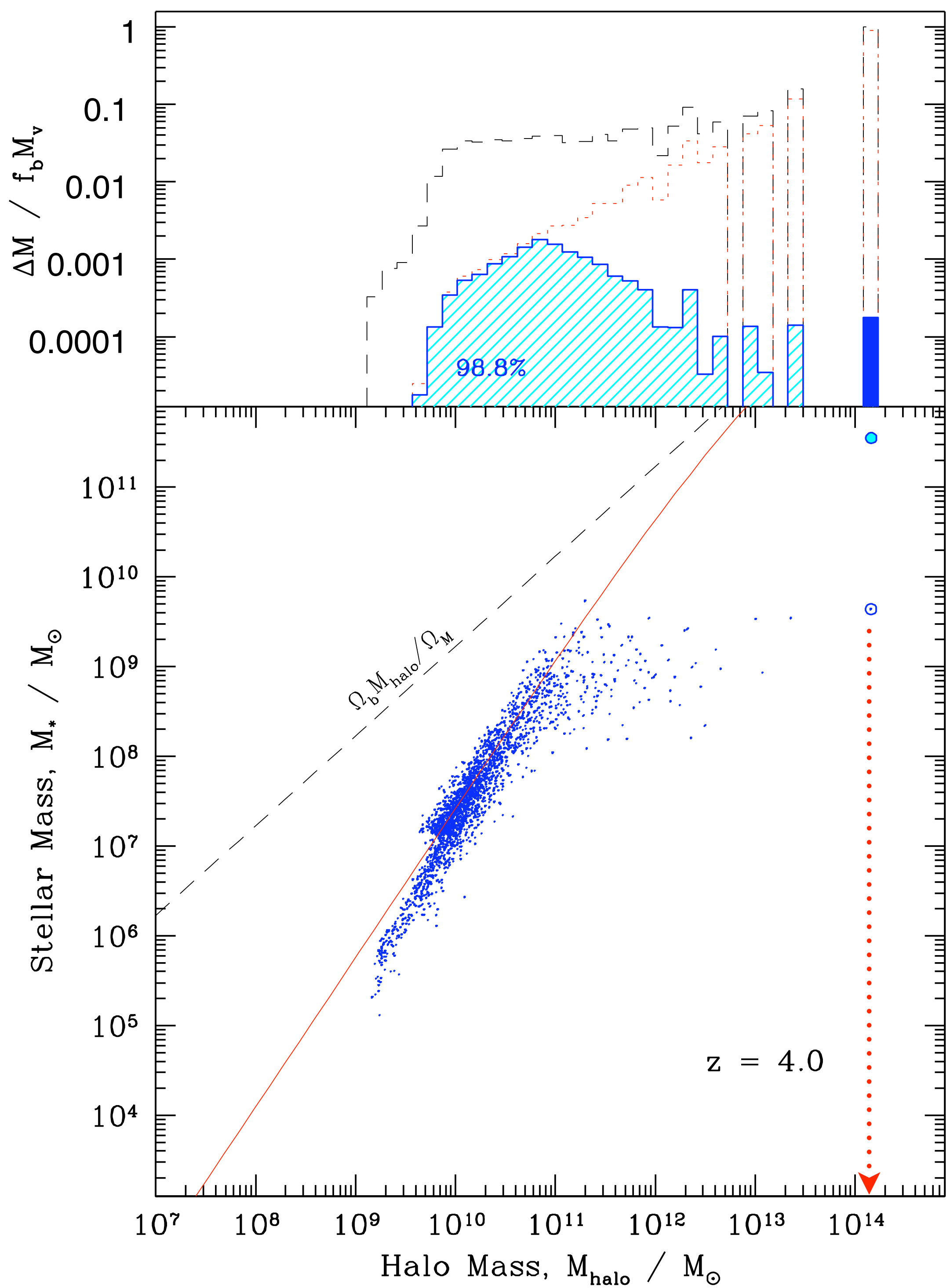

Cluster Mass

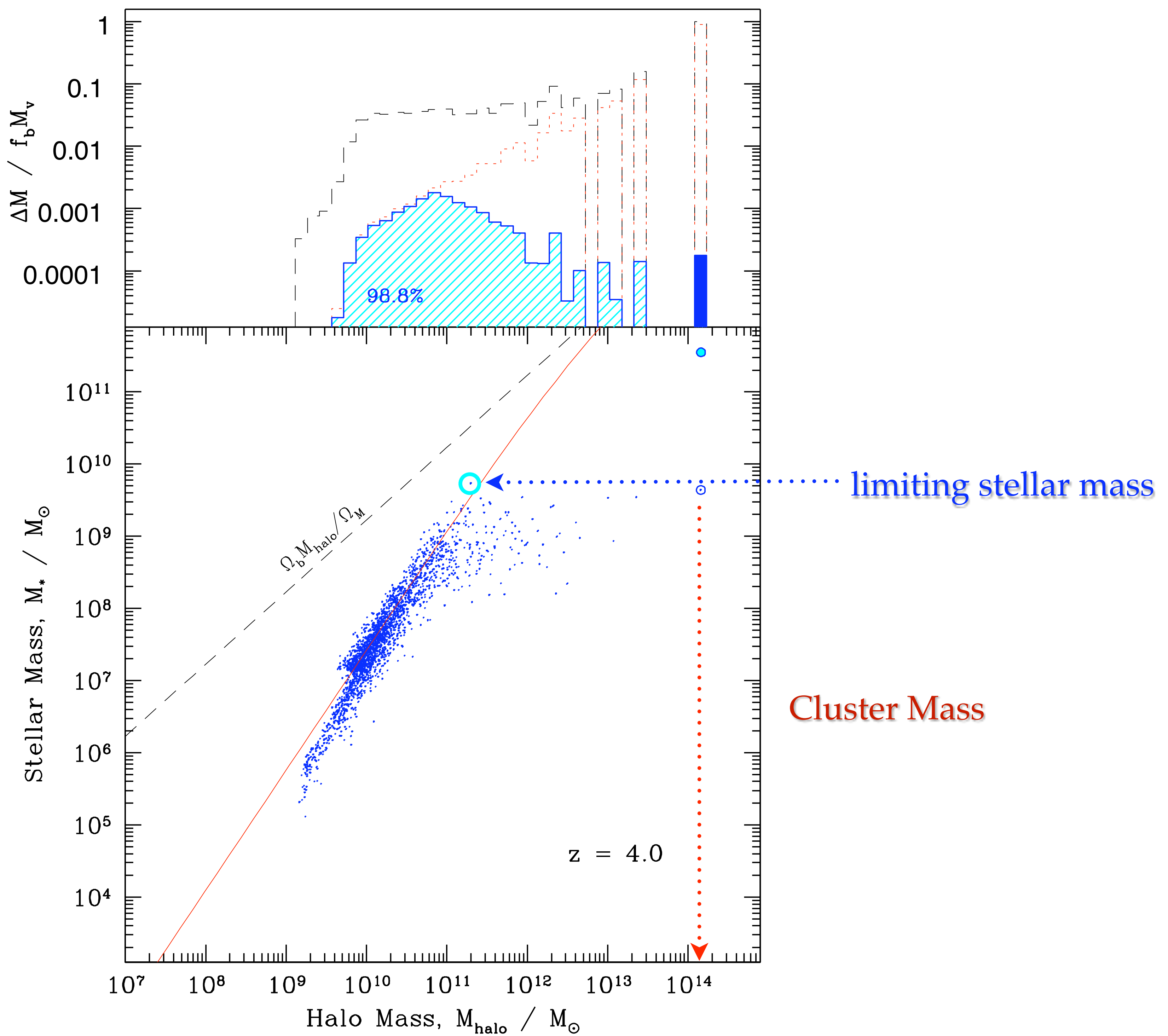

1
0.1
0.01
0.001
0.0001
ΔM / f_b M_v
98.8%
10^11
10^10
10^9
10^8
10^7
10^6
10^5
10^4
Stellar Mass, M_* / M_⊙
Ω_b M_halo / Ω_M
z = 4.0
10^7
10^8
10^9
10^10
10^11
10^12
10^13
10^14
Halo Mass, M_halo / M_⊙
limiting stellar mass
Cluster Mass

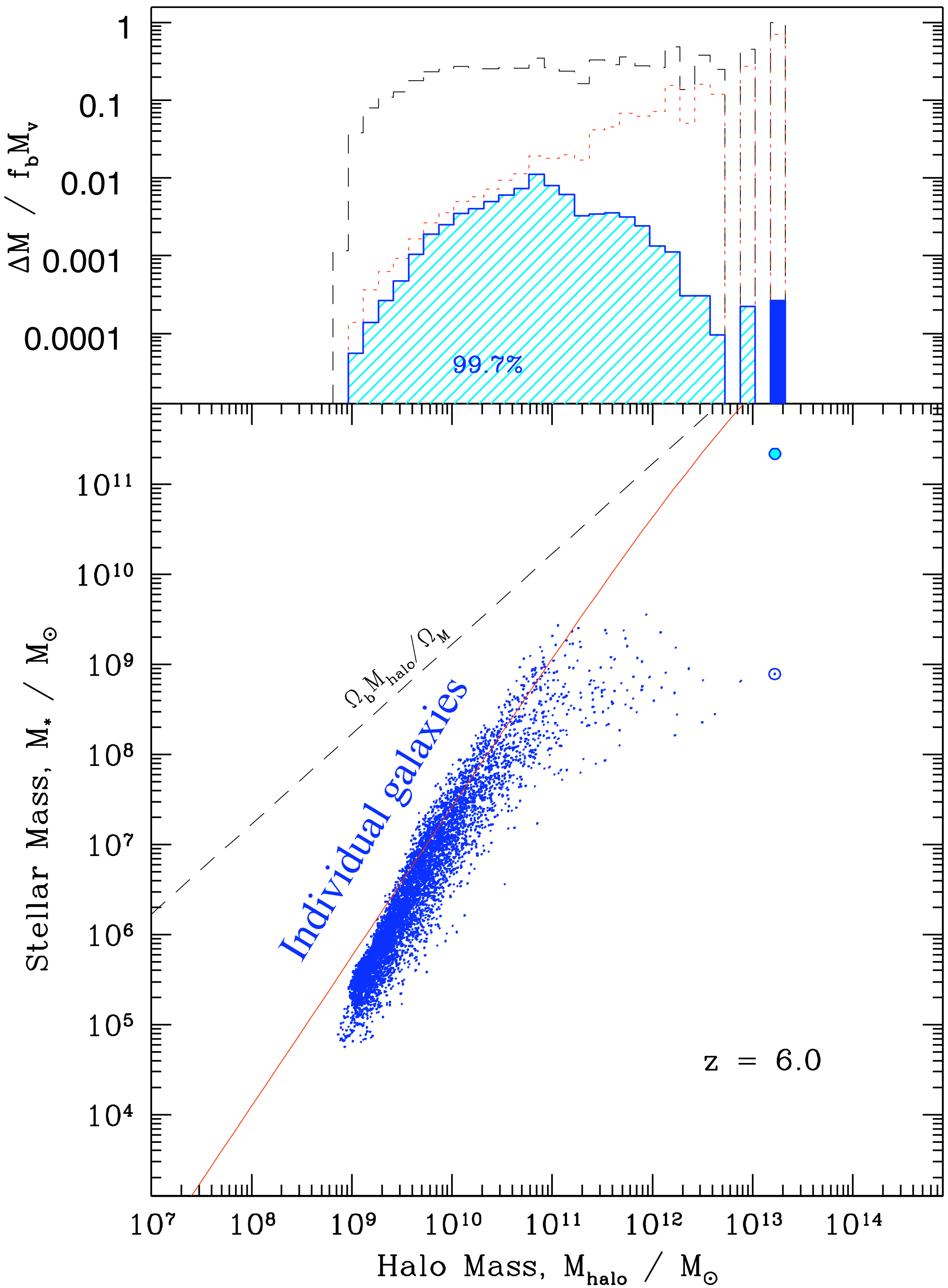

1
0.1
0.01
0.001
0.0001
ΔM / f_b M_v
99.7%
Individual galaxies
Ω_b M_halo/Ω_M
z = 6.0
Stellar Mass, M_* / M_⊙
Halo Mass, M_halo / M_⊙

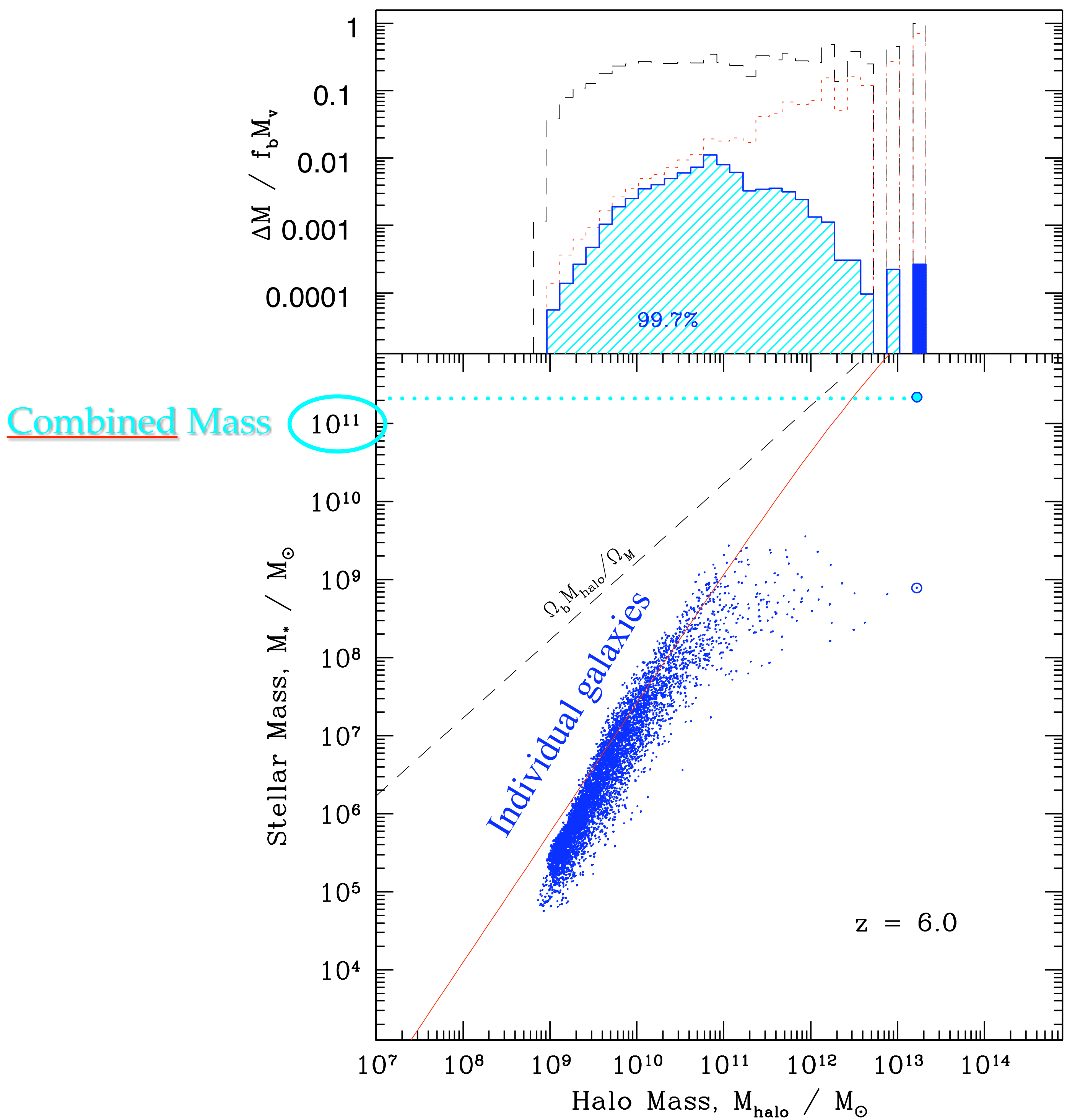

Combined Mass
$\Delta M / f_b M_v$
1
0.1
0.01
0.001
0.0001
99.7%
10^{11}
10^{10}
10^{9}
10^{8}
10^{7}
10^{6}
10^{5}
10^{4}
$\Omega_b M_{halo}/\Omega_M$
Individual galaxies
Stellar Mass, $M_* / M_\odot$
z = 6.0
10^{7} 10^{8} 10^{9} 10^{10} 10^{11} 10^{12} 10^{13} 10^{14}
Halo Mass, $M_{halo} / M_\odot$

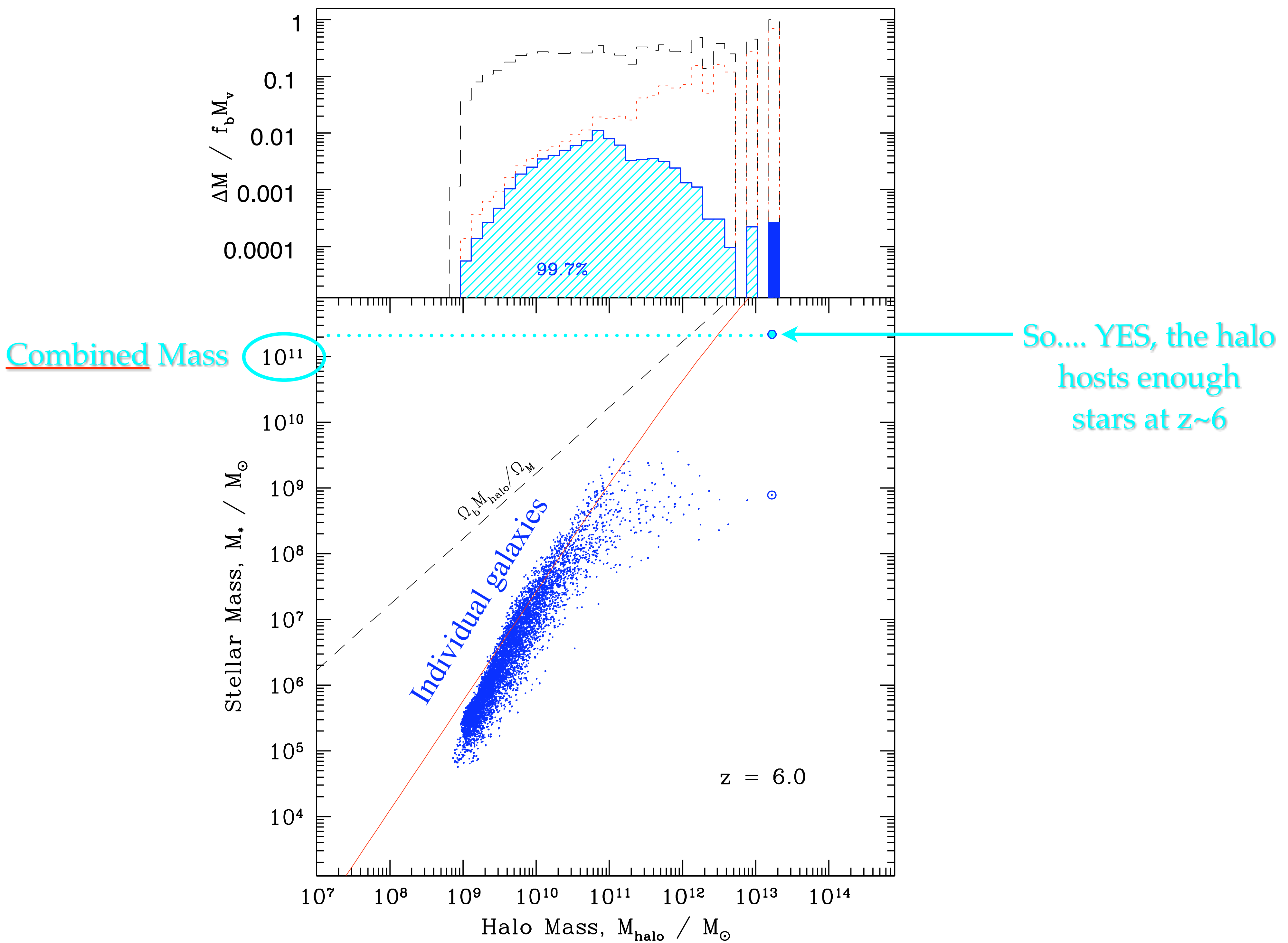

Combined Mass
So.... YES, the halo hosts enough stars at z~6
99.7%
Individual galaxies
$\Omega_b M_{halo}/\Omega_M$
z = 6.0
ΔM / $f_b M_v$
Stellar Mass, M_* / $M_\odot$
Halo Mass, M_{halo} / $M_\odot$

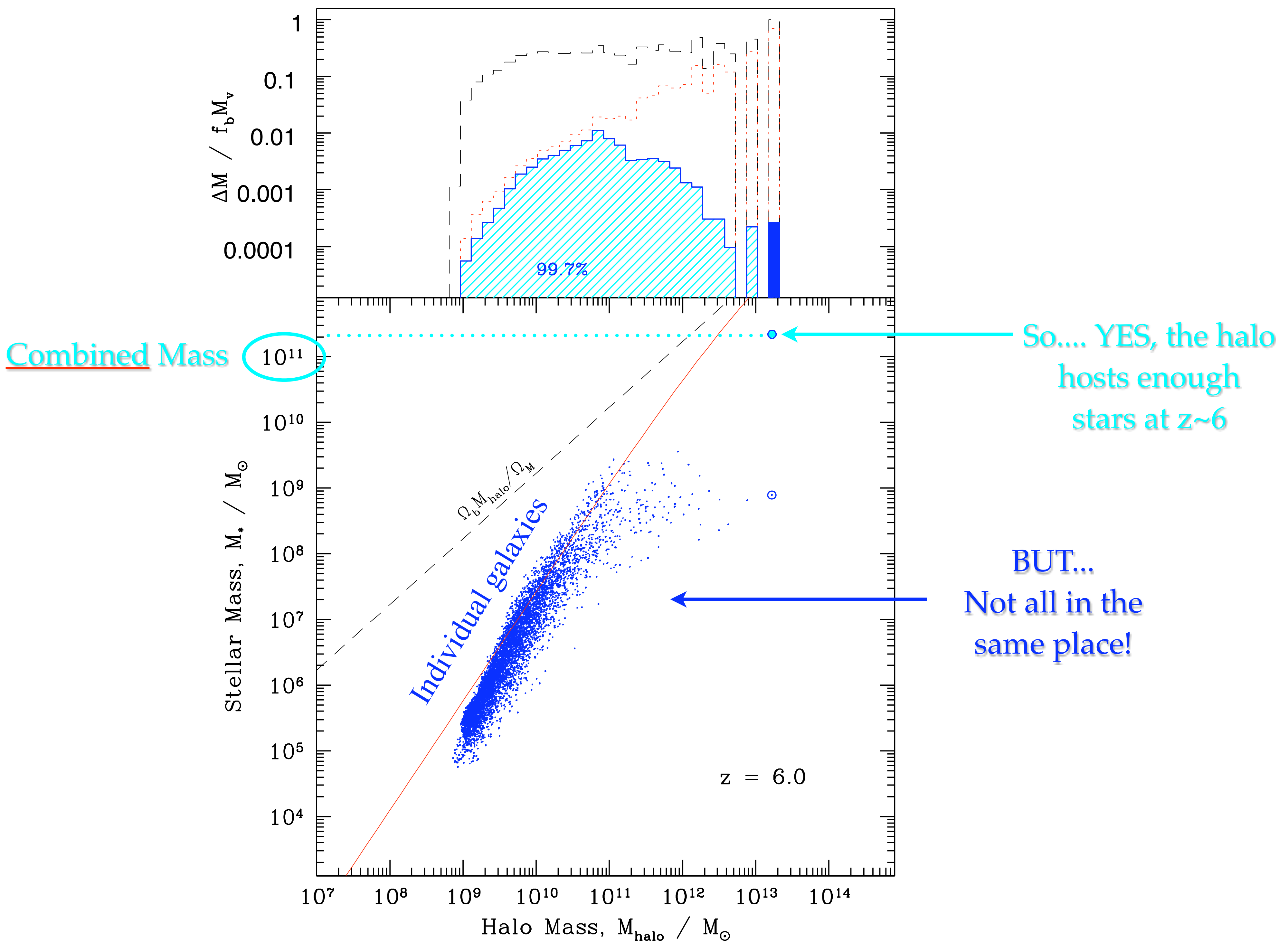

Combined Mass
So.... YES, the halo hosts enough stars at z~6
BUT... Not all in the same place!
Individual galaxies
99.7%
$\Omega_b M_{halo}/\Omega_M$
z = 6.0
ΔM / $f_b M_v$
Stellar Mass, M_* / $M_\odot$
Halo Mass, M_{halo} / $M_\odot$
1
0.1
0.01
0.001
0.0001
10^{11}
10^{10}
10^9
10^8
10^7
10^6
10^5
10^4
10^7 10^8 10^9 10^{10} 10^{11} 10^{12} 10^{13} 10^{14}

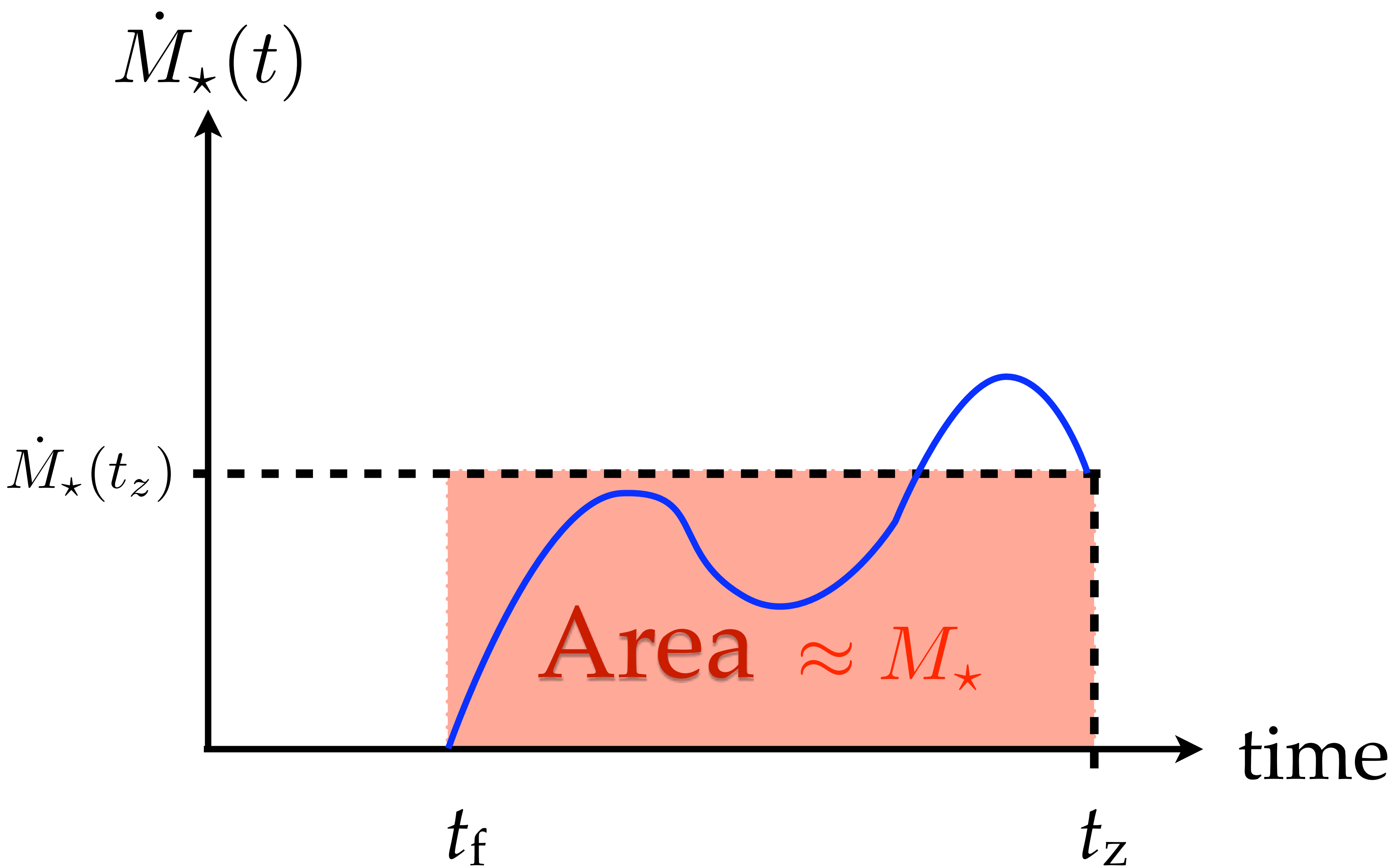

$\dot{M}_\star(t)$
$\dot{M}_\star(t_z)$
Area $\approx M_\star$
time
$t_{\rm f}$
$t_{\rm z}$

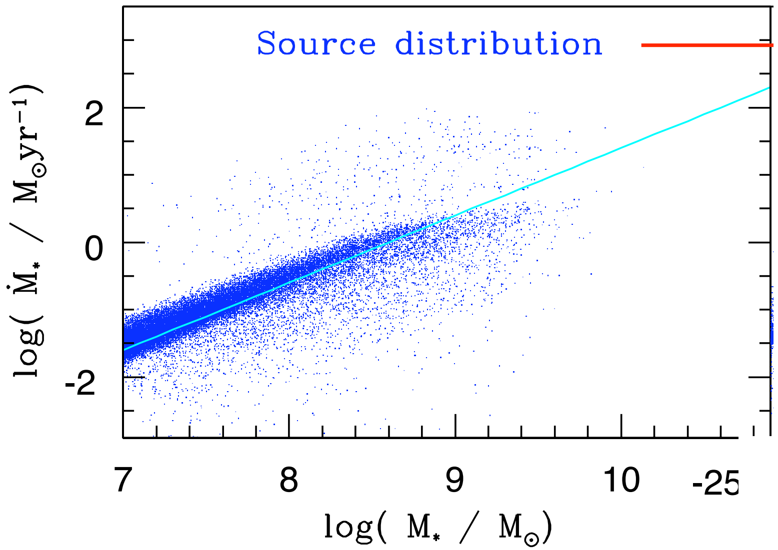

Source distribution
log($\dot{M}_*$ / $M_\odot yr^{-1}$)
2
0
-2
7
8
9
10
-25
log(M_* / $M_\odot$)

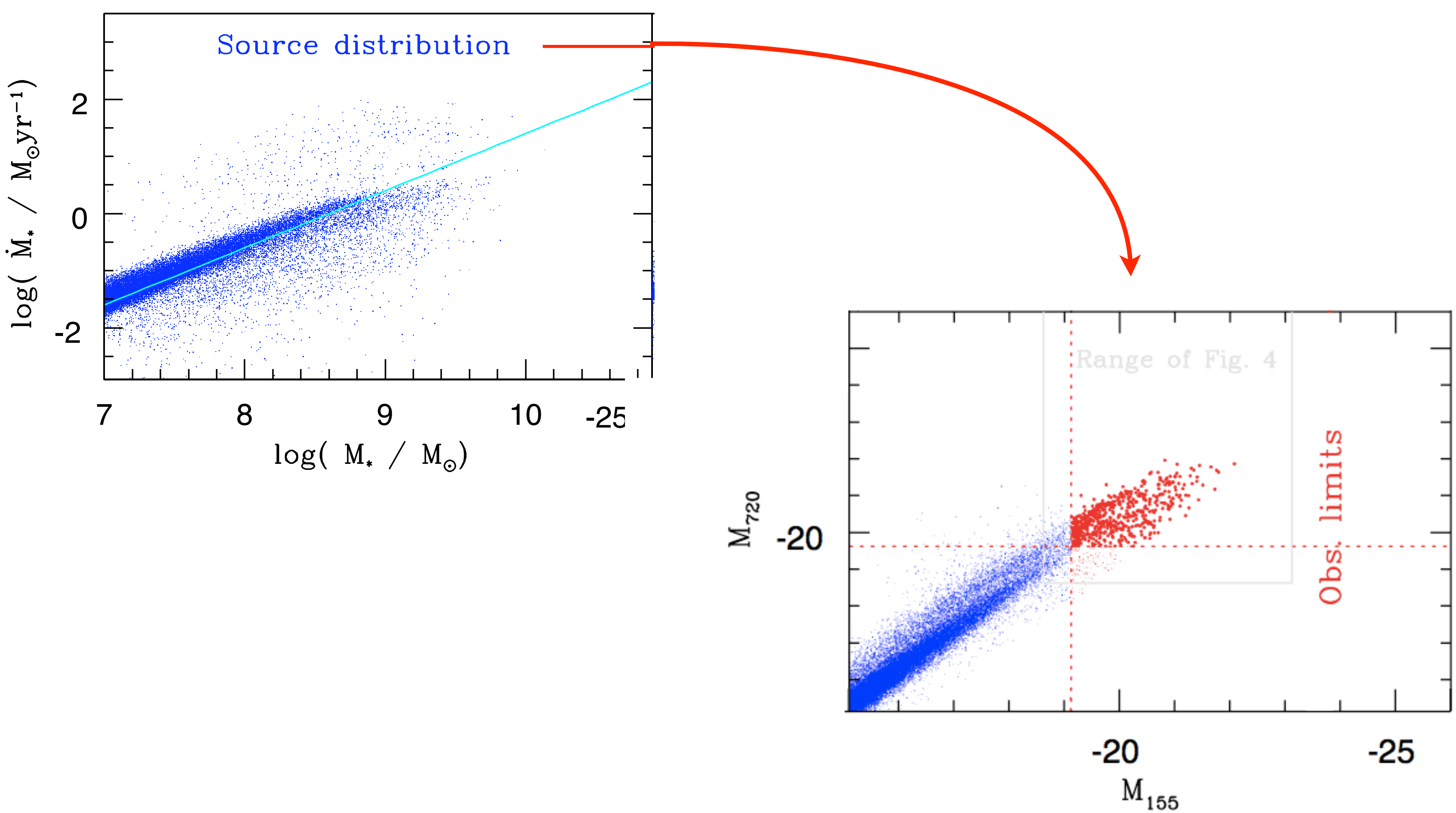
Source distribution
log(Ṁ$_*$ / M$_\odot$yr^{-1})
log(M$_*$ / M$_\odot$)
2
0
-2
7
8
9
10
-25
Range of Fig. 4
Obs. limits
M$_{720}$
-20
M$_{155}$
-20
-25

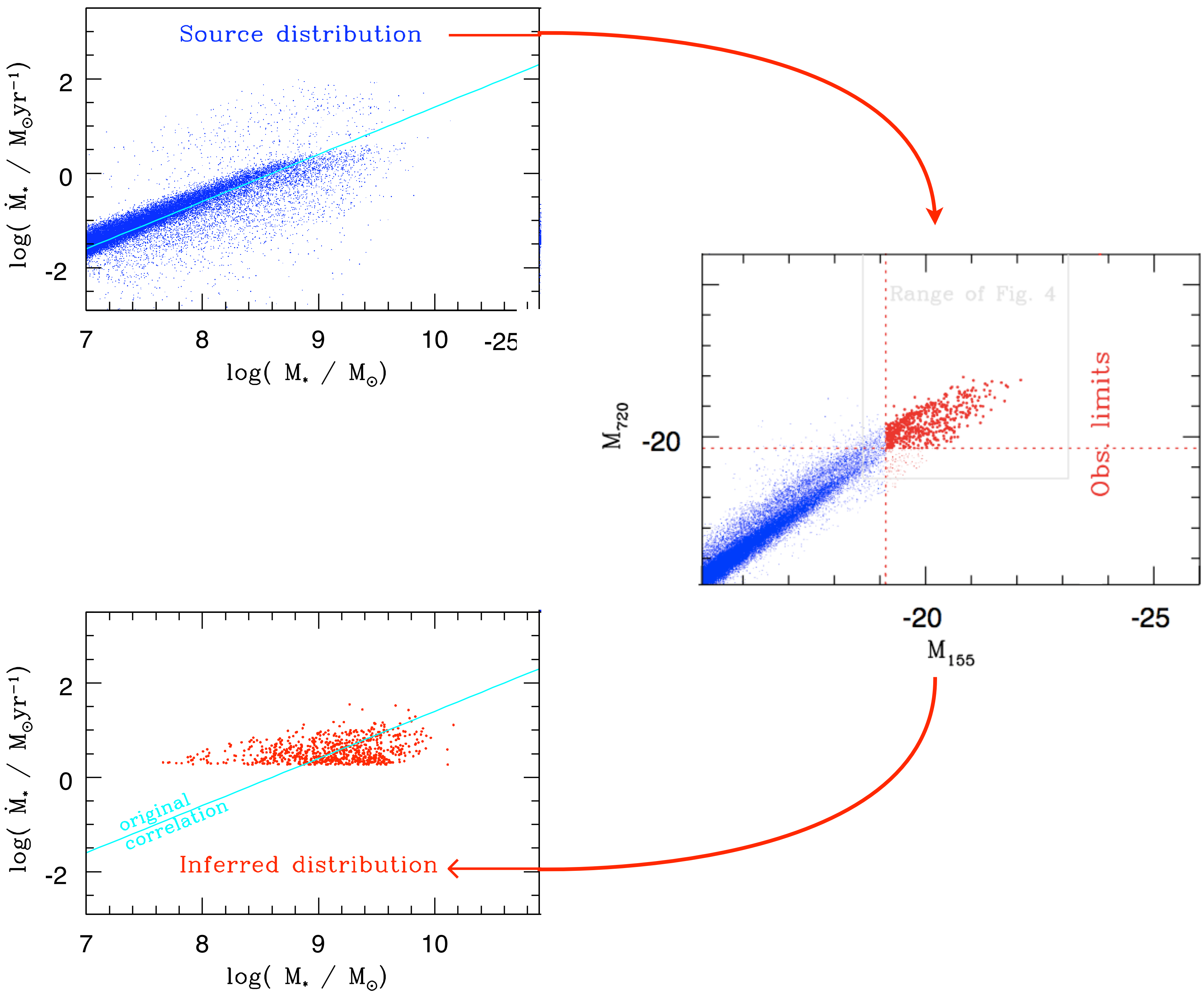

Source distribution
log(Ṁ* / M⊙yr⁻¹)
log(M* / M⊙)
Range of Fig. 4
Obs. limits
M720
M155
original correlation
Inferred distribution

Correlations. Very dangerous...

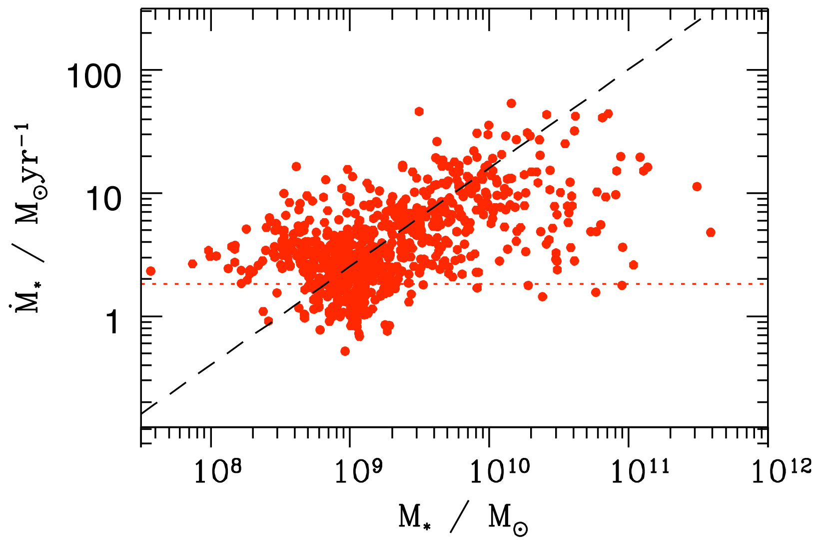

Correlations. Very dangerous...

...you go first!

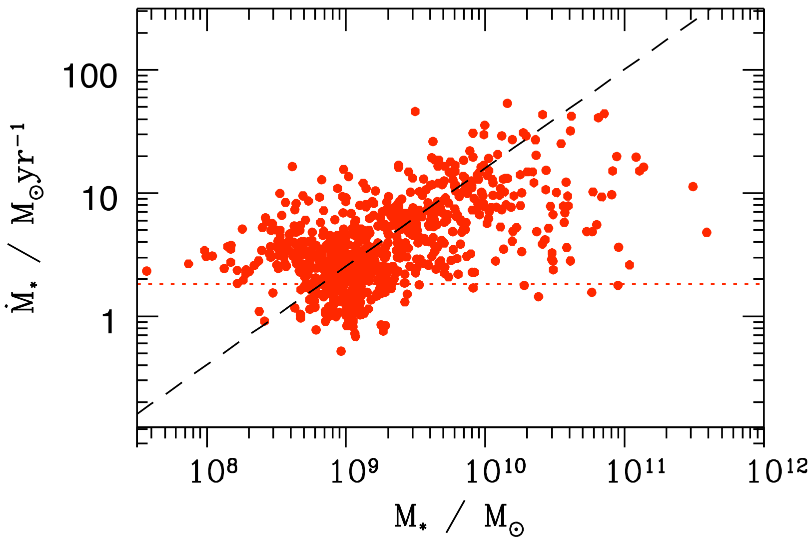

Correlations. Very dangerous...

...you go first!

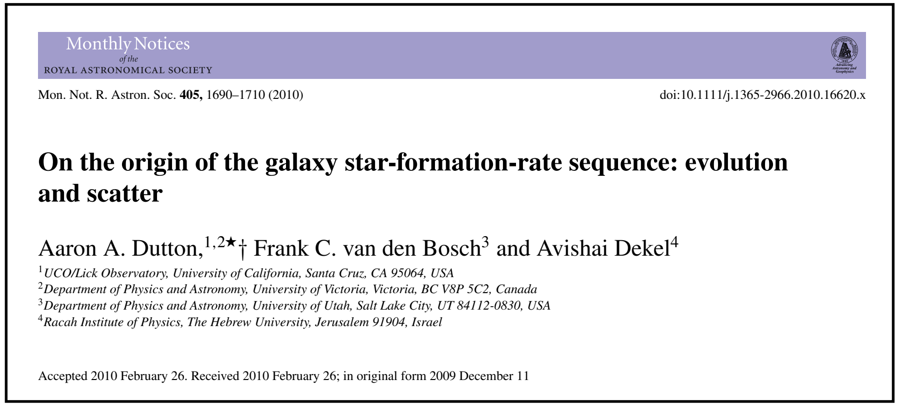

Monthly Notices of the ROYAL ASTRONOMICAL SOCIETY

Mon. Not. R. Astron. Soc. **405,** 1690–1710 (2010) doi:10.1111/j.1365-2966.2010.16620.x

On the origin of the galaxy star-formation-rate sequence: evolution and scatter

Aaron A. Dutton,[1,2★†] Frank C. van den Bosch[3] and Avishai Dekel[4]

[1]*UCO/Lick Observatory, University of California, Santa Cruz, CA 95064, USA*
[2]*Department of Physics and Astronomy, University of Victoria, Victoria, BC V8P 5C2, Canada*
[3]*Department of Physics and Astronomy, University of Utah, Salt Lake City, UT 84112-0830, USA*
[4]*Racah Institute of Physics, The Hebrew University, Jerusalem 91904, Israel*

Accepted 2010 February 26. Received 2010 February 26; in original form 2009 December 11

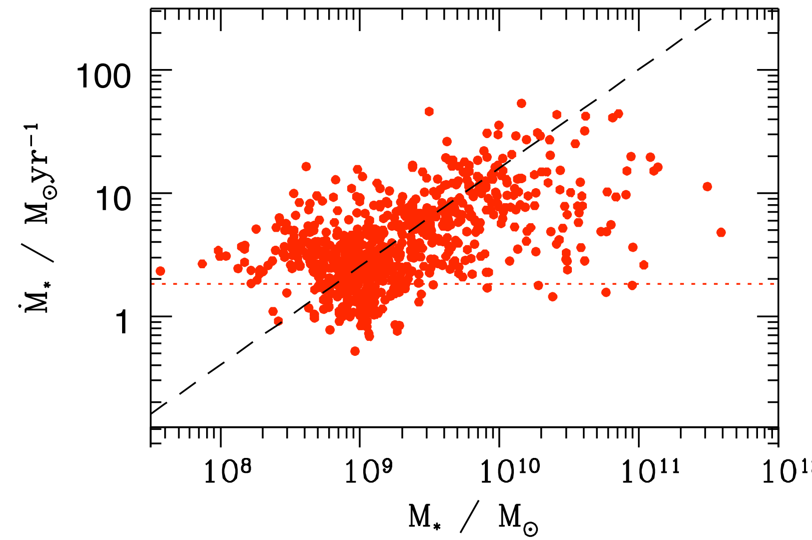

Correlations. Very dangerous...

...you go first!

Monthly Notices of the ROYAL ASTRONOMICAL SOCIETY

Mon. Not. R. Astron. Soc. **405,** 1690–1710 (2010) doi:10.1111/j.1365-2966.2010.16620.x

On the origin of the galaxy star-formation-rate sequence: evolution and scatter

Aaron A. Dutton,[1,2]★† Frank C. van den Bosch[3] and Avishai Dekel[4]

[1] *UCO/Lick Observatory, University of California, Santa Cruz, CA 95064, USA*
[2] *Department of Physics and Astronomy, University of Victoria, Victoria, BC V8P 5C2, Canada*
[3] *Department of Physics and Astronomy, University of Utah, Salt Lake City, UT 84112-0830, USA*
[4] *Racah Institute of Physics, The Hebrew University, Jerusalem 91904, Israel*

Accepted 2010 February 26. Received 2010 February 26; in original form 2009 December 11

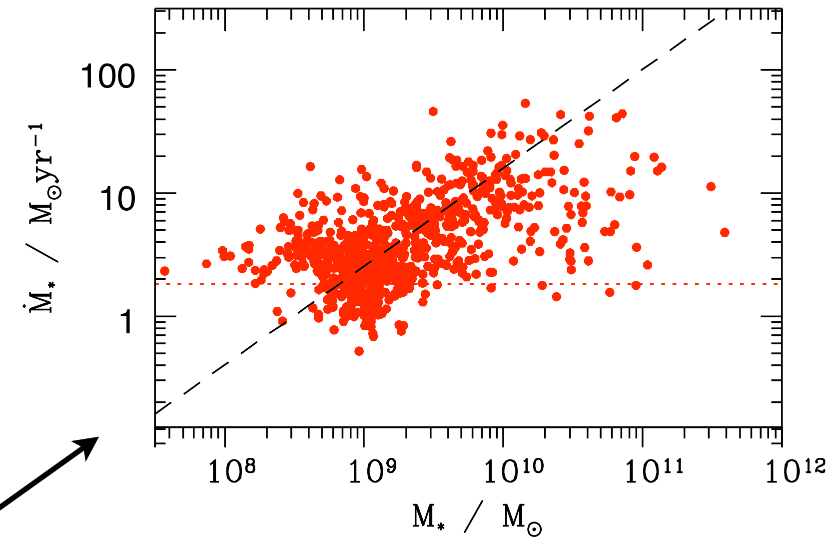

Dutton et al. (2010) think we can see the following correlation:

$$\frac{\dot{M}_\star}{M_\star} \approx \frac{1}{0.62\ \mathrm{Gyr}} \left(\frac{M_\star}{10^{10} M_\odot}\right)^{-0.2}$$

Correlations. Very dangerous...

...you go first!

Monthly Notices of the ROYAL ASTRONOMICAL SOCIETY
Mon. Not. R. Astron. Soc. **405,** 1690–1710 (2010) doi:10.1111/j.1365-2966.2010.16620.x

On the origin of the galaxy star-formation-rate sequence: evolution and scatter

Aaron A. Dutton,[1,2]⋆† Frank C. van den Bosch[3] and Avishai Dekel[4]
[1]*UCO/Lick Observatory, University of California, Santa Cruz, CA 95064, USA*
[2]*Department of Ph*
[3]*Department of Ph*
[4]*Racah Institute of*

Accepted 2010 Feb

Mon. Not. R. Astron. Soc. **000**, 1–4 (2010) Printed 6 September 2010 (MN LaTeX style file v2.2)

Understanding the specific star formation rate of high redshift galaxies: the case for two modes of star formation

Sadegh Khochfar,[1]⋆ Joseph Silk,[2]
[1] *Max-Planck-Institute for Extraterrestrial Physics, Giessenbachstrasse 1, 85748 Garching, Germany*
[2] *Department of Physics, Denys Wilkinson Building, Keble Road, Oxford OX1 3RH, United Kingdom*

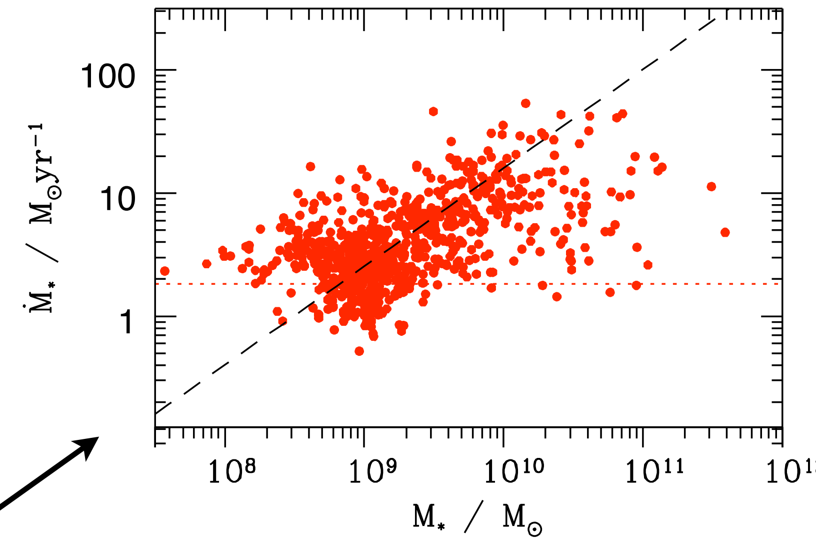

Dutton et al. (2010) think we can see the following correlation:

$$\frac{\dot{M}_\star}{M_\star} \approx \frac{1}{0.62\ \mathrm{Gyr}} \left(\frac{M_\star}{10^{10} M_\odot}\right)^{-0.2}$$

Putting the same data on different axes,
Kockfar & Silk (2009) conclude something different:

Correlations. Very dangerous...

...you go first!

Monthly Notices of the ROYAL ASTRONOMICAL SOCIETY

Mon. Not. R. Astron. Soc. **405,** 1690–1710 (2010) doi:10.1111/j.1365-2966.2010.16620.x

On the origin of the galaxy star-formation-rate sequence: evolution and scatter

Aaron A. Dutton,[1,2★]† Frank C. van den Bosch[3] and Avishai Dekel[4]

[1] *UCO/Lick Observatory, University of California, Santa Cruz, CA 95064, USA*
[2] *Department of Ph*
[3] *Department of Ph*
[4] *Racah Institute of*

Accepted 2010 Feb

Mon. Not. R. Astron. Soc. **000**, 1–4 (2010) Printed 6 September 2010 (MN LATEX style file v2.2)

Understanding the specific star formation rate of high redshift galaxies: the case for two modes of star formation

Sadegh Khochfar,[1★] Joseph Silk,[2]
[1] *Max-Planck-Institute for Extraterrestrial Physics, Giessenbachstrasse 1, 85748 Garching, Germany*
[2] *Department of Physics, Denys Wilkinson Building, Keble Road, Oxford OX1 3RH, United Kingdom*

Dutton et al. (2010) think we can see the following correlation:

$$\frac{\dot{M}_\star}{M_\star} \approx \frac{1}{0.62\ \mathrm{Gyr}} \left(\frac{M_\star}{10^{10} M_\odot}\right)^{-0.2}$$

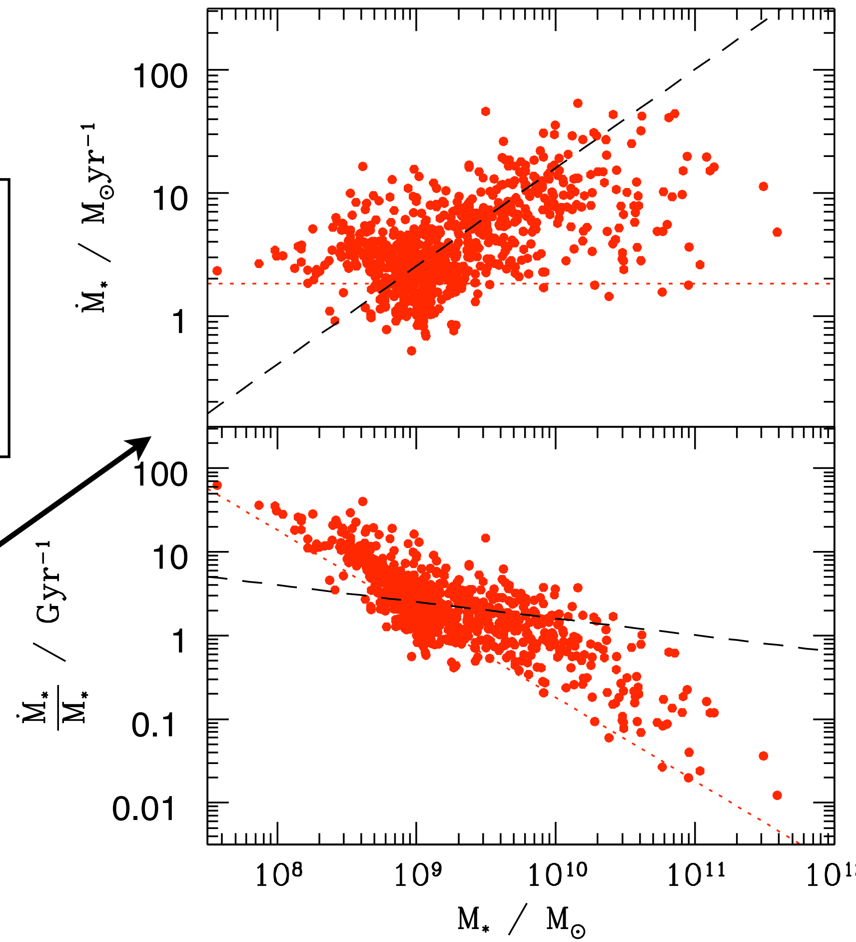

Putting the same data on different axes,
Kockfar & Silk (2009) conclude something different:

Correlations. Very dangerous...

...you go first!

Monthly Notices of the ROYAL ASTRONOMICAL SOCIETY

Mon. Not. R. Astron. Soc. **405,** 1690–1710 (2010) doi:10.1111/j.1365-2966.2010.16620.x

On the origin of the galaxy star-formation-rate sequence: evolution and scatter

Aaron A. Dutton,[1,2★†] Frank C. van den Bosch[3] and Avishai Dekel[4]

[1] *UCO/Lick Observatory, University of California, Santa Cruz, CA 95064, USA*
[2] *Department of Ph*
[3] *Department of Ph*
[4] *Racah Institute of*

Accepted 2010 Feb

Mon. Not. R. Astron. Soc. **000**, 1–4 (2010) Printed 6 September 2010 (MN LaTeX style file v2.2)

Understanding the specific star formation rate of high redshift galaxies: the case for two modes of star formation

Sadegh Khochfar,[1★] Joseph Silk,[2]

[1] *Max-Planck-Institute for Extraterrestrial Physics, Giessenbachstrasse 1, 85748 Garching, Germany*
[2] *Department of Physics, Denys Wilkinson Building, Keble Road, Oxford OX1 3RH, United Kingdom*

Dutton et al. (2010) think we can see the following correlation:

$$\frac{\dot{M}_\star}{M_\star} \approx \frac{1}{0.62\ \mathrm{Gyr}} \left(\frac{M_\star}{10^{10} M_\odot}\right)^{-0.2}$$

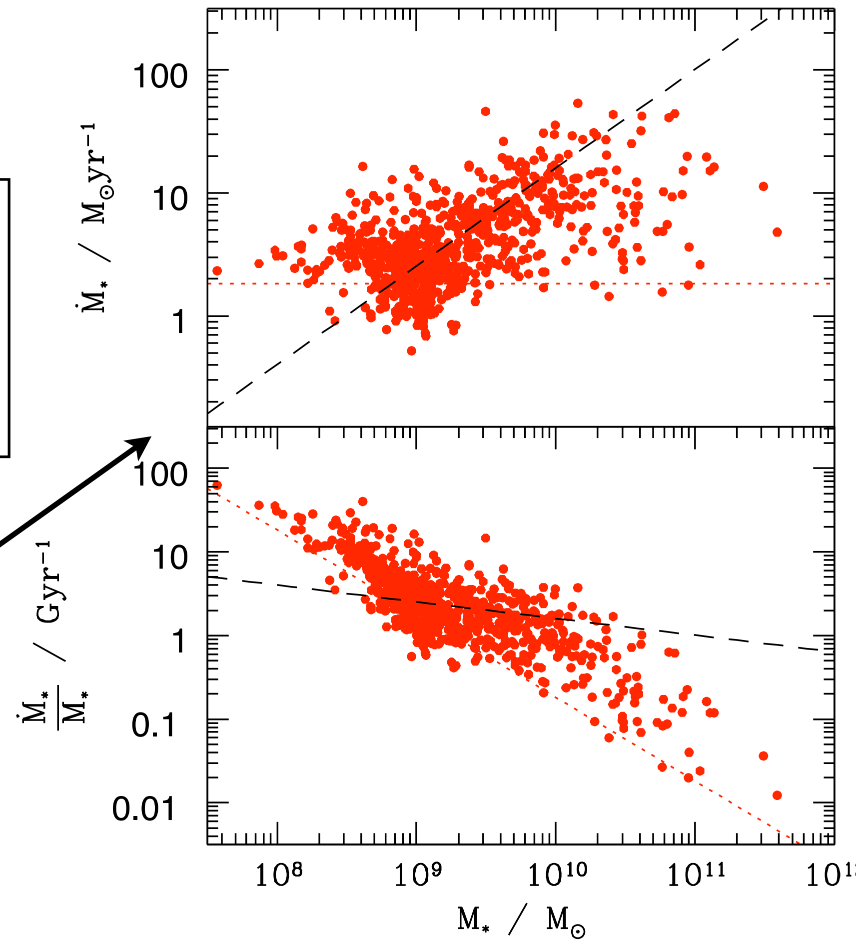

Putting the same data on different axes,
Kockfar & Silk (2009) conclude something different:

“To recover the strong observed mass-dependence of the SSFR, we propose ...”

Mon. Not. R. Astron. Soc. **000**, 1–?? (2002) Printed 28 August 2012 (MN LaTeX style file v2.2)

Evidence for Significant Growth in the Stellar Mass of Brightest Cluster Galaxies over the Past 10 Billion Years.

C. Lidman,[1⋆] J. Suherli,[1,2] A. Muzzin,[3] G. Wilson,[4] R. Demarco,[5] S. Brough,[1] A. Rettura,[4], J. Cox,[4] A. DeGroot,[4] H. K. C. Yee,[6] D. Gilbank,[7] H. Hoekstra,[3] M. Balogh,[8] E. Ellingson,[9] A. Hicks,[10] J. Nantais,[5] A. Noble,[11] M. Lacy,[12] J. Surace,[13] T. Webb[10]

[1] *Australian Astronomical Observatory, PO Box 296, Epping NSW 1710, Australia*
[2] *Bosscha Observatory, Institut Teknologi Bandung, Lembang, Bandung, West Java, Indonesia*
[3] *Leiden Observatory, Leiden University, PO Box 9513, 2300 RA Leiden, The Netherlands*
[4] *Department of Physics and Astronomy, University of California, Riverside, CA 92521*
[5] *Department of Astronomy, Universidad de Concepcion, Casilla 160-C, Concepcion, Chile*
[6] *Department. of Astronomy & Astrophysics, University of Toronto, 50 St. George St., Toronto, Ontario, Canada, M5S 3H4 TBA*
[7] *South African Astronomical Observatory, PO Box 9, Observatory, 7935, South Africa*
[8] *Department of Physics and Astronomy, University of Waterloo, Waterloo, Ontario N2L 3G1, Canada*
[9] *Center for Astrophysics and Space Astronomy, 389UCB, University of Colorado, Boulder, CO 80309, USA*
[10] *Department of Physics and Astronomy, Michigan State University, East Lansing, MI 48824-2320, USA*
[11] *Department of Physics, McGill University, Montral, QC, Canada*
[12] *North American ALMA Science Center, NRAO Headquarters, 520 Edgemont Road, Charlottesville, VA 22903*
[13] *Spitzer Science Center, California Institute of Technology, 220-6, Pasadena, CA, 91125*

Accepted YYYY Month DD. Received YYYY Month DD

ABSTRACT

Using new and published data, we construct a sample of 160 brightest cluster galaxies (BCGs) spanning the redshift interval $0.03 < z < 1.63$. We use this sample, which covers 70% of the history of the universe, to measure the growth in the stellar mass of BCGs after correcting for the correlation between the stellar mass of the BCG and the mass of the cluster in which it lives. We find that the stellar mass of BCGs increase by a factor of 1.8 ± 0.3 between $z = 0.9$ and $z = 0.2$. Compared to earlier works, our result is closer to the predictions of semi-analytic models. However, BCGs at $z = 0.9$, relative to BCGs at $z = 0.2$, are still a factor of 1.5 more massive than the predictions of these models. Star formation rates in BCGs at $z \sim 1$ are generally too low to result in significant amounts of mass. Instead, it is likely that most of the mass build up occurs through mainly dry mergers in which perhaps half of the mass is lost to the intra-cluster medium of the cluster.

Key words: galaxies: clusters: general – galaxies: evolution – galaxies: high-redshift – cosmology: observations

1 INTRODUCTION

Brightest Cluster Galaxies (BCGs) are amongst the largest, most luminous and most massive galaxies in the universe at the present epoch. Located in the cores of rich galaxy clusters, BCGs are easy to identify, both observationally and in simulations. They can also be observed at a time when the universe was less than a third of its current age. They therefore provide an attractive target for testing our understanding of the processes that drive galaxy evolution, albeit in the most massive galaxies of the universe.

In the hierarchical scenario for the formation of structure in our universe, galaxies start off as small fluctuations in the density of matter and build up their stellar mass over time by converting material accreted from their surroundings into stars and by merging with other galaxies (see Baugh 2006, for a review). In semi-analytic models that use the hierarchical scenario as their foundation, the stellar mass of a BCG increases significantly with time. For example, between redshift $z = 1.0$ (corresponding to a look-back time of 6.7 Gyr) to $z = 0$, the semi-analytic model described in De

⋆ E-mail: clidman@aao.gov.au

Mon. Not. R. Astron. Soc. **000**, 1–?? (2002) Printed 28 August 2012 (MN LaTeX style file v2.2)

Evidence for Significant Growth in the Stellar Mass of Brightest Cluster Galaxies over the Past 10 Billion Years.

C. Lidman,[1⋆] J. Suherli,[1,2] A. Muzzin,[3] G. Wilson,[4] R. Demarco,[5] S. Brough,[1] A. Rettura,[4], J. Cox,[4] A. DeGroot,[4] H. K. C. Yee,[6] D. Gilbank,[7] H. Hoekstra,[3] M. Balogh,[8] E. Ellingson,[9] A. Hicks,[10] J. Nantais,[5] A. Noble,[11] M. Lacy,[12] J. Surace,[13] T. Webb[10]

[1] *Australian Astronomical Observatory, PO Box 296, Epping NSW 1710, Australia*
[2] *Bosscha Observatory, Institut Teknologi Bandung, Lembang, Bandung, West Java, Indonesia*
[3] *Leiden Observatory, Leiden University, PO Box 9513, 2300 RA Leiden, The Netherlands*
[4] *Department of Physics and Astronomy, University of California, Riverside, CA 92521*
[5] *Department of Astronomy, Universidad de Concepcion, Casilla 160-C, Concepcion, Chile*
[6] *Department. of Astronomy & Astrophysics, University of Toronto, 50 St. George St., Toronto, Ontario, Canada, M*
[7] *South African Astronomical Observatory, PO Box 9, Observatory, 7935, South Africa*
[8] *Department of Physics and Astronomy, University of Waterloo, Waterloo, Ontario N2L 3G1, Canada*
[9] *Center for Astrophysics and Space Astronomy, 389UCB, University of Colorado, Boulder, CO 80309, USA*
[10] *Department of Physics and Astronomy, Michigan State University, East Lansing, MI 48824-2320, USA*
[11] *Department of Physics, McGill University, Montral, QC, Canada*
[12] *North American ALMA Science Center, NRAO Headquarters, 520 Edgemont Road, Charlottesville, VA 22903*
[13] *Spitzer Science Center, California Institute of Technology, 220-6, Pasadena, CA, 91125*

Accepted YYYY Month DD. Received YYYY Month DD

ABSTRACT

Using new and published data, we construct a sample of 160 brightest c
(BCGs) spanning the redshift interval $0.03 < z < 1.63$. We use this
covers 70% of the history of the universe, to measure the growth in the
BCGs after correcting for the correlation between the stellar mass of th
mass of the cluster in which it lives. We find that the stellar mass of
by a factor of 1.8 ± 0.3 between $z = 0.9$ and $z = 0.2$. Compared to ear
result is closer to the predictions of semi-analytic models. However, BC
relative to BCGs at $z = 0.2$, are still a factor of 1.5 more massive than
of these models. Star formation rates in BCGs at $z \sim 1$ are generally to
in significant amounts of mass. Instead, it is likely that most of the
occurs through mainly dry mergers in which perhaps half of the mas
intra-cluster medium of the cluster.

Key words: galaxies: clusters: general – galaxies: evolution – galaxies
– cosmology: observations

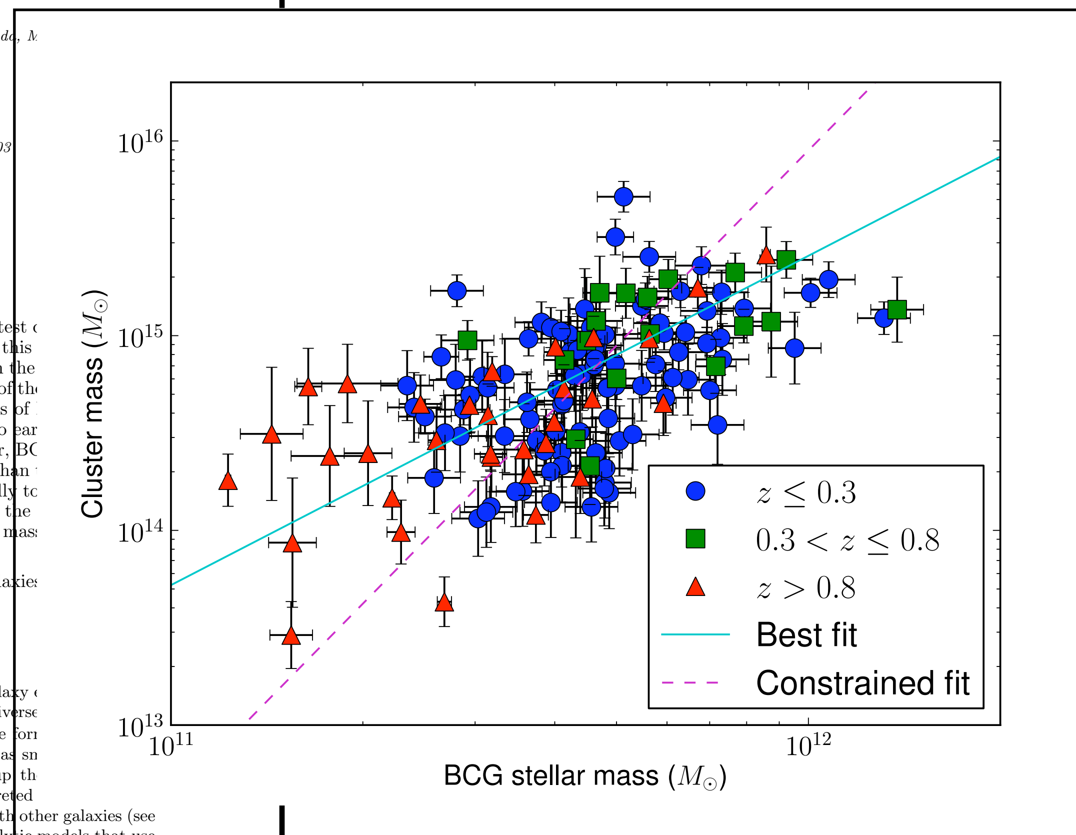

1 INTRODUCTION

Brightest Cluster Galaxies (BCGs) are amongst the largest, most luminous and most massive galaxies in the universe at the present epoch. Located in the cores of rich galaxy clusters, BCGs are easy to identify, both observationally and in simulations. They can also be observed at a time when the universe was less than a third of its current age. They therefore provide an attractive target for testing our under-

standing of the processes that drive galaxy e
in the most massive galaxies of the universe

In the hierarchical scenario for the for
ture in our universe, galaxies start off as sm
in the density of matter and build up th
over time by converting material accreted
roundings into stars and by merging with other galaxies (see Baugh 2006, for a review). In semi-analytic models that use the hierarchical scenario as their foundation, the stellar mass of a BCG increases significantly with time. For example, between redshift $z = 1.0$ (corresponding to a look-back time of 6.7 Gyr) to $z = 0$, the semi-analytic model described in De

⋆ E-mail: clidman@aao.gov.au

Monthly Notices of the ROYAL ASTRONOMICAL SOCIETY

Mon. Not. R. Astron. Soc. **423,** 1596–1609 (2012) doi:10.1111/j.1365-2966.2012.20982.x

Principles of supernova-driven winds

M. J. Stringer,[1,2,3]★ R. G. Bower,[1] S. Cole,[1] C. S. Frenk[1] and T. Theuns[1,4]

[1] *Institute for Computational Cosmology, Department of Physics, University of Durham, South Road, Durham DH1 3LE*
[2] *Observatoire de Paris, LERMA, 61 Av. de l'Observatoire, 75014 Paris, France*
[3] *Kavli Institute for Cosmology, Madingley Road, Cambridge CB3 0HA*
[4] *Department of Physics, University of Antwerp, Campus Groenenborger, Groenenborgerlaan 171, B-2020 Antwerp, Belgium*

Accepted 2012 March 22. Received 2012 February 7; in original form 2011 November 10

ABSTRACT

The formation of galaxies is regulated by a balance between the supply of gas and the rate at which it is ejected. Traditional explanations of gas ejection equate the energy required to escape the galaxy or host halo to an estimate for the energy yield from supernova[e.] ... yield is usually assumed to be a constant fraction of the total available from the supern... or is derived from the assumption of a consistent momentum yield. By applying the[se] i... in the context of a cold dark matter cosmogony, we derive a first-order analytic conne[ction] between these working assumptions and the expected relationship between baryon co[ntent] and galaxy circular velocity, and find that these quick predictions straddle recent observ[ati]... estimates. To examine the premises behind these theories in more detail, we then expl[ore] ... applicability to a set of gasdynamical simulations of idealized galaxies. We show that diff... premises dominate to differing degrees in the simulated outflow, depending on the mas... the system and the resolution with which it is simulated. Using this study to anticipate emergent behaviour at arbitrarily high resolution, we motivate more comprehensive ana... model which allows for the range of velocities with which the gas may exit the system, incorporates both momentum and energy-based constraints on the outflow. Using a trial velocity distribution, this is shown to be compatible with the observed baryon fraction intermediate-mass systems, but implies that current estimates for low-mass systems cann... solely accounted for by supernova winds under commonly held assumptions.

Key words: supernovae: general – ISM: supernova remnants – galaxies: evolution – gala... formation.

1 INTRODUCTION

Any viable theory of the formation and evolution of galaxies should be able to account for the mass of baryons contained, or rather not contained, in the massive collapsed regions that host galaxies. Observational constraints on the location of baryons in the Universe imply that the fraction within these 'haloes' can be many times less than the cosmic baryon fraction, $f_b \approx 0.17$ (e.g. Komatsu et al. 2011), and that the extent of the deficit is clearly dependent on the host's mass. This can be seen from the estimated baryonic and total masses from seven separate surveys which were collected together in one figure in the review by McGaugh et al. (2010); data which are reproduced here in our Fig. 1.

The established explanation for this deficit, dating from long before such observational data were available, is that baryons can be driven from the galaxies – and their host haloes – by supernovae explosions (Matthews & Baker 1971). This account is based on the premise that the energy required to escape the galaxies' gravity is readily available from the supernovae. Because the gravitat... potential barrier will increase with host halo mass, the fraction ... supernova-driven wind which escapes might intuitively be expe... to be greater for lower mass systems, and this does indeed see... be qualitatively upheld by the mass dependence seen in the ... data.

A more quantitative version of this theory was then develope... Larson (1974), who equated this potential barrier with an esti... of the energy yield per supernova (and hence per mass of ... formed). In Section 2, we review the arguments in this classic th... and, by updating the basic premises to include a cold dark m... (CDM) component in the haloes, show how it leads to the first-... theoretical predictions for baryon fractions which are overlaid ... the observational estimates in Fig. 1. We also take the opport... to contrast the scaling expected from the traditional assumptio... consistent energy conversion to the ejected material (Section ...) with the alternative working assumption of a consistent *mome...* yield (Section 2.2).

We then go on, in Section 3, to investigate how modern *simula-tions* of disc galaxies relate to these analytic theories, using aspects of the theory to understand the behaviour which emerges from

★E-mail: martin.stringer@obspm.fr

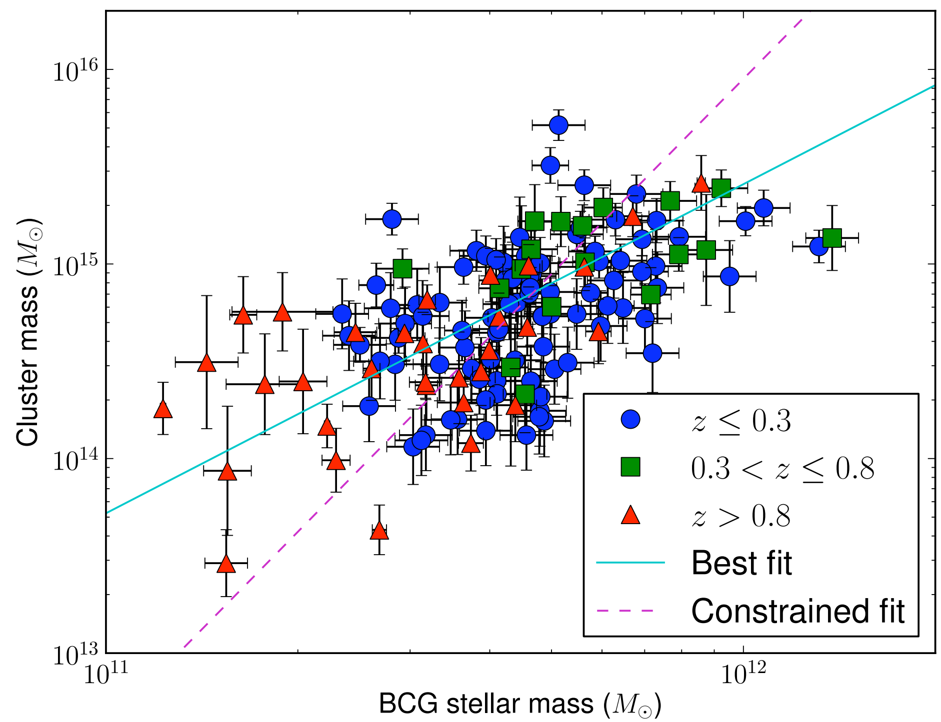

Martin Stringer

Monthly Notices of the Royal Astronomical Society

Mon. Not. R. Astron. Soc. **423,** 1596–1609 (2012) doi:10.1111/j.1365-2966.2012.20982.x

Principles of supernova-driven winds

M. J. Stringer,[1,2,3]★ R. G. Bower,[1] S. Cole,[1] C. S. Frenk[1] and T. Theuns[1,4]

[1] *Institute for Computational Cosmology, Department of Physics, University of Durham, South Road, Durham DH1 3LE*
[2] *Observatoire de Paris, LERMA, 61 Av. de l'Observatoire, 75014 Paris, France*
[3] *Kavli Institute for Cosmology, Madingley Road, Cambridge CB3 0HA*
[4] *Department of Physics, University of Antwerp, Campus Groenenborger, Groenenborgerlaan 171, B-2020 Antwerp, Belgium*

Accepted 2012 March 22. Re

1 INTRODUCTION

Any viable theory of the fo
be able to account for th
not contained, in the mass
Observational constraints
imply that the fraction wit
than the cosmic baryon f
2011), and that the extent
host's mass. This can be s
masses from seven separa
in one figure in the review
are reproduced here in our

The established explar
before such observational
be driven from the galaxie
explosions (Matthews &
the premise that the energ

★E-mail: martin.stringer@ob

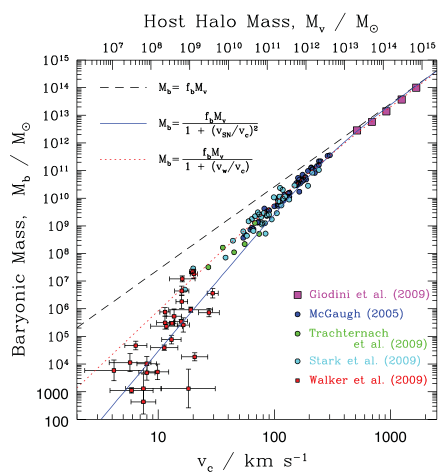

Figure 1. Galactic baryonic mass estimates from several publications, shown as a function of the virialized host halo mass (estimated from observed circular velocity or velocity dispersion). The lines show the simple prediction of self-similarity (dashed line), the prediction based on consistent conversion of supernovae energy to gravitational potential energy gain by the escaped gas (solid line) and a similar prediction based on consistent momentum yield (dotted line) using the values $v_w = v_{SN} = 300\,\mathrm{km\,s^{-1}}$. This plot is deliberately similar in layout to fig. 1 of McGaugh et al. (2010) and uses the same conversion from characteristic speed to host halo mass: $M_v/10^{12}\,\mathrm{M_\odot} \approx (v_c/187\,\mathrm{km\,s^{-1}})^3$. Round symbols represent rotationally supported discs, where v_c is the outermost measurement of circular velocity. Square symbols represent pressure supported systems for which $v_c = \sqrt{3}\sigma$ is assumed, where σ is the observed line-of-sight velocity dispersion.

these numerical experiments, depending on the parameters of the simulated supernovae and the resolution with which the system is simulated. This investigation is then used to motivate revisions to the traditional premises and in Section 4 we present an alternative derivation of the outflow which is built on more realistic assumptions, whilst keeping to the spirit of the original elegant theories.

2 THEORETICAL BACKGROUND

2.1 Consistent energy conversion

The earliest attempt to quantify the mass outflow due to supernova was by Larson (1974). This brought the idea of Matthews & Baker (1971) together with work on the evolution of supernova remnants (Cox 1972) to estimate that 10 per cent of the original supernova energy will be retained as thermal and kinetic energy in the gas, a figure calculated by considering the energy that would still be contained within supernova remnants at the point at which they

ditions that it was considered, 'under most circumstances likely to be encountered in practice', accurate 'to within about a factor of 2'.

This figure could then be incorporated into their model of gas ejection under the additional premise:

'... that all of the available energy of $0.1E_{SN}$ is expended in removing gas from the

This premise can be
energy conversion, in
system to another and
energy gained by the g
relation:

$M_{esc} v_c^2 \approx \eta E_{SN},$

where M_{esc} is the mass
ity of the system (defi
velocity) and η is the f
converted into the ene
nova yield to be propo
can be written as

$M_{esc} \approx \left(\frac{v_{SN}}{v_c}\right)^2 M_\star$

The original calculatio
tive energy release per
per supernova of 100 M
responds, in our notati

The adopted figure f
was attributed to obser
has consistently appea
citation at all. More r
provided by fitting eve
in luminosity of the su
1990), 1993J (e.g. No
et al. 1994), these havi
masses in the range 10-
majority of the superno

The scaling of equa
& Rees (1978) as a co
formation, and the argu
by Dekel & Silk (1986
White & Frenk (1991)
adopt the scaling (if not
though different model
contexts for its applica
day (e.g. De Lucia et a

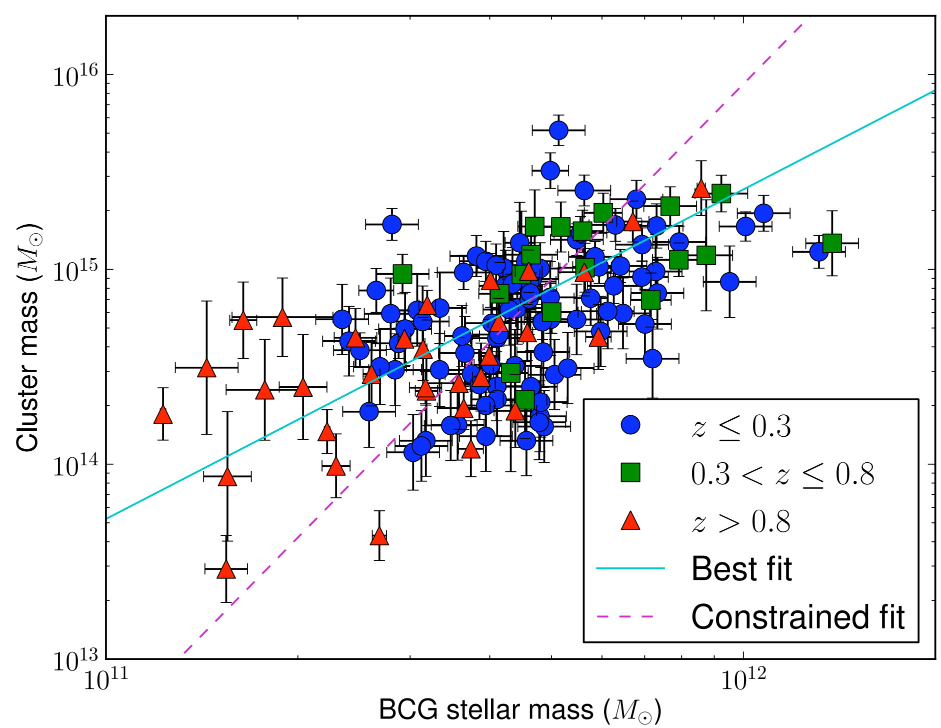

The mapping from supernovae physics to this observed trend in galaxy properties can be appreciated more directly, if more approximately, by simply combining equation (1) with the additional constraint that the retained and escaped masses must add up to give the cosmic fraction, f_b, of their host halo, $(M_b + M_{esc} = f_b M_v)$. This leads to a simple relationship between remaining baryonic mass, M_b, and total virial mass M_v (or characteristic speed v_c) that is plotted[1] in Fig. 1:

$$M_b \approx \frac{f_b M_v}{1 + f_\star (v_{SN}/v_c)^2} \qquad \left[f_\star \equiv \frac{M_\star}{M_b}\right]. \tag{3}$$

Therefore, placed in the context of CDM cosmogony, Larson (1974)

LERMA

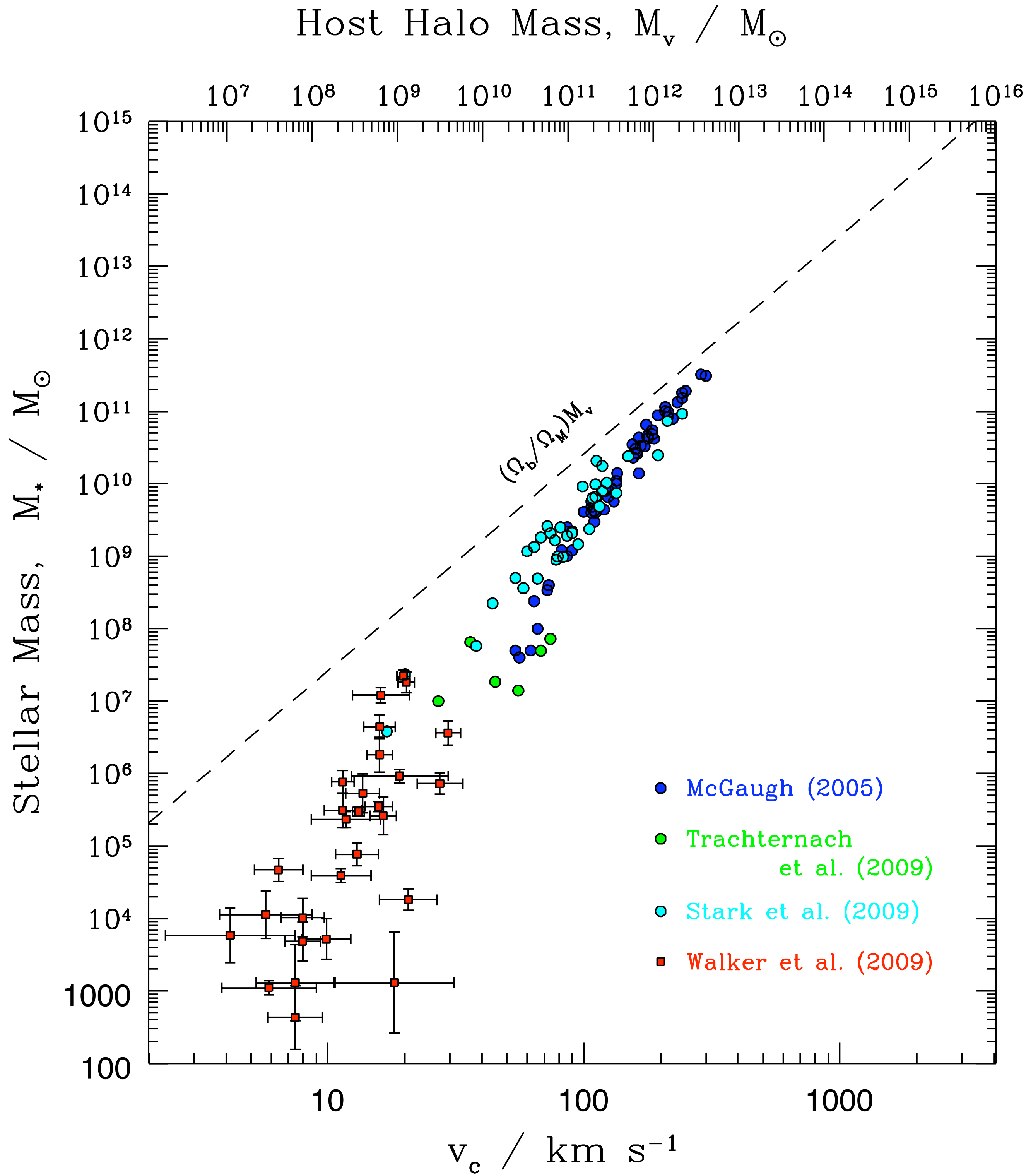

Host Halo Mass, M_v / $M_\odot$
10^7 10^8 10^9 10^{10} 10^{11} 10^{12} 10^{13} 10^{14} 10^{15} 10^{16}
Stellar Mass, M_* / $M_\odot$
10^{15} 10^{14} 10^{13} 10^{12} 10^{11} 10^{10} 10^9 10^8 10^7 10^6 10^5 10^4 1000 100
$(\Omega_b/\Omega_M)M_v$
McGaugh (2005)
Trachternach et. al. (2009)
Stark et al. (2009)
Walker et al. (2009)
10 100 1000
v_c / km s^{-1}

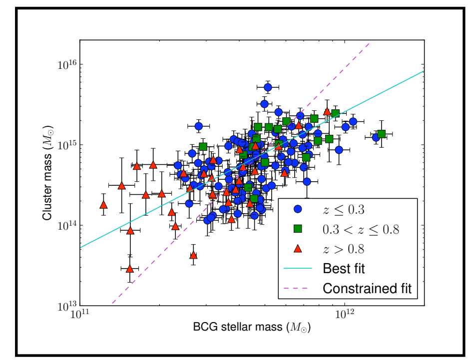

Cluster mass ($M_\odot$)
BCG stellar mass ($M_\odot$)
$z \leq 0.3$
$0.3 < z \leq 0.8$
$z > 0.8$
Best fit
Constrained fit

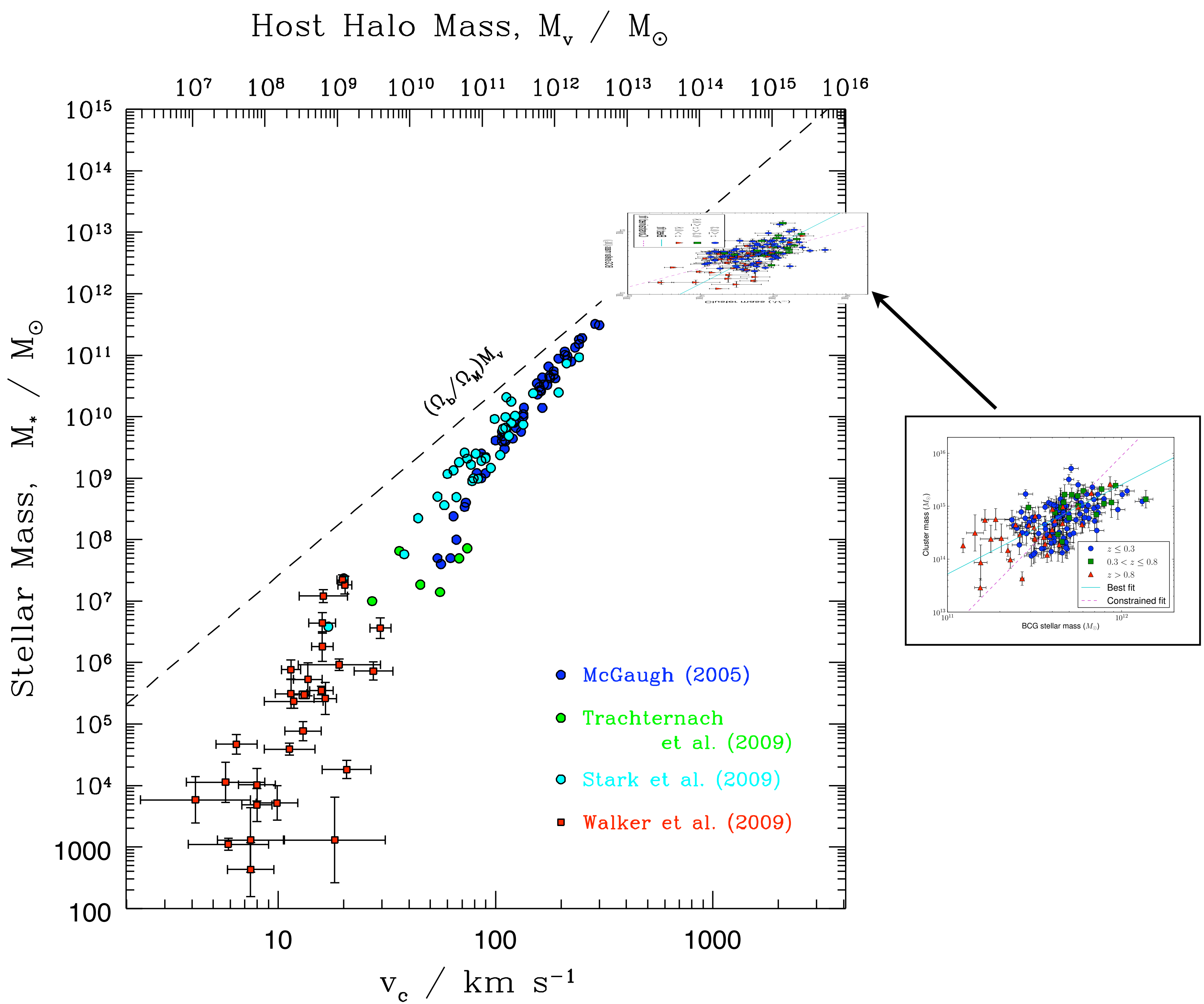

Host Halo Mass, M_v / $M_\odot$
10^7 10^8 10^9 10^{10} 10^{11} 10^{12} 10^{13} 10^{14} 10^{15} 10^{16}
Stellar Mass, M_* / $M_\odot$
10^{15} 10^{14} 10^{13} 10^{12} 10^{11} 10^{10} 10^9 10^8 10^7 10^6 10^5 10^4 1000 100
v_c / km s^{-1}
10 100 1000
$(\Omega_b/\Omega_M)M_v$
McGaugh (2005)
Trachternach et. al. (2009)
Stark et al. (2009)
Walker et al. (2009)
Cluster mass ($M_\odot$)
BCG stellar mass ($M_\odot$)
$z \leq 0.3$
$0.3 < z \leq 0.8$
$z > 0.8$
Best fit
Constrained fit

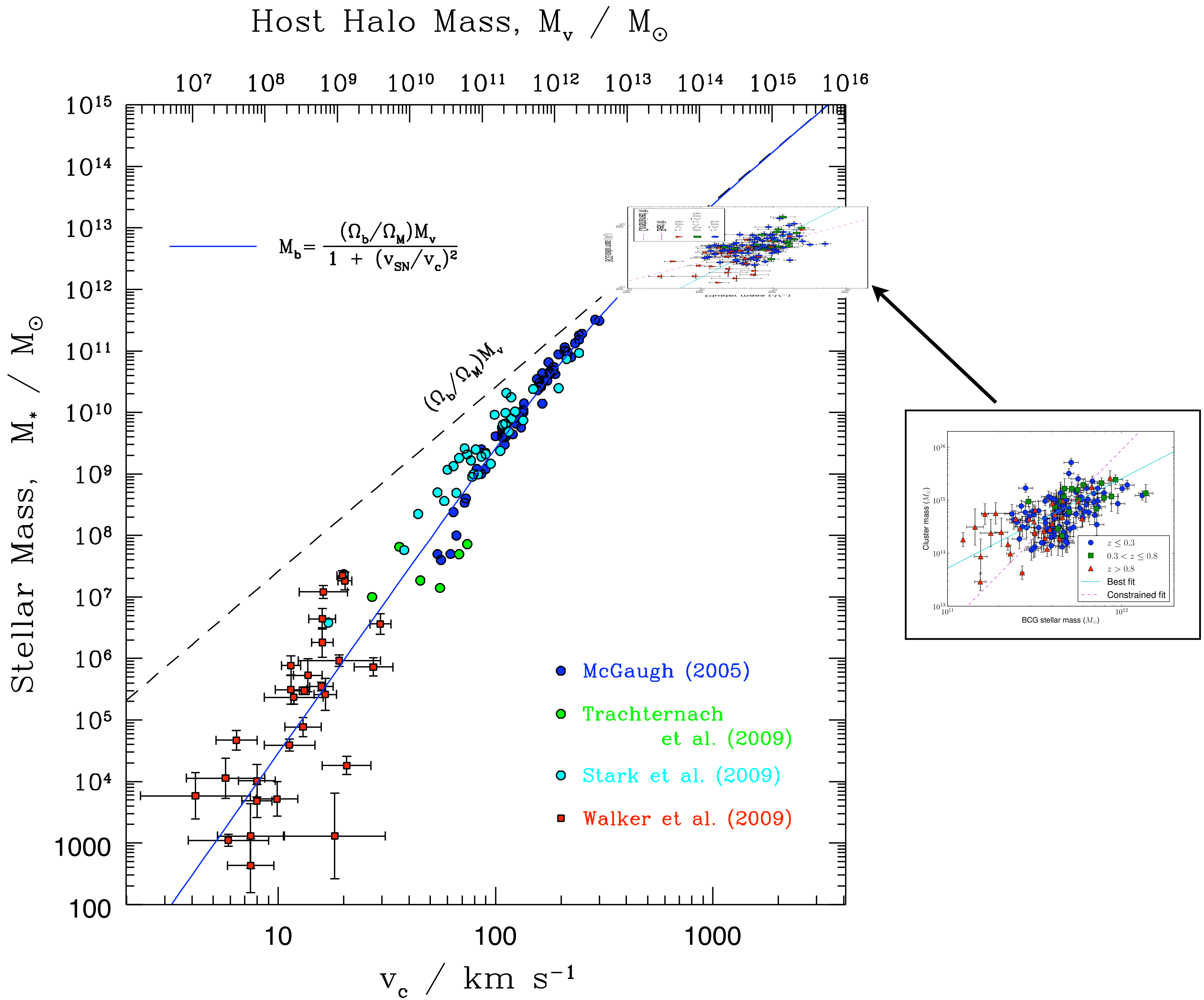

Host Halo Mass, M_v / $M_\odot$
10^7 10^8 10^9 10^{10} 10^{11} 10^{12} 10^{13} 10^{14} 10^{15} 10^{16}
Stellar Mass, M_* / $M_\odot$
10^{15} 10^{14} 10^{13} 10^{12} 10^{11} 10^{10} 10^9 10^8 10^7 10^6 10^5 10^4 1000 100
$M_b = \frac{(\Omega_b/\Omega_M)M_v}{1 + (v_{SN}/v_c)^2}$
$(\Omega_b/\Omega_M)M_v$
McGaugh (2005)
Trachternach et al. (2009)
Stark et al. (2009)
Walker et al. (2009)
10 100 1000
v_c / km s^{-1}
Cluster mass ($M_\odot$)
BCG stellar mass ($M_\odot$)
10^{16} 10^{15} 10^{14} 10^{13}
10^{11} 10^{12}
$z \leq 0.3$
$0.3 < z \leq 0.8$
$z > 0.8$
Best fit
Constrained fit

Growing-up at high redshift: from proto-clusters to galaxy clusters

10-13 September 2012

European Space Astronomy Centre (ESAC)
ESA, Villanueva de la Cañada, Madrid, Spain

Purpose and Goals

Galaxy clusters represent the place where astrophysics and cosmology meet. Recently, the most distant (z>~1.5), massive clusters were discovered in IR and X-ray surveys, and the first high-z clusters discovered through the Sunyaev-Zeldovich (SZ) effect were found thanks to the new telescopes SPT, Planck, ACT. Massive (>~3.10^{14} Msun), high-redshift clusters are expected to be rare in the standard LCDM model. Therefore, robust mass measurements obtained from a combination of high-resolution X-ray and weak/strong lensing data are required to place stringent tests to the current cosmological paradigm. On the other hand, the underlying galaxy populations of these high-z clusters start to show signs of evolution relative to nearby systems, e.g. a reversal of star formation ("infrared Butchler-Oemler" effect). In this respect, the FIR Herschel data offers a new observational window, expected to provide valuable insights on their star-formation properties. Concurrently, significant progress had been done in the study of proto-clusters at z>1.6. A multi-wavelength approach is thus mandatory to gain a deeper understanding on the physical properties of these distant systems, obtain accurate mass measurements, and constrain the formation epoch of galaxy clusters. The aim of this conference is to discuss the latest results in this field obtained with data at previously unexplored wavelengths, and investigate future prospects with upcoming facilities such as ALMA, E-ELT, etc.

Growing-up at high redshift: from proto-clusters to galaxy clusters

10-13 September 2012

European Space Astronomy Centre (ESAC)
ESA, Villanueva de la Cañada, Madrid, Spain

Purpose and Goals

Galaxy clusters represent the place where astrophysics and cosmology meet. Recently, the most distant (z>~1.5), massive clusters were discovered in IR and X-ray surveys, and the first high-z clusters discovered through the Sunyaev-Zeldovich (SZ) effect were found thanks to the new telescopes SPT, Planck, ACT. Massive >~3.10^{14} Msun, high-redshift clusters are expected to be rare in the standard LCDM model. Therefore, robust mass measurements obtained from a combination of high-resolution X-ray and weak/strong lensing data are required to place stringent tests to the current cosmological paradigm. On the other hand, the underlying galaxy populations of these high-z clusters start to show signs of evolution relative to nearby systems, e.g. a reversal of star formation ("infrared Butchler-Oemler" effect). In this respect, the FIR Herschel data offers a new observational window, expected to provide valuable insights on their star-formation properties. Concurrently, significant progress had been done in the study of proto-clusters at z>1.6. A multi-wavelength approach is thus mandatory to gain a deeper understanding on the physical properties of these distant systems, obtain accurate mass measurements, and constrain the formation epoch of galaxy clusters. The aim of this conference is to discuss the latest results in this field obtained with data at previously unexplored wavelengths, and investigate future prospects with upcoming facilities such as ALMA, E-ELT, etc.

Growing-up at high redshift: from proto-clusters to galaxy clusters

10-13 September 2012

European Space Astronomy Centre (ESAC)
ESA, Villanueva de la Cañada, Madrid, Spain

Purpose and Goals

Galaxy clusters represent the place where astrophysics and cosmology meet. Recently, the most distant ($z>\sim1.5$), massive clusters were discovered in IR and X-ray surveys, and the first high-z clusters discovered through the Sunyaev-Zeldovich (SZ) effect were found thanks to the new telescopes SPT, Planck, ACT. Massive ($>\sim3.10^{14}$ Msun), high-redshift clusters are expected to be rare in the standard LCDM model. Therefore, robust mass measurements obtained from a combination of high-resolution X-ray and weak/strong lensing data are required to place stringent tests to the current cosmological paradigm. On the other hand, the underlying galaxy populations of these high-z clusters start to show signs of evolution relative to nearby systems, e.g. a reversal of star formation ("infrared Butchler-Oemler" effect). In this respect, the FIR Herschel data offers a new observational window, expected to provide valuable insights on their star-formation properties. Concurrently, significant progress had been done in the study of proto-clusters at $z>1.6$. A multi-wavelength approach is thus mandatory to gain a deeper understanding on the physical properties of these distant systems, obtain accurate mass measurements, and constrain the formation epoch of galaxy clusters. The aim of this conference is to discuss the latest results in this field obtained with data at previously unexplored wavelengths, and investigate future prospects with upcoming facilities such as ALMA, E-ELT, etc.

Growing-up at high redshift: from proto-clusters to galaxy clusters

10-13 September 2012

European Space Astronomy Centre (ESAC)
ESA, Villanueva de la Cañada, Madrid, Spain

Purpose and Goals

Galaxy clusters represent the place where astrophysics and cosmology meet. Recently, the most distant (z>~1.5), massive clusters were discovered in IR and X-ray surveys, and the first high-z clusters discovered through the Sunyaev-Zeldovich (SZ) effect were found thanks to the new telescopes SPT, Planck, ACT. Massive >~3.10^{14} Msun, high-redshift clusters are expected to be rare in the standard LCDM model. Therefore, robust mass measurements obtained from a combination of high-resolution X-ray and weak/strong lensing data are required to place stringent tests to the current cosmological paradigm. On the other hand, the underlying galaxy populations of these high-z clusters start to show signs of evolution relative to nearby systems, e.g. a reversal of star formation ("infrared Butchler-Oemler" effect). In this respect, the FIR Herschel data offers a new observational window, expected to provide valuable insights on their star-formation properties. Concurrently, significant progress had been done in the study of proto-clusters at z>1.6. A multi-wavelength approach is thus mandatory to gain a deeper understanding on the physical properties of these distant systems, obtain accurate mass measurements, and constrain the formation epoch of galaxy clusters. The aim of this conference is to discuss the latest results in this field obtained with data at previously unexplored wavelengths, and investigate future prospects with upcoming facilities such as ALMA, E-ELT, etc.

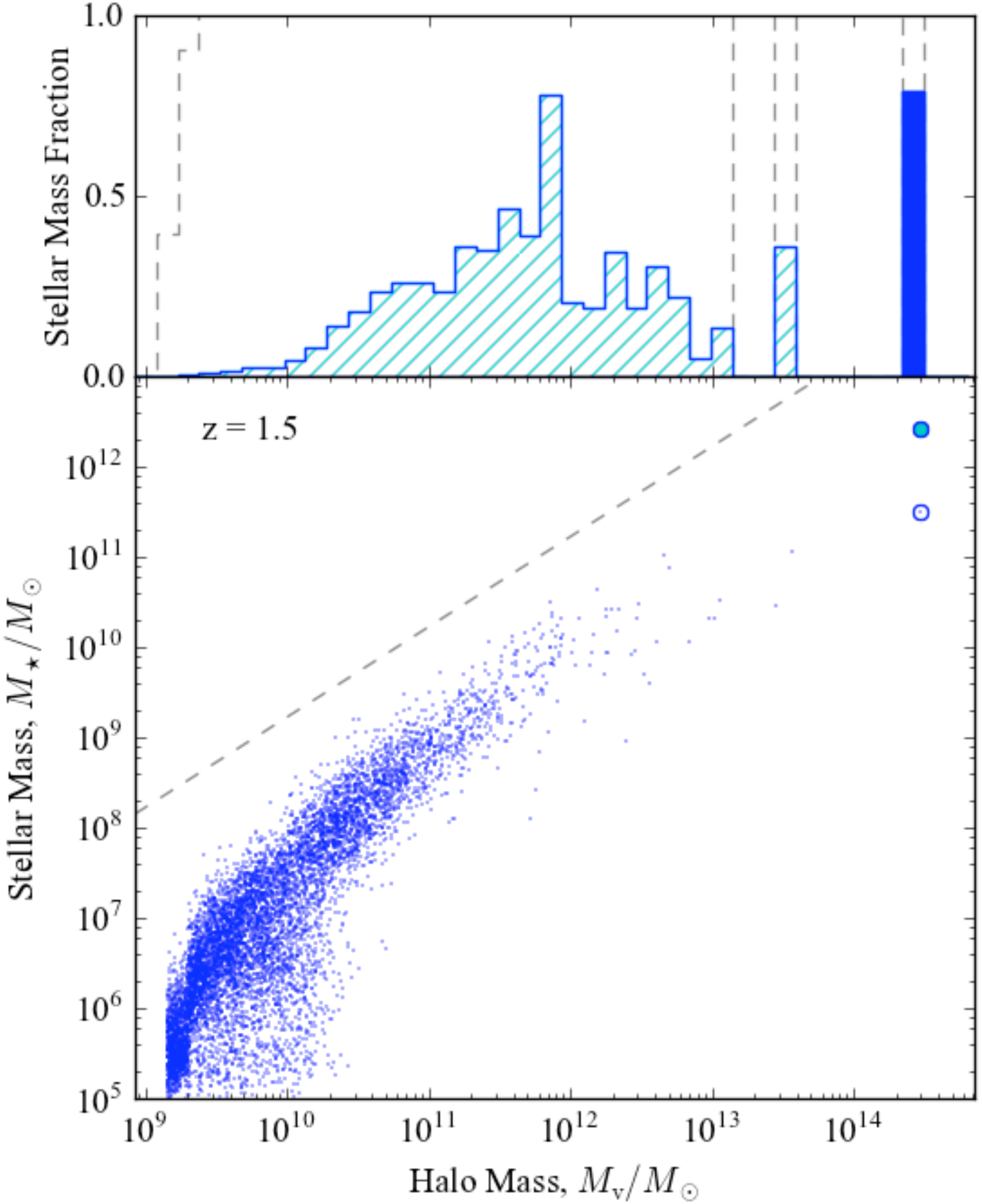

Stellar Mass Fraction
1.0
0.5
0.0
z = 1.5
Stellar Mass, $M_\star/M_\odot$
10^{5}
10^{6}
10^{7}
10^{8}
10^{9}
10^{10}
10^{11}
10^{12}
Halo Mass, $M_{\rm v}/M_\odot$
10^{9}
10^{10}
10^{11}
10^{12}
10^{13}
10^{14}

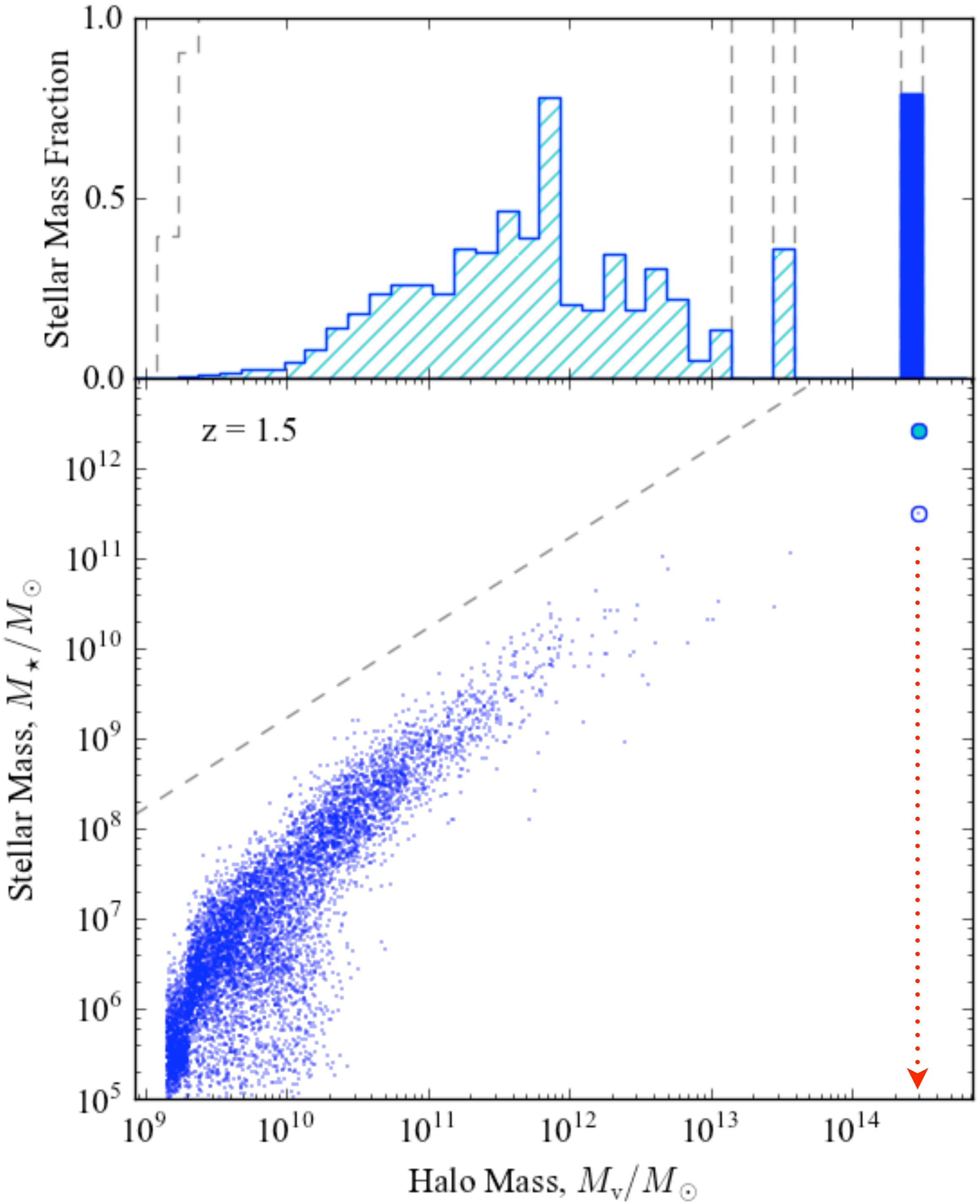

Cluster Mass probability
under LCDM

~1-10 Gpc^{-3}

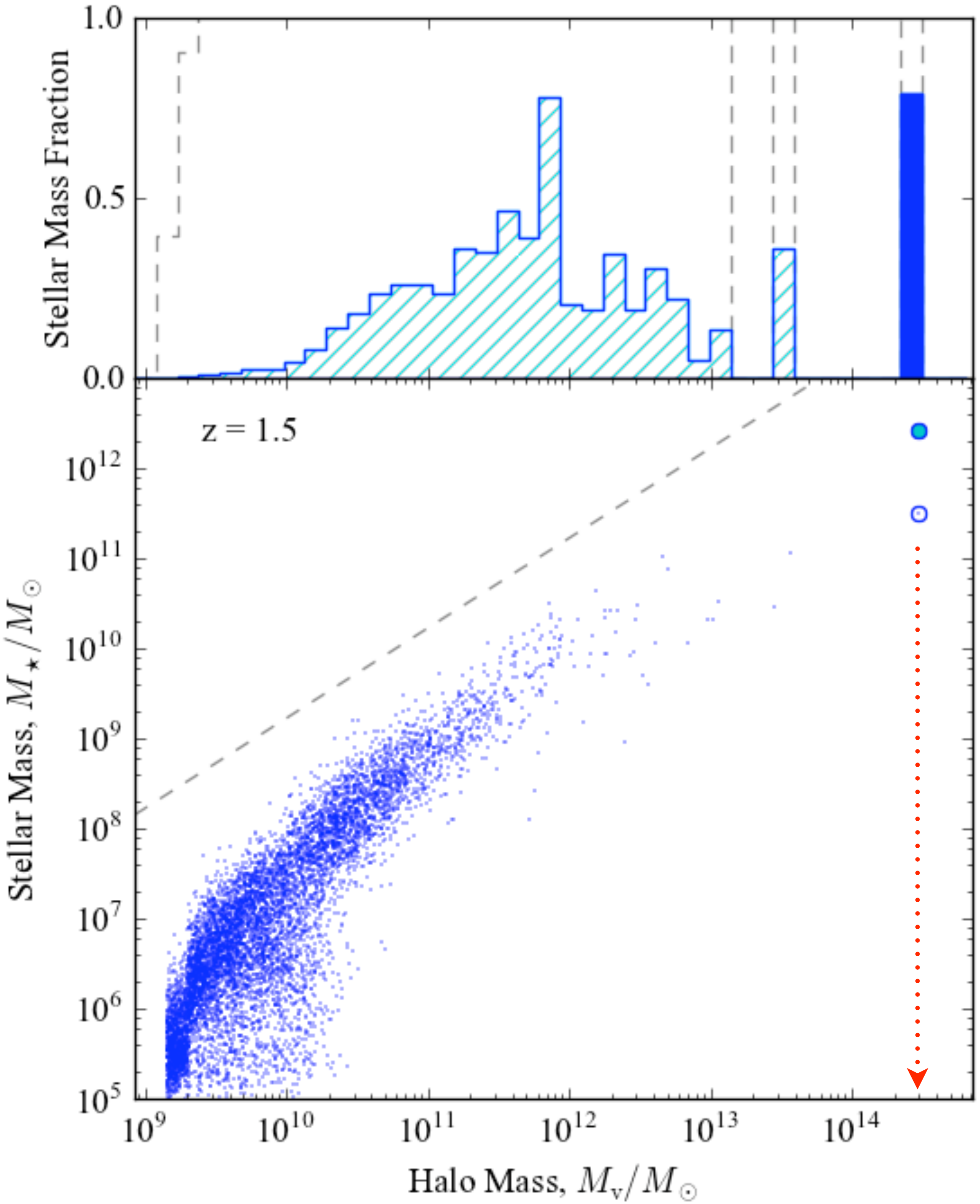

Cluster Mass probability
under LCDM

~1-10 Gpc^{-3}

~ 100s per Hubble Volume

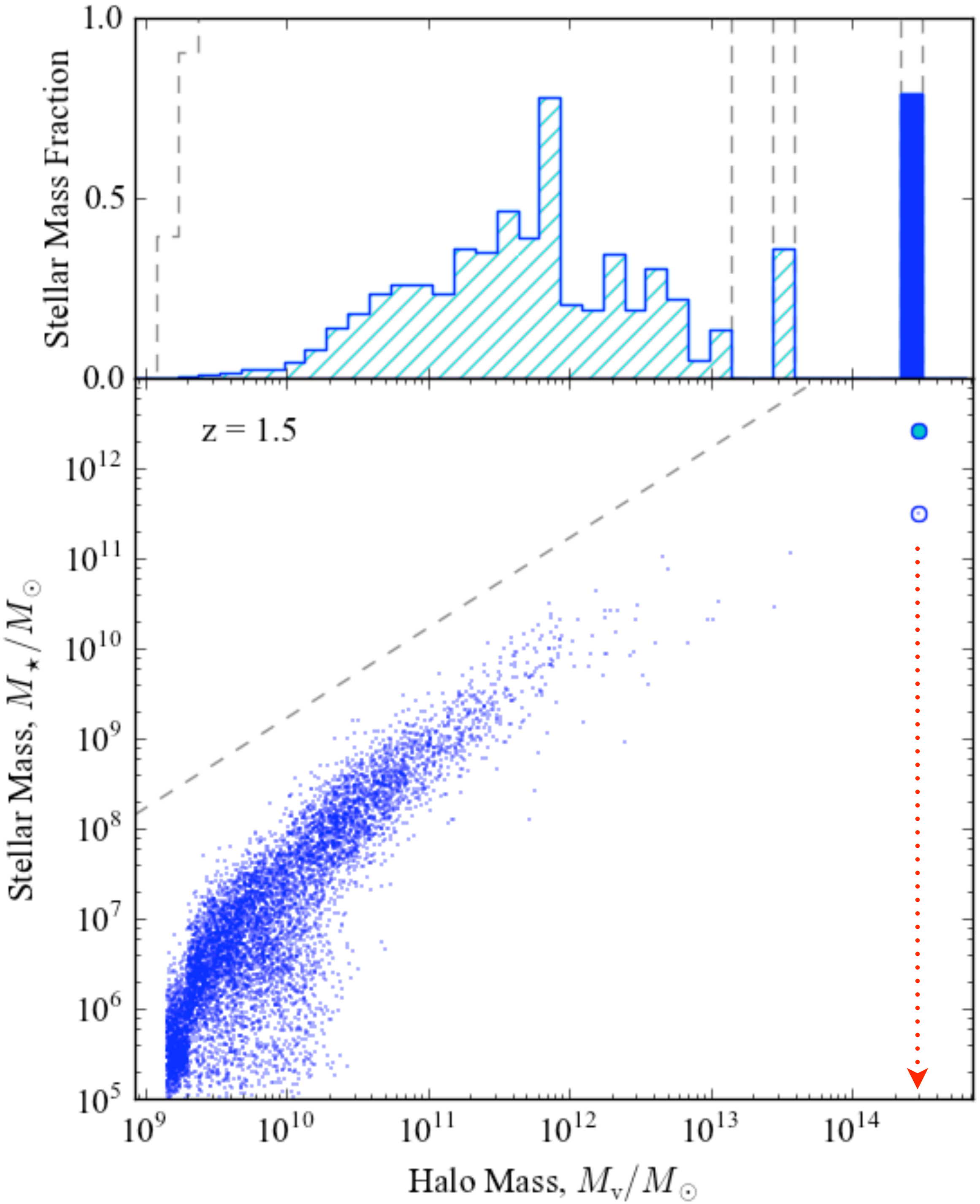

But the BCG mass
is still limited

Cluster Mass probability
under LCDM

~1-10 Gpc^{-3}

~ 100s per Hubble Volume

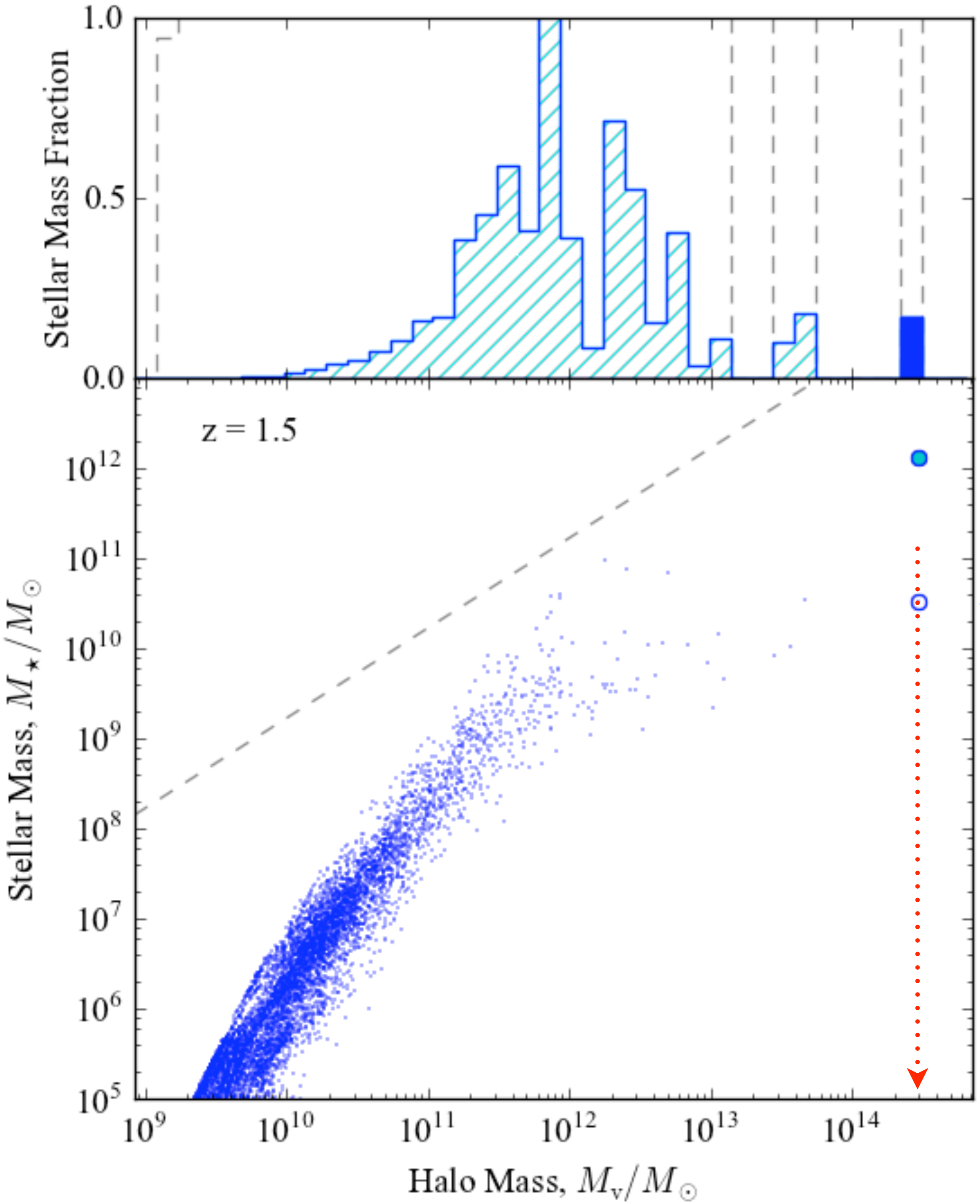

With a model including
AGN feedback
(Bower et al, 2005)
the BCG is even fainter

The Astrophysical Journal, 737:22 (10pp), 2011 August 10 doi:10.1088/0004-637X/737/1/22

DETECTION OF A HOT GASEOUS HALO AROUND THE GIANT SPIRAL GALAXY NGC 1961

Michael E. Anderson and Joel N. Bregman
Department of Astronomy, University of Michigan, Ann Arbor, MI 48109, USA;
michevan@umich.edu, jbregman@umich.edu
Received 2011 January 5; accepted 2011 May 20; published 2011 July 26

ABSTRACT

Hot gaseous halos are predicted around all large galaxies and are critically important for our understanding of galaxy formation, but they have never been detected at distances beyond a few kpc around a spiral galaxy. We used the ACIS-I instrument on board *Chandra* to search for diffuse X-ray emission around an ideal candidate galaxy: the isolated giant spiral NGC 1961. We observed four quadrants around the galaxy for 30 ks each, carefully subtracting background and point-source emission, and found diffuse emission that appears to extend to 40–50 kpc. We fit β-models to the emission and estimate a hot halo mass within 50 kpc of $5 \times 10^9\ M_\odot$. When this profile is extrapolated to 500 kpc (the approximate virial radius), the implied hot halo mass is 1–3 $\times\ 10^{11}\ M_\odot$. These mass estimates assume a gas metallicity of $Z = 0.5\ Z_\odot$. This galaxy's hot halo is a large reservoir of gas, but falls significantly below observational upper limits set by pervious searches, and suggests that NGC 1961 is missing 75% of its baryons relative to the cosmic mean, which would tentatively place it below an extrapolation of the baryon Tully–Fisher relationship of less massive galaxies. The cooling rate of the gas is no more than 0.4 $M_\odot$ yr^{-1}, more than an order of magnitude below the gas consumption rate through star formation. We discuss the implications of this halo for galaxy formation models.

Key words: galaxies: halos – galaxies: individual (NGC 1961) – X-rays: galaxies

Online-only material: color figures

1. INTRODUCTION

Hot gaseous halos around galaxies have been an important prediction of galaxy formation models since White & Rees (1978). Theory predicts these hot halos form as matter accretes onto the dark matter halo and the baryons shock to the virial temperature (White & Frenk 1991; also see the review by Benson 2010). Depending on the details of the assumed preheating, heating from galactic feedback, and cooling rates, these hot halos are often predicted to contain as much or more baryonic mass as the galaxies within the halos (Sommer-Larsen 2006; Fukugita & Peebles 2006), making them cosmologically important as reservoirs of the "missing baryons" from galaxies (although see also Anderson & Bregman 2010). The hot halo is also thought to produce the galactic color–magnitude bimodality (Dekel & Birnboim 2006) and to help explain galactic "downsizing" in the star formation history (Bower et al. 2006; De Lucia et al. 2006).

Hot halos have been extensively observed in soft X-rays (roughly 0.5–2 keV) around early-type galaxies (Forman et al. 1985; O'Sullivan et al. 2001; Mulchaey & Jeltema 2010). The halos are typically luminous ($L_{\mathrm{X},0.5\text{–}2\,\mathrm{keV}} \sim 10^{39}$–$10^{41}$ for non-BCG ellipticals), mass-dependent (for most definitions of L_X and L_K, $L_\mathrm{X} \propto L_\mathrm{K}^2$), and are often visible out to many tens of kpc. But these halos are difficult to connect to the formation of the galaxies because coronal gas can also be produced in the mergers and associated star formation that occurred when the galaxy became elliptical (Read & Ponman 1998), and because it is difficult to disentangle halo gas with the intergroup medium (IGM) in which most large ellipticals reside (Dressler 1980).

In contrast, hot halos around quiescent disk galaxies should be much more direct tracers of the galaxy formation process. While the morphology–density relation makes it difficult to disentangle elliptical galaxies from their dense environments, it also ensures a large supply of isolated spiral galaxies in low-density environments. Late-type disks are destroyed by strong mergers (e.g., Robertson et al. 2006), and it is easy to identify and exclude starbursting galaxies, so it should be straightforward to search for hot halos around quiescent isolated spirals and to connect these halos to models of galaxy formation.

Unfortunately, the search for extended soft X-ray emission around isolated spirals has so far been unsuccessful. There are several detections of emission a few kpc above the disk (Strickland et al. 2004a; Li et al. 2006; Tüllmann et al. 2006; Rasmussen et al. 2009; Owen & Warwick 2009; Yamasaki et al. 2009), but these observations are linked to the star formation in the galaxy and probably represent galactic fountains. In terms of more extended emission, Li et al. (2007) observe gas around the Sombrero galaxy out to 20 kpc, but this galaxy is significantly bulge-dominated, and the extended emission has been linked to a galactic bulge-driven wind. Finally, Pedersen et al. (2006) claimed to detect extended hot halo emission around NGC 5746, but this emission disappeared after subsequent reanalysis with newer calibration files (Rasmussen et al. 2009).

A recent paper (Crain et al. 2010b) attributes these detections of extended emission to galactic coronae, instead of the standard explanation of the emission as a fountain or a wind originating from within the galaxy. This interpretation is in disagreement with the standard understanding of galactic fountains in spiral galaxies, but regardless of interpretation it still is true that no hot halo has been detected around a disk galaxy at a radius of more than a few kpc.

In this paper, we present an analysis of observations by the ACIS-I array on board the *Chandra X-ray Observatory* of the environs of the extremely massive spiral galaxy NGC 1961, in which we detect X-ray emission out to at least 40 kpc and attribute the emission to a hot halo. The outline of the paper is as follows. In Section 2, we discuss the properties of NGC 1961 and the details of our observation. In Section 3, we discuss the reduction of the data and explain various approaches to flat

The Astrophysical Journal, 737:22 (10pp), 2011 August 10 doi:10.1088/0004-637X/737/1/22

DETECTION OF A HOT GASEOUS HALO AROUND THE GIANT SPIRAL GALAXY NGC 1961

Michael E. Anderson and Joel N. Bregman
Department of Astronomy, University of Michigan, Ann Arbor, MI 48109, USA;
michevan@umich.edu, jbregman@umich.edu
Received 2011 January 5; accepted 2011 May 20; published 2011 July 26

ABSTRACT

Hot gaseous halos are predicted around all large galaxies and are critically important for our understanding of galaxy formation, but they have never been detected at distances beyond a few kpc around a spiral galaxy. We used the ACIS-I instrument on board *Chandra* to search for diffuse X-ray emission around an ideal candidate galaxy: the isolated giant spiral NGC 1961. We observed four quadrants around the galaxy for 30 ks each, carefully subtracting background and point-source emission, and found diffuse emission that appears to extend to 40–50 kpc. We fit β-models to the emission and estimate a hot halo mass within 50 kpc of $5 \times 10^9\ M_\odot$. When this profile is extrapolated to 500 kpc (the approximate virial radius), the implied hot halo mass is $1\text{–}3 \times 10^{11}\ M_\odot$. These mass estimates assume a gas metallicity of $Z = 0.5\ Z_\odot$. This galaxy's hot halo is a large reservoir of gas, but falls significantly below observational upper limits set by pervious searches, and suggests that NGC 1961 is missing 75% of its baryons relative to the cosmic mean, which would tentatively place it below an extrapolation of the baryon Tully–Fisher relationship of less massive galaxies. The cooling rate of the gas is no more than $0.4\ M_\odot\ \mathrm{yr}^{-1}$, more than an order of magnitude below the gas consumption rate through star formation. We discuss the implications of this halo for galaxy formation models.

Key words: galaxies: halos – galaxies: individual (NGC 1961) – X-rays: galaxies

Online-only material: color figures

1. INTRODUCTION

Hot gaseous halos around galaxies have been an important prediction of galaxy formation models since White & Rees (1978). Theory predicts these hot halos form as matter accretes onto the dark matter halo and the baryons shock to the virial temperature (White & Frenk 1991; also see the review by Benson 2010). Depending on the details of the assumed pre-heating, heating from galactic feedback, and cooling rates, these hot halos are often predicted to contain as much or more baryonic mass as the galaxies within the halos (Sommer-Larsen 2006; Fukugita & Peebles 2006), making them cosmologically important as reservoirs of the "missing baryons" from galaxies (although see also Anderson & Bregman 2010). The hot halo is also thought to produce the galactic color–magnitude bimodality (Dekel & Birnboim 2006) and to help explain galactic "downsizing" in the star formation history (Bower et al. 2006; De Lucia et al. 2006).

Hot halos have been extensively observed in soft X-rays (roughly 0.5–2 keV) around early-type galaxies (Forman et al. 1985; O'Sullivan et al. 2001; Mulchaey & Jeltema 2010). The halos are typically luminous ($L_{X,0.5\text{–}2\,\mathrm{keV}} \sim 10^{39}\text{–}10^{41}$ for non-BCG ellipticals), mass-dependent (for most definitions of L_X and L_K, $L_X \propto L_K^2$), and are often visible out to many tens of kpc. But these halos are difficult to connect to the formation of the galaxies because coronal gas can also be produced in the mergers and associated star formation that occurred when the galaxy became elliptical (Read & Ponman 1998), and because it is difficult to disentangle halo gas with the intergroup medium (IGM) in which most large ellipticals reside (Dressler 1980).

In contrast, hot halos around quiescent disk galaxies should be much more direct tracers of the galaxy formation process. While the morphology–density relation makes it difficult to disentangle elliptical galaxies from their dense environments, it also ensures a large supply of isolated spiral galaxies in low-density environments. Late-type disks are destroyed by strong mergers (e.g., Robertson et al. 2006), and it is easy to identify and exclude starbursting galaxies, so it should be straightforward to search for hot halos around quiescent isolated spirals and to connect these halos to models of galaxy formation.

Unfortunately, the search for extended soft X-ray emission around isolated spirals has so far been unsuccessful. There are several detections of emission a few kpc above the disk (Strickland et al. 2004a; Li et al. 2006; Tüllmann et al. 2006; Rasmussen et al. 2009; Owen & Warwick 2009; Yamasaki et al. 2009), but these observations are linked to the star formation in the galaxy and probably represent galactic fountains. In terms of more extended emission, Li et al. (2007) observe gas around the Sombrero galaxy out to 20 kpc, but this galaxy is significantly bulge-dominated, and the extended emission has been linked to a galactic bulge-driven wind. Finally, Pedersen et al. (2006) claimed to detect extended hot halo emission around NGC 5746, but this emission disappeared after subsequent reanalysis with newer calibration files (Rasmussen et al. 2009).

A recent paper (Crain et al. 2010b) attributes these detections of extended emission to galactic coronae, instead of the standard explanation of the emission as a fountain or a wind originating from within the galaxy. This interpretation is in disagreement with the standard understanding of galactic fountains in spiral galaxies, but regardless of interpretation it still is true that no hot halo has been detected around a disk galaxy at a radius of more than a few kpc.

In this paper, we present an analysis of observations by the ACIS-I array on board the *Chandra X-ray Observatory* of the environs of the extremely massive spiral galaxy NGC 1961, in which we detect X-ray emission out to at least 40 kpc and attribute the emission to a hot halo. The outline of the paper is as follows. In Section 2, we discuss the properties of NGC 1961 and the details of our observation. In Section 3, we discuss the reduction of the data and explain various approaches to flat

7.3. Halo Cooling Rates and Implications for Galaxy Formation

We can estimate the cooling radius of this hot halo and the implied accretion rate onto the galaxy, which has implications for setting and regulating the star formation rate in the galaxy. We define the cooling radius as the radius for which the cooling time is 10 Gyr, using the expression for cooling time from Fukugita & Peebles (2006):

$$\tau(r) = \frac{1.5nkT}{\Lambda n_e\,(n - n_e)} \approx \frac{1.5kT\ \times 1.92}{\Lambda n_e \times 0.92}, \tag{1}$$

where the latter expression assumes primeval helium abundance so that the total particle density $n = 1.92 n_e$. For $T = 10^{6.85}$ K and $Z = 0.5\,Z_\odot$, $\Lambda = 10^{-22.85}$ erg cm^3 s^{-1} (Sutherland & Dopita 1993). Thus, the cooling radius occurs at $n_e = 6.8 \times 10^{-4}$ cm^{-3}. For the range of best-fit β-model profiles listed above, this corresponds to a cooling radius between 17.8 and 18.2 kpc, and an interior hot halo mass of $8.9\text{–}10.2 \times 10^8\ M_\odot$. It is difficult to estimate the accretion rate onto the disk from this hot halo, since the heating rate is unconstrained, but we can make an order-of-magnitude estimate by dividing the hot gas thermal energy within the 10 Gyr cooling radius by the luminosity within that radius; this yields a cooling time of 2.0–2.4 Gyr for material within the cooling radius, or an effective cooling rate of $0.4\,M_\odot$ yr^{-1}. In contrast, we can estimate the star formation rate in NGC 1961 from the total Hα luminosity ($7.6 \pm 0.9 \times 10^{41}$ erg s^{-1}) using the relation in Kennicutt (1998): star formation rate SFR $= 7.9 \times 10^{-42}$ $L(\mathrm{H}\alpha) = 6.0 \pm 0.7\ M_\odot$ yr^{-1}. The halo accretion rate is therefore insufficient to produce the star formation rate of the galaxy. More relevant for galaxy formation, the halo accretion rate is two orders of magnitude too low to assemble the stellar mass of this galaxy within a Hubble time. If we preserve β and r_0 for the halo, but increase S_0 to add the present-day stellar mass of $3.1 \times 10^{11}\ M_\odot$ to the halo, the cooling rate becomes 1.2–1.8 $M_\odot$ yr^{-1}, which is still insufficient to assemble the stellar mass by a factor of 20.

The Astrophysical Journal, 737:22 (10pp), 2011 August 10 doi:10.1088/0004-637X/737/1/22

DETECTION OF A HOT GASEOUS HALO AROUND THE GIANT SPIRAL GALAXY NGC 1961

Michael E. Anderson and Joel N. Bregman
Department of Astronomy, University of Michigan, Ann Arbor, MI 48109, USA;
michevan@umich.edu, jbregman@umich.edu
Received 2011 January 5; accepted 2011 May 20; published 2011 July 26

ABSTRACT

Hot gaseous halos are predicted around all large galaxies and are critically important for our understanding of galaxy formation, but they have never been detected at distances beyond a few kpc around a spiral galaxy. We used the ACIS-I instrument on board *Chandra* to search for diffuse X-ray emission around an ideal candidate galaxy: the isolated giant spiral NGC 1961. We observed four quadrants around the galaxy for 30 ks each, carefully subtracting background and point-source emission, and found diffuse emission that appears to extend to 40–50 kpc. We fit β-models to the emission and estimate a hot halo mass within 50 kpc of $5 \times 10^9\ M_\odot$. When this profile is extrapolated to 500 kpc (the approximate virial radius), the implied hot halo mass is $1\text{–}3 \times 10^{11}\ M_\odot$. These mass estimates assume a gas metallicity of $Z = 0.5\ Z_\odot$. This galaxy's hot halo is a large reservoir of gas, but falls significantly below observational upper limits set by pervious searches, and suggests that NGC 1961 is missing 75% of its baryons relative to the cosmic mean, which would tentatively place it below an extrapolation of the baryon Tully–Fisher relationship of less massive galaxies. The cooling rate of the gas is no more than $0.4\ M_\odot\ \text{yr}^{-1}$, more than an order of magnitude below the gas consumption rate through star formation. We discuss the implications of this halo for galaxy formation models.

Key words: galaxies: halos – galaxies: individual (NGC 1961) – X-rays: galaxies

Online-only material: color figures

1. INTRODUCTION

Hot gaseous halos around galaxies have been an important prediction of galaxy formation models since White & Rees (1978). Theory predicts these hot halos form as matter accretes onto the dark matter halo and the baryons shock to the virial temperature (White & Frenk 1991; also see the review by Benson 2010). Depending on the details of the assumed pre-heating, heating from galactic feedback, and cooling rates, these hot halos are often predicted to contain as much or more baryonic mass as the galaxies within the halos (Sommer-Larsen 2006; Fukugita & Peebles 2006), making them cosmologically important as reservoirs of the "missing baryons" from galaxies (although see also Anderson & Bregman 2010). The hot halo is also thought to produce the galactic color–magnitude bimodality (Dekel & Birnboim 2006) and to help explain galactic "downsizing" in the star formation history (Bower et al. 2006; De Lucia et al. 2006).

Hot halos have been extensively observed in soft X-rays (roughly 0.5–2 keV) around early-type galaxies (Forman et al. 1985; O'Sullivan et al. 2001; Mulchaey & Jeltema 2010). The halos are typically luminous ($L_{X,0.5\text{–}2\,\text{keV}} \sim 10^{39}\text{–}10^{41}$ for non-BCG ellipticals), mass-dependent (for most definitions of L_X and L_K, $L_X \propto L_K^2$), and are often visible out to many tens of kpc. But these halos are difficult to connect to the formation of the galaxies because coronal gas can also be produced in the mergers and associated star formation that occurred when the galaxy became elliptical (Read & Ponman 1998), and because it is difficult to disentangle halo gas with the intergroup medium (IGM) in which most large ellipticals reside (Dressler 1980).

In contrast, hot halos around quiescent disk galaxies should be much more direct tracers of the galaxy formation process. While the morphology–density relation makes it difficult to disentangle elliptical galaxies from their dense environments, it also ensures a large supply of isolated spiral galaxies in low-density environments. Late-type disks are destroyed by strong mergers (e.g., Robertson et al. 2006), and it is easy to identify and exclude starbursting galaxies, so it should be straightforward to search for hot halos around quiescent isolated spirals and to connect these halos to models of galaxy formation.

Unfortunately, the search for extended soft X-ray emission around isolated spirals has so far been unsuccessful. There are several detections of emission a few kpc above the disk (Strickland et al. 2004a; Li et al. 2006; Tüllmann et al. 2006; Rasmussen et al. 2009; Owen & Warwick 2009; Yamasaki et al. 2009), but these observations are linked to the star formation in the galaxy and probably represent galactic fountains. In terms of more extended emission, Li et al. (2007) observe gas around the Sombrero galaxy out to 20 kpc, but this galaxy is significantly bulge-dominated, and the extended emission has been linked to a galactic bulge-driven wind. Finally, Pedersen et al. (2006) claimed to detect extended hot halo emission around NGC 5746, but this emission disappeared after subsequent reanalysis with newer calibration files (Rasmussen et al. 2009).

A recent paper (Crain et al. 2010b) attributes these detections of extended emission to galactic coronae, instead of the standard explanation of the emission as a fountain or a wind originating from within the galaxy. This interpretation is in disagreement with the standard understanding of galactic fountains in spiral galaxies, but regardless of interpretation it still is true that no hot halo has been detected around a disk galaxy at a radius of more than a few kpc.

In this paper, we present an analysis of observations by the ACIS-I array on board the *Chandra X-ray Observatory* of the environs of the extremely massive spiral galaxy NGC 1961, in which we detect X-ray emission out to at least 40 kpc and attribute the emission to a hot halo. The outline of the paper is as follows. In Section 2, we discuss the properties of NGC 1961 and the details of our observation. In Section 3, we discuss the reduction of the data and explain various approaches to flat

7.3. Halo Cooling Rates and Implications for Galaxy Formation

We can estimate the cooling radius of this hot halo and the implied accretion rate onto the galaxy, which has implications for setting and regulating the star formation rate in the galaxy. We define the cooling radius as the radius for which the cooling time is 10 Gyr, using the expression for cooling time from Fukugita & Peebles (2006):

$$\tau(r) = \frac{1.5nkT}{\Lambda n_e (n - n_e)} \approx \frac{1.5kT \times 1.92}{\Lambda n_e \times 0.92}, \tag{1}$$

where the latter expression assumes primeval helium abundance so that the total particle density $n = 1.92 n_e$. For $T = 10^{6.85}$ K and $Z = 0.5\,Z_\odot$, $\Lambda = 10^{-22.85}$ erg cm^3 s^{-1} (Sutherland & Dopita 1993). Thus, the cooling radius occurs at $n_e = 6.8 \times 10^{-4}$ cm^{-3}. For the range of best-fit β-model profiles listed above, this corresponds to a cooling radius between 17.8 and 18.2 kpc, and an interior hot halo mass of $8.9\text{–}10.2 \times 10^8\ M_\odot$. It is difficult to estimate the accretion rate onto the disk from this hot halo, since the heating rate is unconstrained, but we can make an order-of-magnitude estimate by dividing the hot gas thermal energy within the 10 Gyr cooling radius by the luminosity within that radius; this yields a cooling time of 2.0–2.4 Gyr for material within the cooling radius, or an effective cooling rate of $0.4\,M_\odot$ yr^{-1}. In contrast, we can estimate the star formation rate in NGC 1961 from the total Hα luminosity ($7.6 \pm 0.9 \times 10^{41}$ erg s^{-1}) using the relation in Kennicutt (1998): star formation rate SFR $= 7.9 \times 10^{-42}$ $L(\text{H}\alpha) = 6.0 \pm 0.7\ M_\odot$ yr^{-1}. The halo accretion rate is therefore insufficient to produce the star formation rate of the galaxy. More relevant for galaxy formation, the halo accretion rate is two orders of magnitude too low to assemble the stellar mass of this galaxy within a Hubble time. If we preserve β and r_0 for the halo, but increase S_0 to add the present-day stellar mass of $3.1 \times 10^{11}\ M_\odot$ to the halo, the cooling rate becomes 1.2–1.8 $M_\odot$ yr^{-1}, which is still insufficient to assemble the stellar mass by a factor of 20.

The Astrophysical Journal, 737:22 (10pp), 2011 August 10 doi:10.1088/0004-637X/737/1/22

DETECTION OF A HOT GASEOUS HALO AROUND THE GIANT SPIRAL GALAXY NGC 1961

Michael E. Anderson and Joel N. Bregman
Department of Astronomy, University of Michigan, Ann Arbor, MI 48109, USA;
michevan@umich.edu, jbregman@umich.edu
Received 2011 January 5; accepted 2011 May 20; published 2011 July 26

ABSTRACT

Hot gaseous halos are predicted around all large galaxies and are critically important for our understanding of galaxy formation, but they have never been detected at distances beyond a few kpc around a spiral galaxy. We used the ACIS-I instrument on board *Chandra* to search for diffuse X-ray emission around an ideal candidate galaxy: the isolated giant spiral NGC 1961. We observed four quadrants around the galaxy for 30 ks each, carefully subtracting background and point-source emission, and found diffuse emission that appears to extend to 40–50 kpc. We fit β-models to the emission and estimate a hot halo mass within 50 kpc of $5 \times 10^9\ M_\odot$. When this profile is extrapolated to 500 kpc (the approximate virial radius), the implied hot halo mass is $1\text{–}3 \times 10^{11}\ M_\odot$. These mass estimates assume a gas metallicity of $Z = 0.5\ Z_\odot$. This galaxy's hot halo is a large reservoir of gas, but falls significantly below observational upper limits set by pervious searches, and suggests that NGC 1961 is missing 75% of its baryons relative to the cosmic mean, which would tentatively place it below an extrapolation of the baryon Tully–Fisher relationship of less massive galaxies. The cooling rate of the gas is no more than $0.4\ M_\odot\ \mathrm{yr}^{-1}$, more than an order of magnitude below the gas consumption rate through star formation. We discuss the implications of this halo for galaxy formation models.

Key words: galaxies: halos – galaxies: individual (NGC 1961) – X-rays: galaxies

Online-only material: color figures

1. INTRODUCTION

Hot gaseous halos around galaxies have been an important prediction of galaxy formation models since White & Rees (1978). Theory predicts these hot halos form as matter accretes onto the dark matter halo and the baryons shock to the virial temperature (White & Frenk 1991; also see the review by Benson 2010). Depending on the details of the assumed pre-heating, heating from galactic feedback, and cooling rates, these hot halos are often predicted to contain as much or more baryonic mass as the galaxies within the halos (Sommer-Larsen 2006; Fukugita & Peebles 2006), making them cosmologically important as reservoirs of the "missing baryons" from galaxies (although see also Anderson & Bregman 2010). The hot halo is also thought to produce the galactic color–magnitude bimodality (Dekel & Birnboim 2006) and to help explain galactic "downsizing" in the star formation history (Bower et al. 2006; De Lucia et al. 2006).

Hot halos have been extensively observed in soft X-rays (roughly 0.5–2 keV) around early-type galaxies (Forman et al. 1985; O'Sullivan et al. 2001; Mulchaey & Jeltema 2010). The halos are typically luminous ($L_{X,0.5\text{–}2\,\mathrm{keV}} \sim 10^{39}\text{–}10^{41}$ for non-BCG ellipticals), mass-dependent (for most definitions of L_X and L_K, $L_X \propto L_K^2$), and are often visible out to many tens of kpc. But these halos are difficult to connect to the formation of the galaxies because coronal gas can also be produced in the mergers and associated star formation that occurred when the galaxy became elliptical (Read & Ponman 1998), and because it is difficult to disentangle halo gas with the intergroup medium (IGM) in which most large ellipticals reside (Dressler 1980).

In contrast, hot halos around quiescent disk galaxies should be much more direct tracers of the galaxy formation process. While the morphology–density relation makes it difficult to disentangle elliptical galaxies from their dense environments, it also ensures a large supply of isolated spiral galaxies in low-density environments. Late-type disks are destroyed by strong mergers (e.g., Robertson et al. 2006), and it is easy to identify and exclude starbursting galaxies, so it should be straightforward to search for hot halos around quiescent isolated spirals and to connect these halos to models of galaxy formation.

Unfortunately, the search for extended soft X-ray emission around isolated spirals has so far been unsuccessful. There are several detections of emission a few kpc above the disk (Strickland et al. 2004a; Li et al. 2006; Tüllmann et al. 2006; Rasmussen et al. 2009; Owen & Warwick 2009; Yamasaki et al. 2009), but these observations are linked to the star formation in the galaxy and probably represent galactic fountains. In terms of more extended emission, Li et al. (2007) observe gas around the Sombrero galaxy out to 20 kpc, but this galaxy is significantly bulge-dominated, and the extended emission has been linked to a galactic bulge-driven wind. Finally, Pedersen et al. (2006) claimed to detect extended hot halo emission around NGC 5746, but this emission disappeared after subsequent reanalysis with newer calibration files (Rasmussen et al. 2009).

A recent paper (Crain et al. 2010b) attributes these detections of extended emission to galactic coronae, instead of the standard explanation of the emission as a fountain or a wind originating from within the galaxy. This interpretation is in disagreement with the standard understanding of galactic fountains in spiral galaxies, but regardless of interpretation it still is true that no hot halo has been detected around a disk galaxy at a radius of more than a few kpc.

In this paper, we present an analysis of observations by the ACIS-I array on board the *Chandra X-ray Observatory* of the environs of the extremely massive spiral galaxy NGC 1961, in which we detect X-ray emission out to at least 40 kpc and attribute the emission to a hot halo. The outline of the paper is as follows. In Section 2, we discuss the properties of NGC 1961 and the details of our observation. In Section 3, we discuss the reduction of the data and explain various approaches to flat

7.3. *Halo Cooling Rates and Implications for Galaxy Formation*

We can estimate the cooling radius of this hot halo and the implied accretion rate onto the galaxy, which has implications for setting and regulating the star formation rate in the galaxy. We define the cooling radius as the radius for which the cooling time is 10 Gyr, using the expression for cooling time from Fukugita & Peebles (2006):

$$\tau(r) = \frac{1.5nkT}{\Lambda n_e (n - n_e)} \approx \frac{1.5kT \times 1.92}{\Lambda n_e \times 0.92}, \tag{1}$$

where the latter expression assumes primeval helium abundance so that the total particle density $n = 1.92 n_e$. For $T = 10^{6.85}$ K and $Z = 0.5\,Z_\odot$, $\Lambda = 10^{-22.85}$ erg cm^3 s^{-1} (Sutherland & Dopita 1993). Thus, the cooling radius occurs at $n_e = 6.8 \times 10^{-4}$ cm^{-3}. For the range of best-fit β-model profiles listed above, this corresponds to a cooling radius between 17.8 and 18.2 kpc, and an interior hot halo mass of $8.9\text{–}10.2 \times 10^8\ M_\odot$. It is difficult to estimate the accretion rate onto the disk from this hot halo, since the heating rate is unconstrained, but we can make an order-of-magnitude estimate by dividing the hot gas thermal energy within the 10 Gyr cooling radius by the luminosity within that radius; this yields a cooling time of 2.0–2.4 Gyr for material within the cooling radius, or an effective cooling rate of $0.4\,M_\odot$ yr^{-1}. In contrast, we can estimate the star formation rate in NGC 1961 from the total Hα luminosity ($7.6 \pm 0.9 \times 10^{41}$ erg s^{-1}) using the relation in Kennicutt (1998): star formation rate SFR $= 7.9 \times 10^{-42}\ L(\mathrm{H}\alpha) = 6.0 \pm 0.7\ M_\odot$ yr^{-1}. The halo accretion rate is therefore insufficient to produce the star formation rate of the galaxy. More relevant for galaxy formation, the halo accretion rate is two orders of magnitude too low to assemble the stellar mass of this galaxy within a Hubble time. If we preserve β and r_0 for the halo, but increase S_0 to add the present-day stellar mass of $3.1 \times 10^{11}\ M_\odot$ to the halo, the cooling rate becomes 1.2–1.8 $M_\odot$ yr^{-1}, which is still insufficient to assemble the stellar mass by a factor of 20.

The Astrophysical Journal, 737:22 (10pp), 2011 August 10 doi:10.1088/0004-637X/737/1/22

DETECTION OF A HOT GASEOUS HALO AROUND THE GIANT SPIRAL GALAXY NGC 1961

Michael E. Anderson and Joel N. Bregman
Department of Astronomy, University of Michigan, Ann Arbor, MI 48109, USA;
michevan@umich.edu, jbregman@umich.edu
Received 2011 January 5; accepted 2011 May 20; published 2011 July 26

ABSTRACT

Hot gaseous halos are predicted around all large galaxies and are critically important for our understanding of galaxy formation, but they have never been detected at distances beyond a few kpc around a spiral galaxy. We used the ACIS-I instrument on board *Chandra* to search for diffuse X-ray emission around an ideal candidate galaxy: the isolated giant spiral NGC 1961. We observed four quadrants around the galaxy for 30 ks each, carefully subtracting background and point-source emission, and found diffuse emission that appears to extend to 40–50 kpc. We fit β-models to the emission and estimate a hot halo mass within 50 kpc of $5 \times 10^9\ M_\odot$. When this profile is extrapolated to 500 kpc (the approximate virial radius), the implied hot halo mass is 1–3 $\times\ 10^{11}\ M_\odot$. These mass estimates assume a gas metallicity of $Z = 0.5\ Z_\odot$. This galaxy's hot halo is a large reservoir of gas, but falls significantly below observational upper limits set by pervious searches, and suggests that NGC 1961 is missing 75% of its baryons relative to the cosmic mean, which would tentatively place it below an extrapolation of the baryon Tully–Fisher relationship of less massive galaxies. The cooling rate of the gas is no more than $0.4\ M_\odot\ \mathrm{yr}^{-1}$, more than an order of magnitude below the gas consumption rate through star formation. We discuss the implications of this halo for galaxy formation models.

Key words: galaxies: halos – galaxies: individual (NGC 1961) – X-rays: galaxies

Online-only material: color figures

1. INTRODUCTION

Hot gaseous halos around galaxies have been an important prediction of galaxy formation models since White & Rees (1978). Theory predicts these hot halos form as matter accretes onto the dark matter halo and the baryons shock to the virial temperature (White & Frenk 1991; also see the review by Benson 2010). Depending on the details of the assumed pre-heating, heating from galactic feedback, and cooling rates, these hot halos are often predicted to contain as much or more baryonic mass as the galaxies within the halos (Sommer-Larsen 2006; Fukugita & Peebles 2006), making them cosmologically important as reservoirs of the "missing baryons" from galaxies (although see also Anderson & Bregman 2010). The hot halo is also thought to produce the galactic color–magnitude bimodality (Dekel & Birnboim 2006) and to help explain galactic "down-sizing" in the star formation history (Bower et al. 2006; De Lucia et al. 2006).

Hot halos have been extensively observed in soft X-rays (roughly 0.5–2 keV) around early-type galaxies (Forman et al. 1985; O'Sullivan et al. 2001; Mulchaey & Jeltema 2010). The halos are typically luminous ($L_{X,0.5\text{–}2\,\mathrm{keV}} \sim 10^{39}$–$10^{41}$ for non-BCG ellipticals), mass-dependent (for most definitions of L_X and L_K, $L_X \propto L_K^2$), and are often visible out to many tens of kpc. But these halos are difficult to connect to the formation of the galaxies because coronal gas can also be produced in the mergers and associated star formation that occurred when the galaxy became elliptical (Read & Ponman 1998), and because it is difficult to disentangle halo gas with the intergroup medium (IGM) in which most large ellipticals reside (Dressler 1980).

In contrast, hot halos around quiescent disk galaxies should be much more direct tracers of the galaxy formation process. While the morphology–density relation makes it difficult to disentangle elliptical galaxies from their dense environments, it also ensures a large supply of isolated spiral galaxies in low-density environments. Late-type disks are destroyed by strong mergers (e.g., Robertson et al. 2006), and it is easy to identify and exclude starbursting galaxies, so it should be straightforward to search for hot halos around quiescent isolated spirals and to connect these halos to models of galaxy formation.

Unfortunately, the search for extended soft X-ray emission around isolated spirals has so far been unsuccessful. There are several detections of emission a few kpc above the disk (Strickland et al. 2004a; Li et al. 2006; Tüllmann et al. 2006; Rasmussen et al. 2009; Owen & Warwick 2009; Yamasaki et al. 2009), but these observations are linked to the star formation in the galaxy and probably represent galactic fountains. In terms of more extended emission, Li et al. (2007) observe gas around the Sombrero galaxy out to 20 kpc, but this galaxy is significantly bulge-dominated, and the extended emission has been linked to a galactic bulge-driven wind. Finally, Pedersen et al. (2006) claimed to detect extended hot halo emission around NGC 5746, but this emission disappeared after subsequent reanalysis with newer calibration files (Rasmussen et al. 2009).

A recent paper (Crain et al. 2010b) attributes these detections of extended emission to galactic coronae, instead of the standard explanation of the emission as a fountain or a wind originating from within the galaxy. This interpretation is in disagreement with the standard understanding of galactic fountains in spiral galaxies, but regardless of interpretation it still is true that no hot halo has been detected around a disk galaxy at a radius of more than a few kpc.

In this paper, we present an analysis of observations by the ACIS-I array on board the *Chandra X-ray Observatory* of the environs of the extremely massive spiral galaxy NGC 1961, in which we detect X-ray emission out to at least 40 kpc and attribute the emission to a hot halo. The outline of the paper is as follows. In Section 2, we discuss the properties of NGC 1961 and the details of our observation. In Section 3, we discuss the reduction of the data and explain various approaches to flat

7.3. Halo Cooling Rates and Implications for Galaxy Formation

We can estimate the cooling radius of this hot halo and the implied accretion rate onto the galaxy, which has implications for setting and regulating the star formation rate in the galaxy. We define the cooling radius as the radius for which the cooling time is 10 Gyr, using the expression for cooling time from Fukugita & Peebles (2006):

$$\tau(r) = \frac{1.5nkT}{\Lambda n_e (n - n_e)} \approx \frac{1.5kT \times 1.92}{\Lambda n_e \times 0.92}, \qquad (1)$$

where the latter expression assumes primeval helium abundance so that the total particle density $n = 1.92n_e$. For $T = 10^{6.85}$ K and $Z = 0.5\,Z_\odot$, $\Lambda = 10^{-22.85}$ erg cm^3 s^{-1} (Sutherland & Dopita 1993). Thus, the cooling radius occurs at $n_e = 6.8 \times 10^{-4}$ cm^{-3}. For the range of best-fit β-model profiles listed above, this corresponds to a cooling radius between 17.8 and 18.2 kpc, and an interior hot halo mass of 8.9–10.2 $\times\ 10^8\ M_\odot$. It is difficult to estimate the accretion rate onto the disk from this hot halo, since the heating rate is unconstrained, but we can make an order-of-magnitude estimate by dividing the hot gas thermal energy within the 10 Gyr cooling radius by the luminosity within that radius; this yields a cooling time of 2.0–2.4 Gyr for material within the cooling radius, or an effective cooling rate of $0.4\,M_\odot\ \mathrm{yr}^{-1}$. In contrast, we can estimate the star formation rate in NGC 1961 from the total Hα luminosity ($7.6 \pm 0.9 \times 10^{41}$ erg s^{-1}) using the relation in Kennicutt (1998): star formation rate SFR $= 7.9 \times 10^{-42}$ $L(\mathrm{H}\alpha) = 6.0 \pm 0.7\ M_\odot\ \mathrm{yr}^{-1}$. The halo accretion rate is therefore insufficient to produce the star formation rate of the galaxy. More relevant for galaxy formation, the halo accretion rate is two orders of magnitude too low to assemble the stellar mass of this galaxy within a Hubble time. If we preserve β and r_0 for the halo, but increase S_0 to add the present-day stellar mass of $3.1 \times 10^{11}\ M_\odot$ to the halo, the cooling rate becomes 1.2–1.8 $M_\odot$ yr^{-1}, which is still insufficient to assemble the stellar mass by a factor of 20.

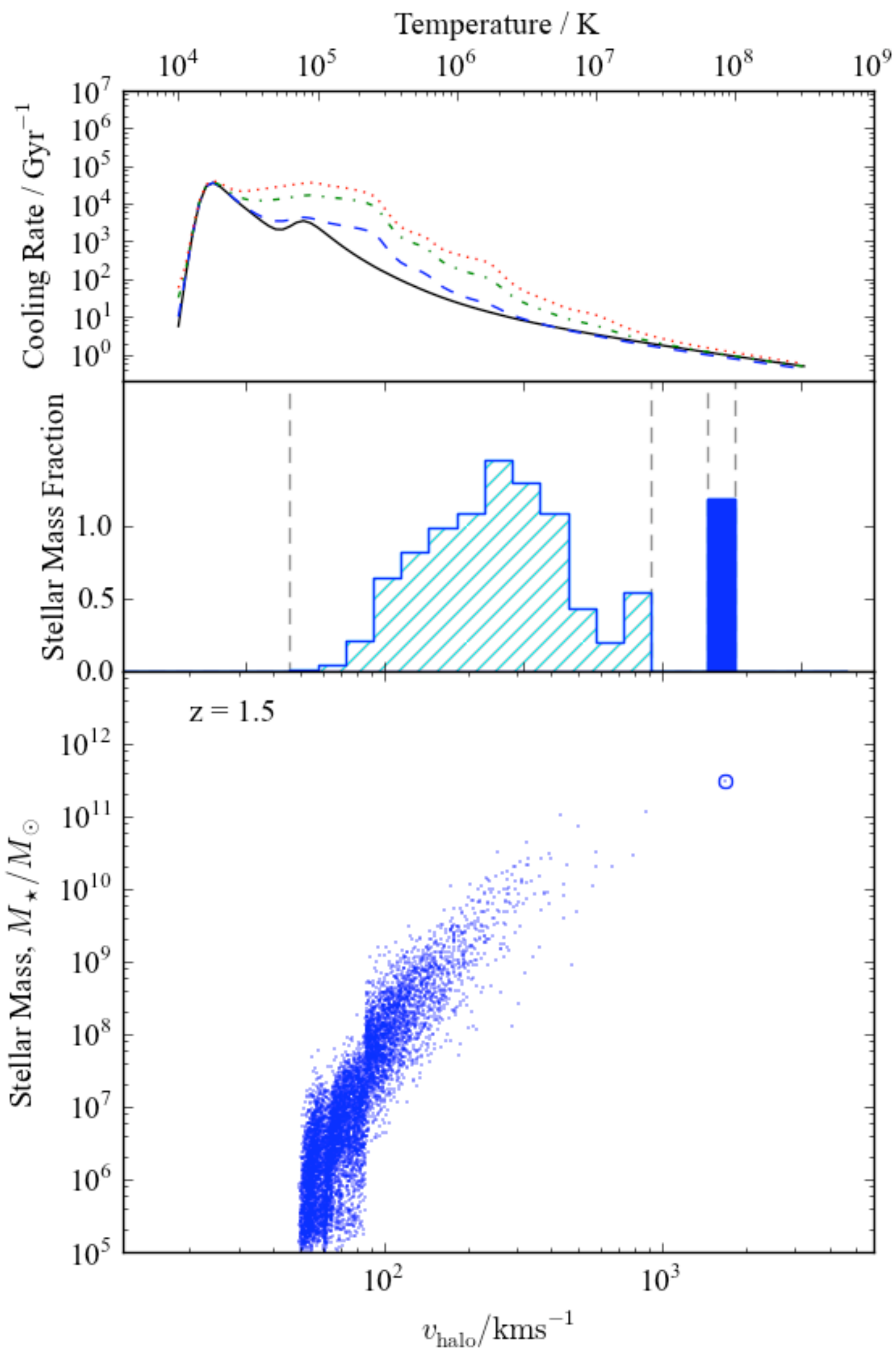

Temperature / K
10^4
10^5
10^6
10^7
10^8
10^9
Cooling Rate / Gyr^{-1}
Stellar Mass Fraction
z = 1.5
Stellar Mass, $M_\star/M_\odot$
$v_{\rm halo}/{\rm kms}^{-1}$

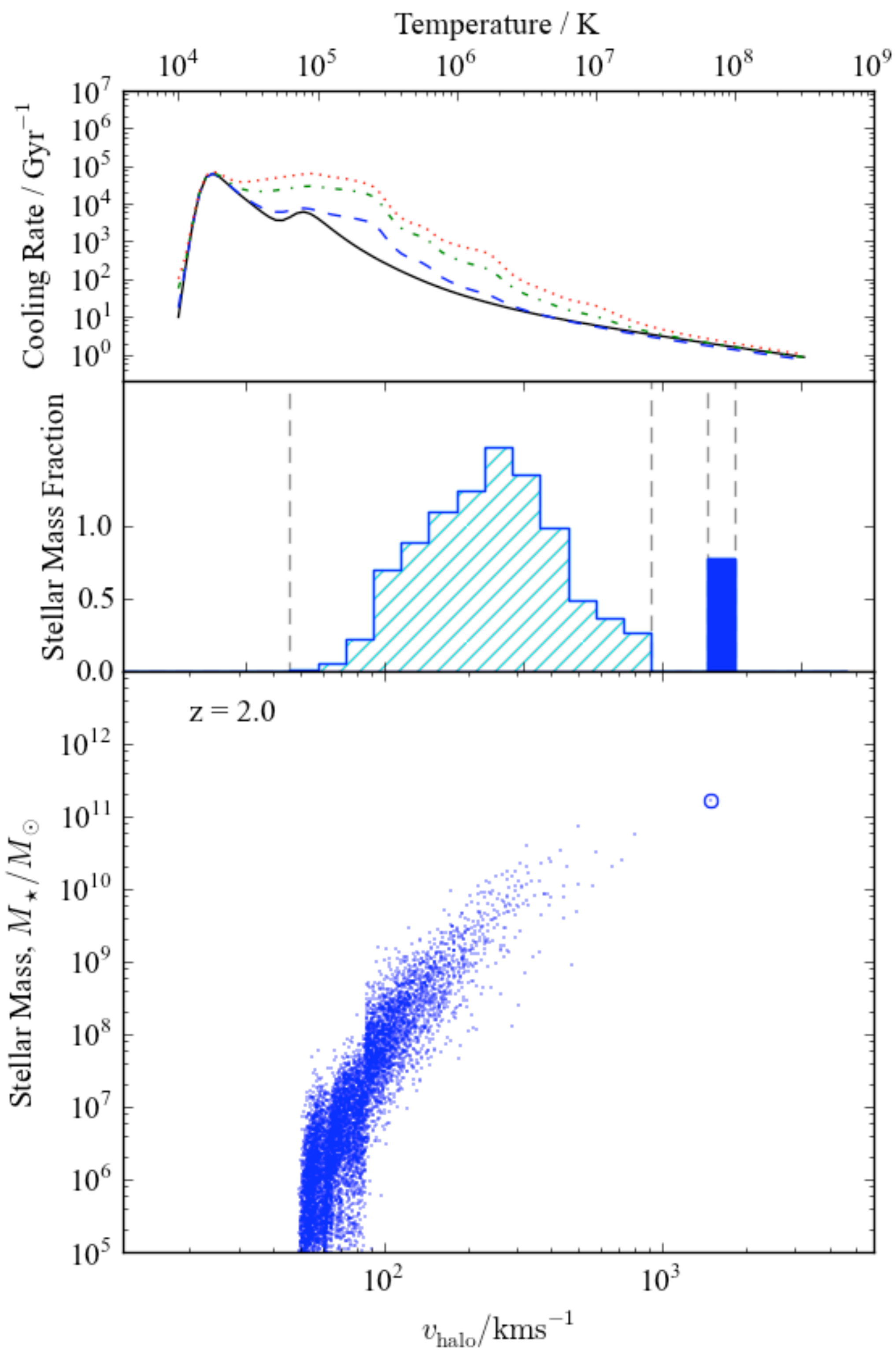

Temperature / K
Cooling Rate / Gyr^{-1}
Stellar Mass Fraction
z = 2.0
Stellar Mass, $M_\star / M_\odot$
$v_{\rm halo}/{\rm kms}^{-1}$

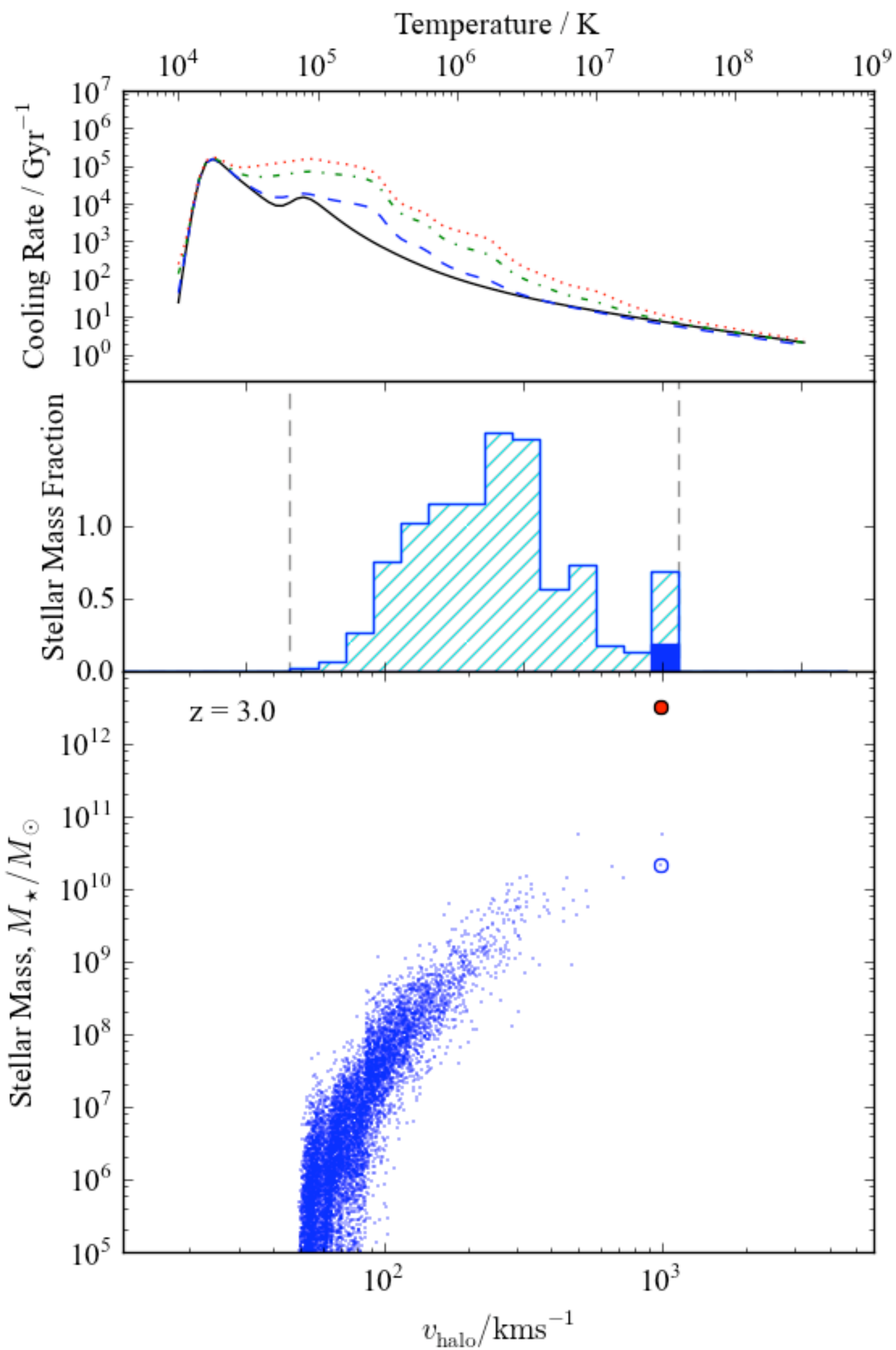

Temperature / K
Cooling Rate / Gyr^{-1}
Stellar Mass Fraction
z = 3.0
Stellar Mass, $M_\star/M_\odot$
$v_{\rm halo}/{\rm kms}^{-1}$

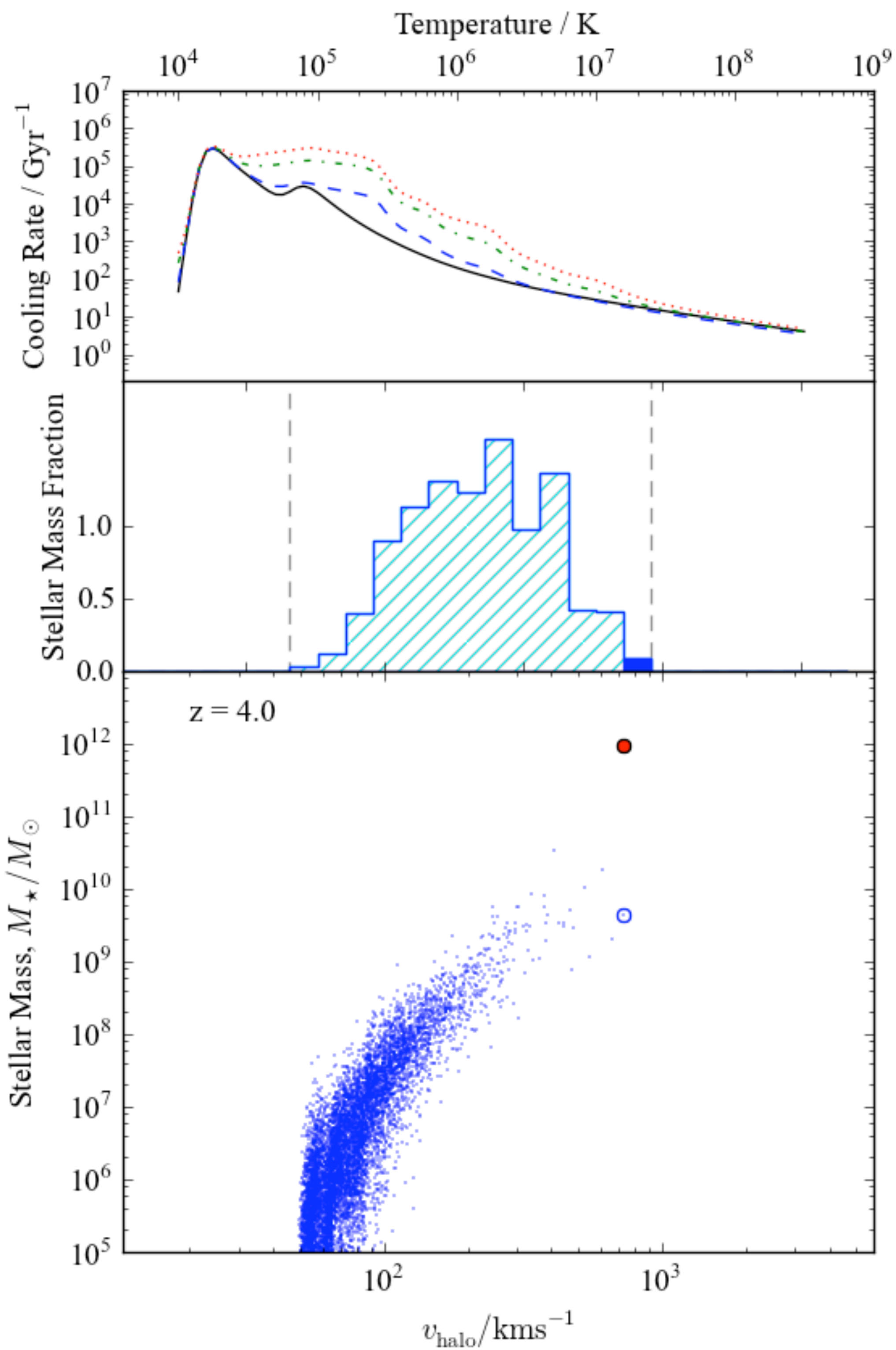

Temperature / K
Cooling Rate / Gyr^{-1}
Stellar Mass Fraction
z = 4.0
Stellar Mass, $M_\star/M_\odot$
$v_{\rm halo}/{\rm kms}^{-1}$

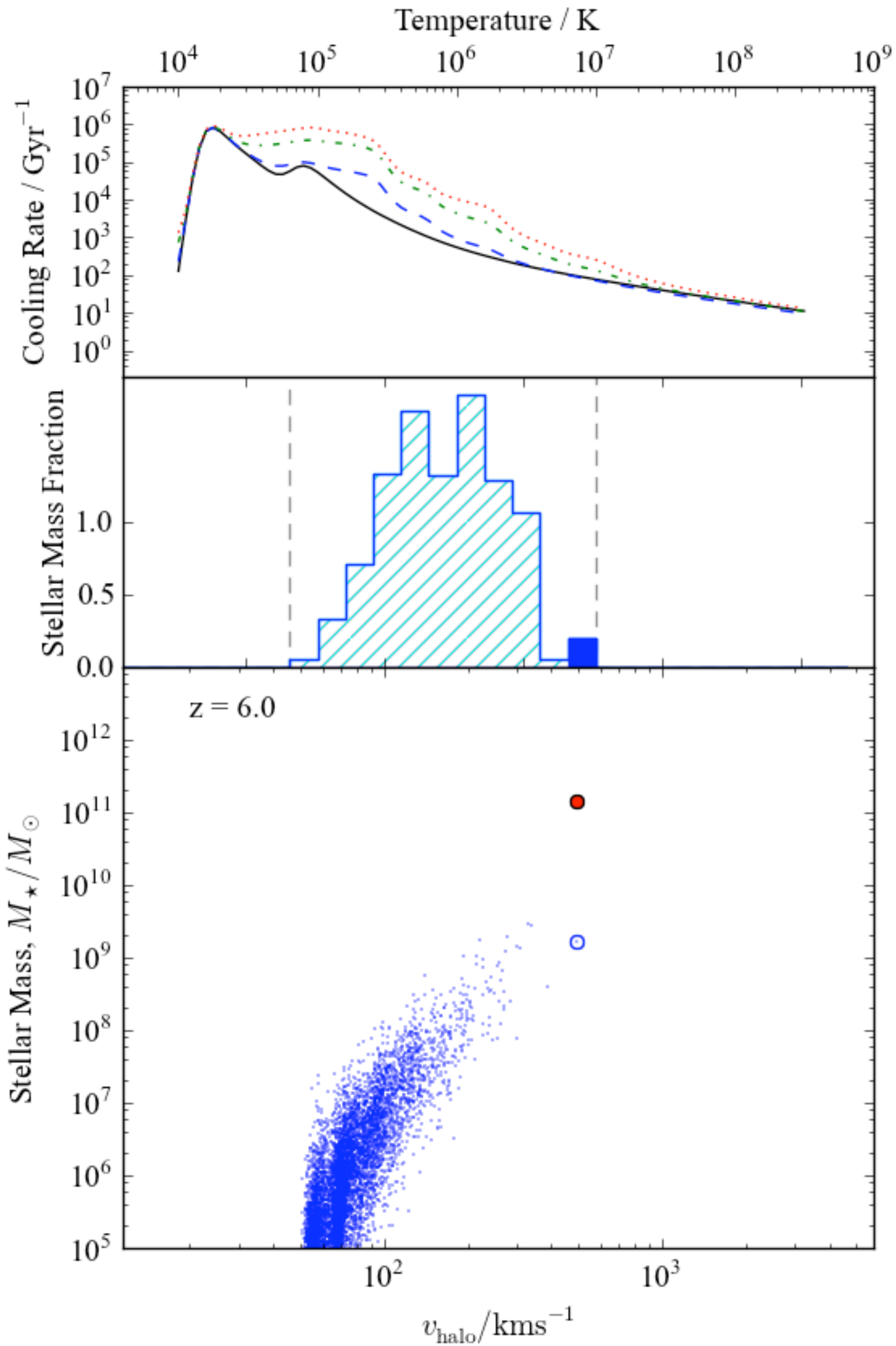

Temperature / K
Cooling Rate / Gyr^{-1}
Stellar Mass Fraction
z = 6.0
Stellar Mass, $M_\star / M_\odot$
$v_{\rm halo}/{\rm kms}^{-1}$

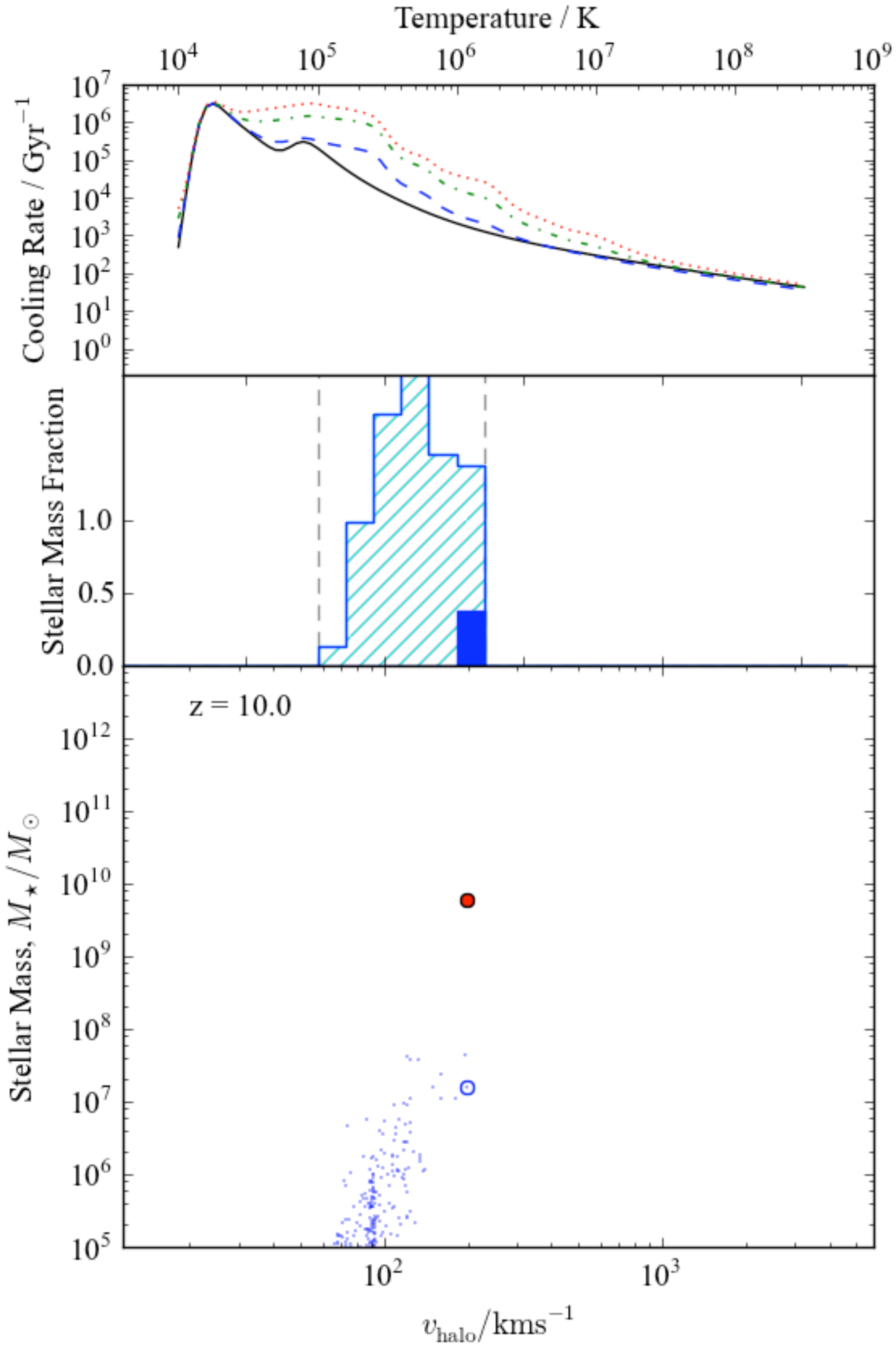

Temperature / K
Cooling Rate / Gyr^{-1}
Stellar Mass Fraction
z = 10.0
Stellar Mass, $M_\star / M_\odot$
$v_{\rm halo}/{\rm kms}^{-1}$

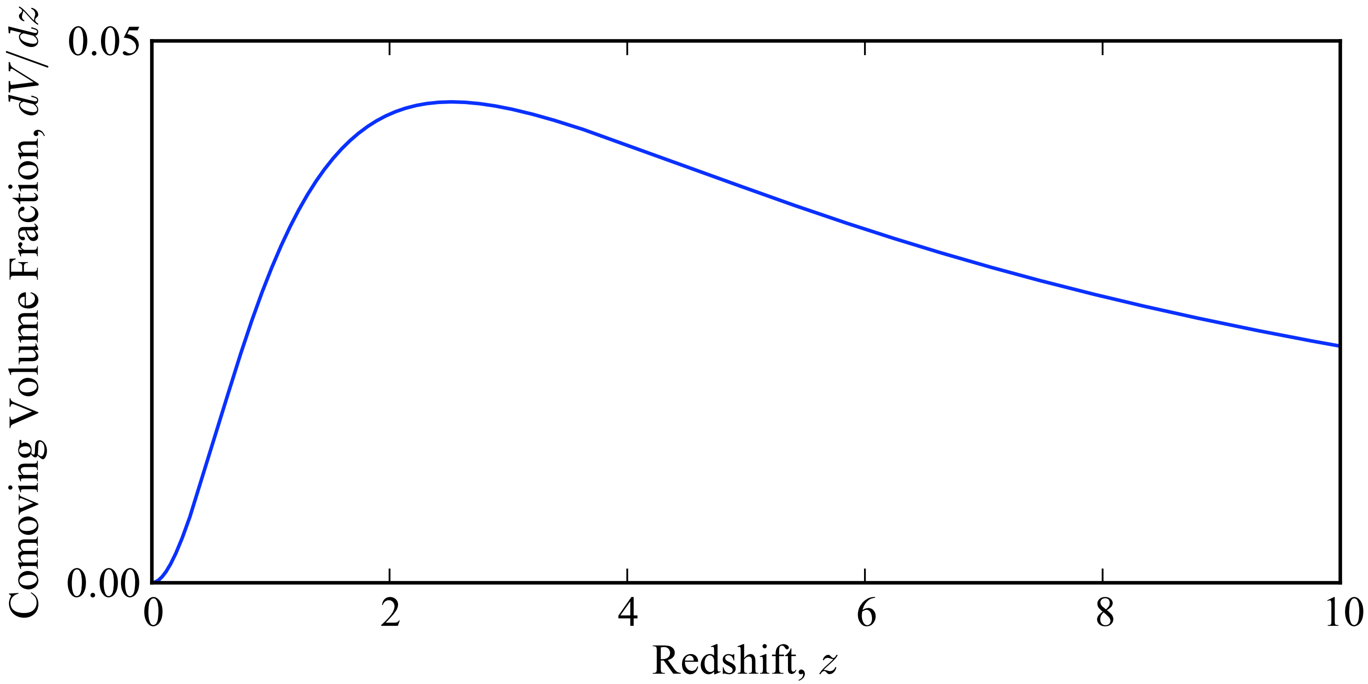

Comoving Volume Fraction, dV/dz
0.05
0.00
0
2
4
6
8
10
Redshift, z

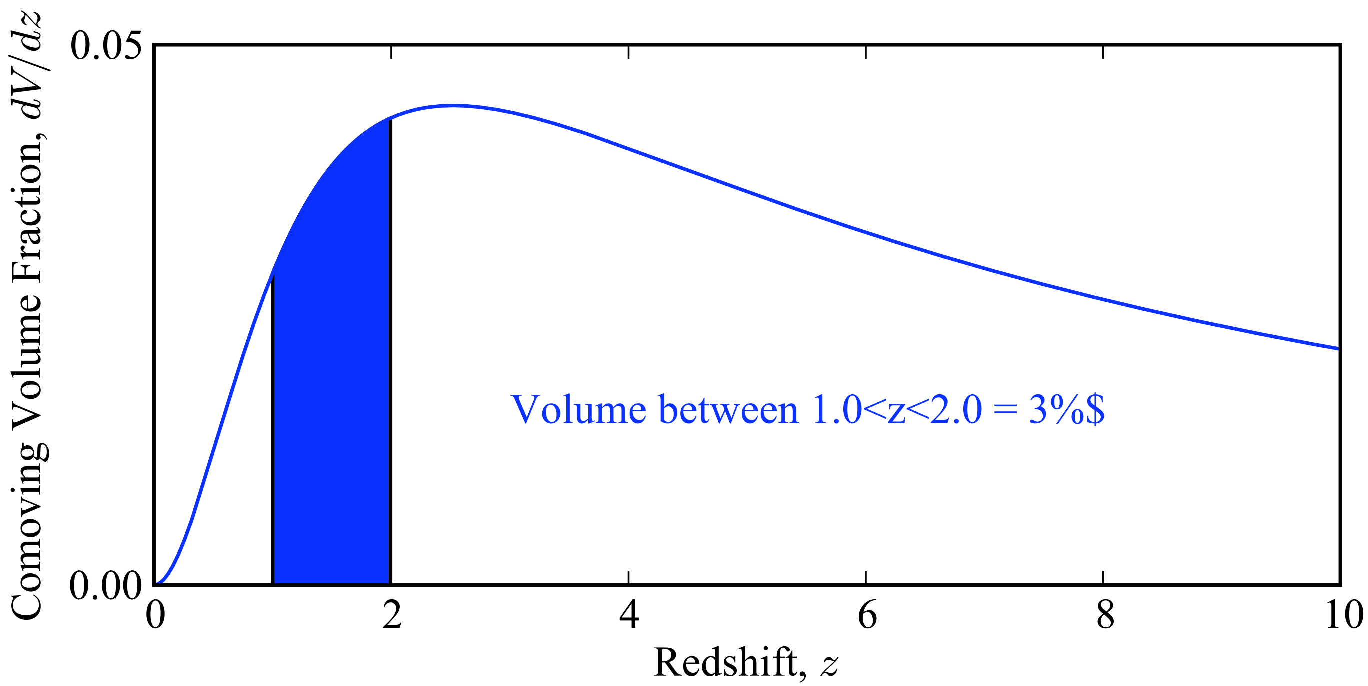

Comoving Volume Fraction, dV/dz
0.05
0.00
Volume between 1.0<z<2.0 = 3%$
0
2
4
6
8
10
Redshift, z

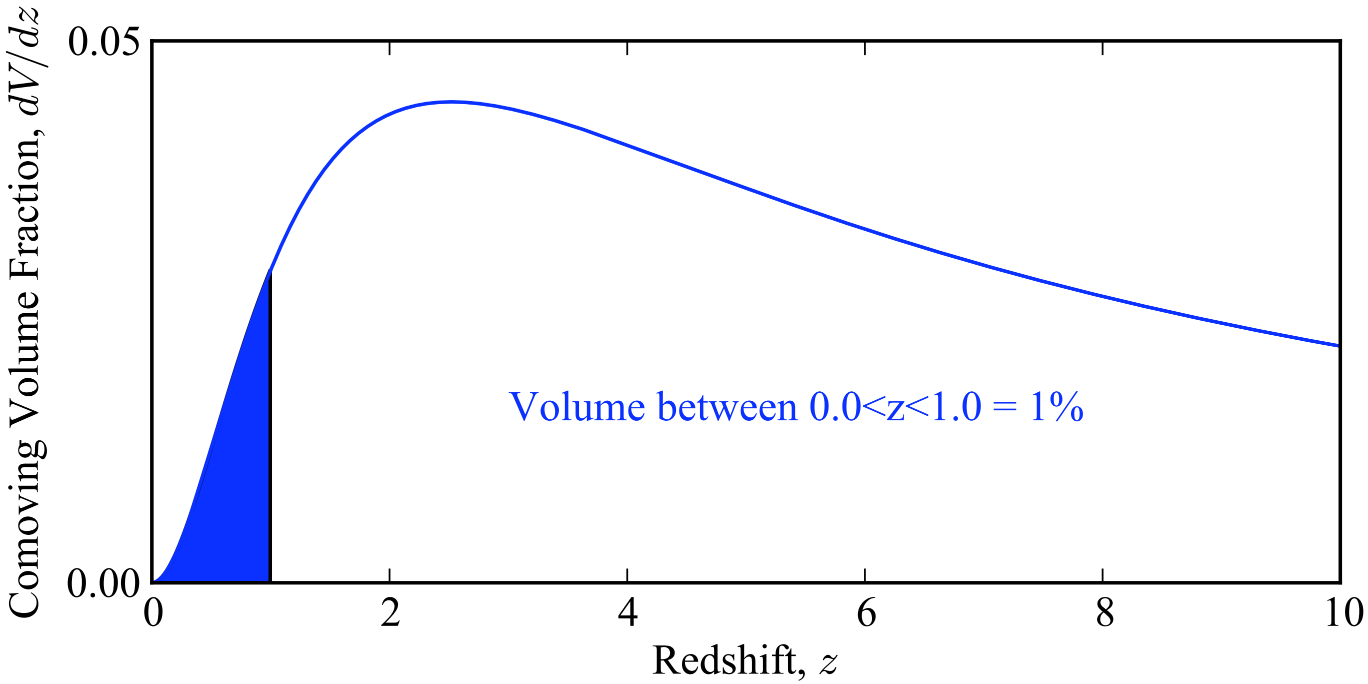
0.05
0.00
0
2
4
6
8
10
Comoving Volume Fraction, dV/dz
Redshift, z
Volume between 0.0<z<1.0 = 1%

Accepted to ApJ
Preprint typeset using LaTeX style emulateapj v. 5/2/11

CAN MINOR MERGING ACCOUNT FOR THE SIZE GROWTH OF QUIESCENT GALAXIES? NEW RESULTS FROM THE CANDELS SURVEY

Andrew B. Newman[1], Richard S. Ellis[1], Kevin Bundy[2], and Tommaso Treu[3]
[1] Cahill Center for Astronomy & Astrophysics, California Institute of Technology, MS 249-17, Pasadena, CA 91125, USA
[2] Institute for the Physics and Mathematics of the Universe, University of Tokyo, Kashiwa 277-8582, Japan
[3] Department of Physics, University of California, Santa Barbara, CA 93106, USA
Accepted to ApJ

ABSTRACT

The presence of extremely compact galaxies at $z \sim 2$ and their subsequent growth in physical size has been the cause of much puzzlement. We revisit the question using deep infrared Wide Field Camera 3 data to probe the rest-frame optical structure of 935 galaxies selected with $0.4 < z < 2.5$ and stellar masses $M_* > 10^{10.7} M_\odot$ in the UKIRT Ultra Deep Survey and GOODS-South fields of the CANDELS survey. At each redshift, the most compact sources are those with little or no star formation, and the mean size of these systems at fixed stellar mass grows by a factor of 3.5 ± 0.3 over this redshift interval. The data are sufficiently deep to identify companions to these hosts whose stellar masses are ten times smaller. By searching for these around 404 quiescent hosts within a physical annulus $10\ h^{-1}$ kpc $< R < 30\ h^{-1}$ kpc, we estimate the minor merger rate over $0.4 < z < 2$. We find that $13\% - 18\%$ of quiescent hosts have likely physical companions with stellar mass ratios of 0.1 or greater. Mergers of these companions will typically increase the host mass by $6\% \pm 2\%$ per merger timescale. We estimate the minimum growth rate necessary to explain the declining abundance of compact galaxies. Using a simple model motivated by recent numerical simulations, we then assess whether mergers of the faint companions with their hosts are sufficient to explain this minimal rate. We find that mergers may explain most of the size evolution observed at $z \lesssim 1$ if a relatively short merger timescale is assumed, but the rapid growth seen at higher redshift likely requires additional physical processes.

Subject headings: galaxies: evolution — galaxies: formation — galaxies: fundamental parameters — galaxies: structure

1. INTRODUCTION

The compact nature of massive quiescent galaxies at redshifts $z \simeq 2$ was a surprising discovery when it was announced some years ago (e.g., Daddi et al. 2005; Trujillo et al. 2006; Buitrago et al. 2008; van Dokkum et al. 2008). Many red galaxies with stellar masses $M_* \simeq 10^{11} M_\odot$ have effective radii $R_e \simeq 1$ kpc, $3-5$ times smaller than comparably massive early-type galaxies in the local universe. This suggests that they grew significantly in size, but much less in stellar mass. Initially there was some suspicion that the stellar masses of the $z \simeq 2$ sources were overestimated, but deep spectroscopic data (Cappellari et al. 2009; Newman et al. 2010; van de Sande et al. 2011) have verified dynamically the high masses of selected $1 < z < 2$ sources and, in conjunction with the abundance of dynamical masses for lower redshift sources (Treu et al. 2005; van der Wel et al. 2005), provided a valuable, independent confirmation of the size evolution.

Only two physical explanations have been put forward to explain this remarkable growth in size while avoiding the overproduction of present-day high-mass galaxies. Adiabatic expansion through significant mass loss can lead to size growth (Fan et al. 2008, 2010). A galaxy that loses mass as a result of winds driven by an active nucleus or supernovae, for example, will adjust its size in response to the shallower central potential. However, the "puffing up" arising from baryonic mass loss occurs only when the system is highly active and young in terms of its stellar population (Ragone-Figueroa & Granato 2011, see also Bezanson et al. 2009), so it is difficult to see how this mechanism can account for the gradual and persistent growth in size observed for compact sources that are mostly quiescent in nature.

In a hierarchical picture of galaxy formation, mergers are expected to lead to growth in size and stellar mass. Whereas major mergers, involving nearly equal-mass components, will lead to comparable growth in both size and mass, minor mergers involving lower-mass companions can produce more efficient size growth (Bezanson et al. 2009; Naab et al. 2009; Hopkins et al. 2010c). This mechanism requires a high rate of occurrence of minor mergers, a significant fraction of which must involve gas-poor companions. Although the major merger rate is observationally constrained reasonably well over $0 < z < 1$ (e.g., Kartaltepe et al. 2007; Lin et al. 2008; Bundy et al. 2009; de Ravel et al. 2009; Lotz et al. 2011) and via a few measurements up to $z \simeq 3$ (e.g., Bluck et al. 2009; Man et al. 2011), the rate at which minor merging occurs requires exquisitely deep photometric data. For this hypothesis, the key question is whether observations confirm that minor merging occurs at the required rate.

The infrared Wide Field Camera 3 (WFC3/IR) on board the Hubble Space Telescope (*HST*) enables us to address the question of whether minor merging is sufficiently frequent to account for the size growth of compact sources since $z \simeq 2$. The CANDELS survey (GO 12444/5; PIs: H. C. Ferguson and S. M. Faber) provides an excellent resource for addressing this question since,

anewman@astro.caltech.edu

ACCEPTED TO APJ
Preprint typeset using LaTeX style emulateapj v. 5/2/11

CAN MINOR MERGING ACCOUNT FOR THE SIZE GROWTH OF QUIESCENT GALAXIES? NEW RESULTS FROM THE CANDELS SURVEY

ANDREW B. NEWMAN[1], RICHARD S. ELLIS[1], KEVIN BUNDY[2], AND TOMMASO TREU[3]
[1] Cahill Center for Astronomy & Astrophysics, California Institute of Technology, MS 249-17, Pasadena, CA 91125, USA
[2] Institute for the Physics and Mathematics of the Universe, University of Tokyo, Kashiwa 277-8582, Japan
[3] Department of Physics, University of California, Santa Barbara, CA 93106, USA
Accepted to ApJ

ABSTRACT

The presence of extremely compact galaxies at $z \sim 2$ and their subsequent growth in physical size has been the cause of much puzzlement. We revisit the question using deep infrared Wide Field Camera 3 data to probe the rest-frame optical structure of 935 galaxies selected with $0.4 < z < 2.5$ and stellar masses $M_* > 10^{10.7} M_\odot$ in the UKIRT Ultra Deep Survey and GOODS-South fields of the CANDELS survey. At each redshift, the most compact sources are those with little or no star formation, and the mean size of these systems at fixed stellar mass grows by a factor of 3.5 ± 0.3 over this redshift interval. The data are sufficiently deep to identify companions to these hosts whose stellar masses are ten times smaller. By searching for these around 404 quiescent hosts within a physical annulus $10\ h^{-1}$ kpc $< R < 30\ h^{-1}$ kpc, we estimate the minor merger rate over $0.4 < z < 2$. We find that $13\% - 18\%$ of quiescent hosts have likely physical companions with stellar mass ratios of 0.1 or greater. Mergers of these companions will typically increase the host mass by $6\% \pm 2\%$ per merger timescale. We estimate the minimum growth rate necessary to explain the declining abundance of compact galaxies. Using a simple model motivated by recent numerical simulations, we then assess whether mergers of the faint companions with their hosts are sufficient to explain this minimal rate. We find that mergers may explain most of the size evolution observed at $z \lesssim 1$ if a relatively short merger timescale is assumed, but the rapid growth seen at higher redshift likely requires additional physical processes.

Subject headings: galaxies: evolution — galaxies: formation — galaxies: fundamental parameters — galaxies: structure

1. INTRODUCTION

The compact nature of massive quiescent galaxies at redshifts $z \simeq 2$ was a surprising discovery when it was announced some years ago (e.g., Daddi et al. 2005; Trujillo et al. 2006; Buitrago et al. 2008; van Dokkum et al. 2008). Many red galaxies with stellar masses $M_* \simeq 10^{11} M_\odot$ have effective radii $R_e \simeq 1$ kpc, $3-5$ times smaller than comparably massive early-type galaxies in the local universe. This suggests that they grew significantly in size, but much less in stellar mass. Initially there was some suspicion that the stellar masses of the $z \simeq 2$ sources were overestimated, but deep spectroscopic data (Cappellari et al. 2009; Newman et al. 2010; van de Sande et al. 2011) have verified dynamically the high masses of selected $1 < z < 2$ sources and, in conjunction with the abundance of dynamical masses for lower redshift sources (Treu et al. 2005; van der Wel et al. 2005), provided a valuable, independent confirmation of the size evolution.

Only two physical explanations have been put forward to explain this remarkable growth in size while avoiding the overproduction of present-day high-mass galaxies. Adiabatic expansion through significant mass loss can lead to size growth (Fan et al. 2008, 2010). A galaxy that loses mass as a result of winds driven by an active nucleus or supernovae, for example, will adjust its size in response to the shallower central potential. However, the "puffing up" arising from baryonic mass loss occurs only when the system is highly active and young in terms of its stellar population (Ragone-Figueroa & Granato 2011, see also Bezanson et al. 2009), so it is difficult to see how this mechanism can account for the gradual and persistent growth in size observed for compact sources that are mostly quiescent in nature.

In a hierarchical picture of galaxy formation, mergers are expected to lead to growth in size and stellar mass. Whereas major mergers, involving nearly equal-mass components, will lead to comparable growth in both size and mass, minor mergers involving lower-mass companions can produce more efficient size growth (Bezanson et al. 2009; Naab et al. 2009; Hopkins et al. 2010c). This mechanism requires a high rate of occurrence of minor mergers, a significant fraction of which must involve gas-poor companions. Although the major merger rate is observationally constrained reasonably well over $0 < z < 1$ (e.g., Kartaltepe et al. 2007; Lin et al. 2008; Bundy et al. 2009; de Ravel et al. 2009; Lotz et al. 2011) and via a few measurements up to $z \simeq 3$ (e.g., Bluck et al. 2009; Man et al. 2011), the rate at which minor merging occurs requires exquisitely deep photometric data. For this hypothesis, the key question is whether observations confirm that minor merging occurs at the required rate.

The infrared Wide Field Camera 3 (WFC3/IR) on board the Hubble Space Telescope (*HST*) enables us to address the question of whether minor merging is sufficiently frequent to account for the size growth of compact sources since $z \simeq 2$. The CANDELS survey (GO 12444/5; PIs: H. C. Ferguson and S. M. Faber) provides an excellent resource for addressing this question since,

anewman@astro.caltech.edu

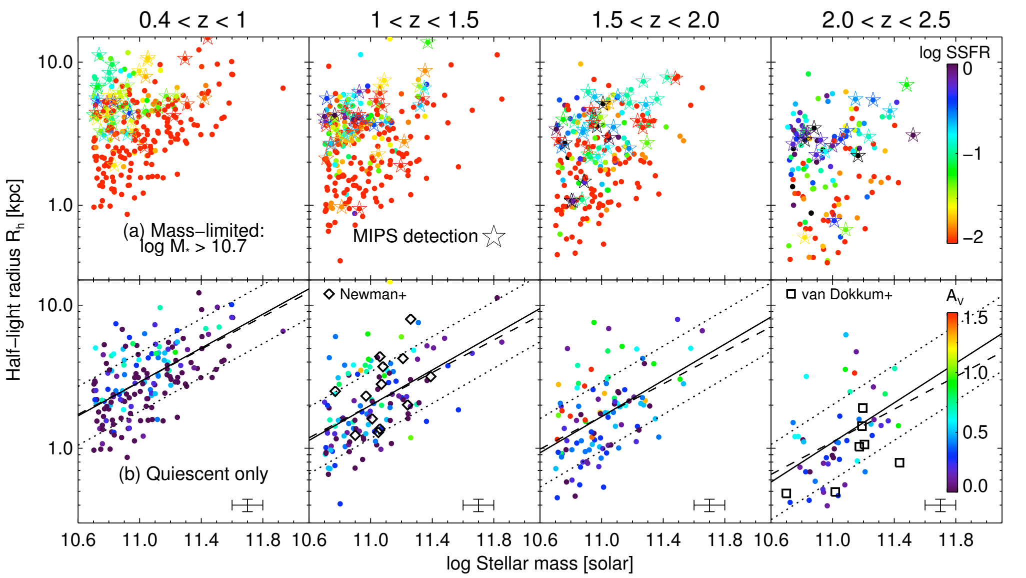

Martin Stringer

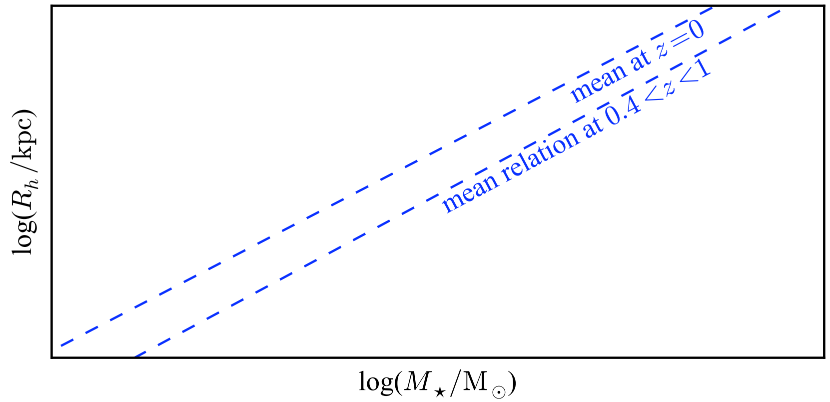

mean at $z=0$
mean relation at $0.4<z<1$
$\log(R_h/\mathrm{kpc})$
$\log(M_\star/\mathrm{M}_\odot)$

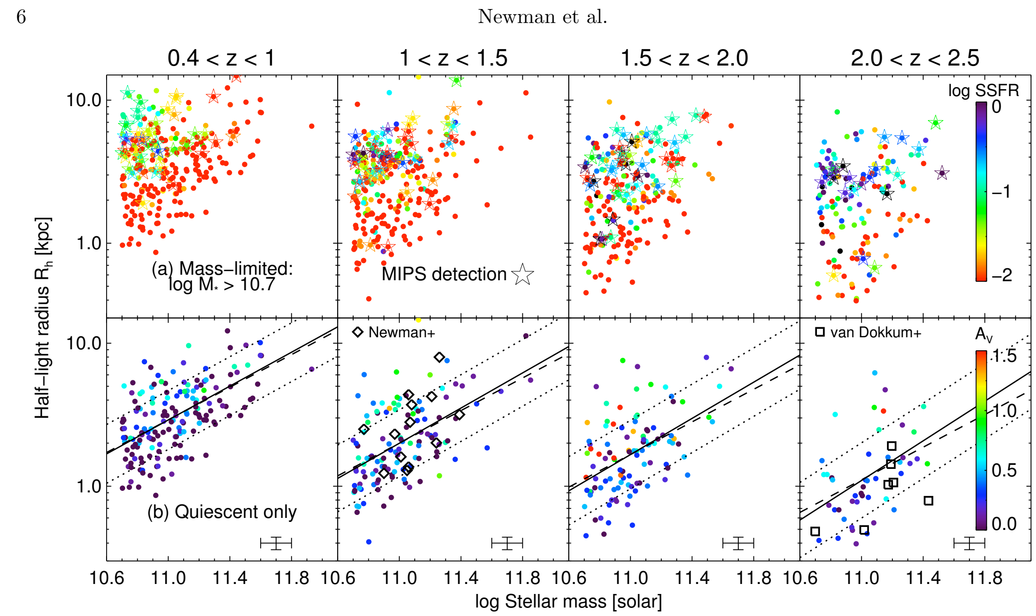

6
Newman et al.
0.4 < z < 1
1 < z < 1.5
1.5 < z < 2.0
2.0 < z < 2.5
log SSFR
(a) Mass–limited: log M* > 10.7
MIPS detection
(b) Quiescent only
Newman+
van Dokkum+
A_V
Half–light radius R_h [kpc]
log Stellar mass [solar]

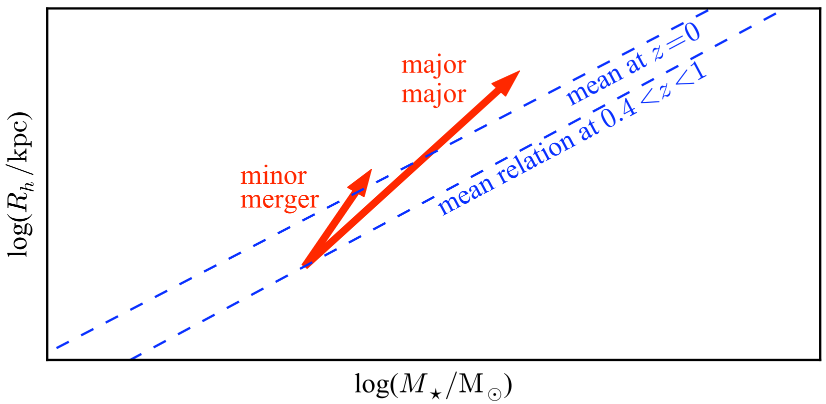

major
major
minor
merger
mean at $z=0$
mean relation at $0.4<z<1$
$\log(R_h/\mathrm{kpc})$
$\log(M_\star/\mathrm{M}_\odot)$

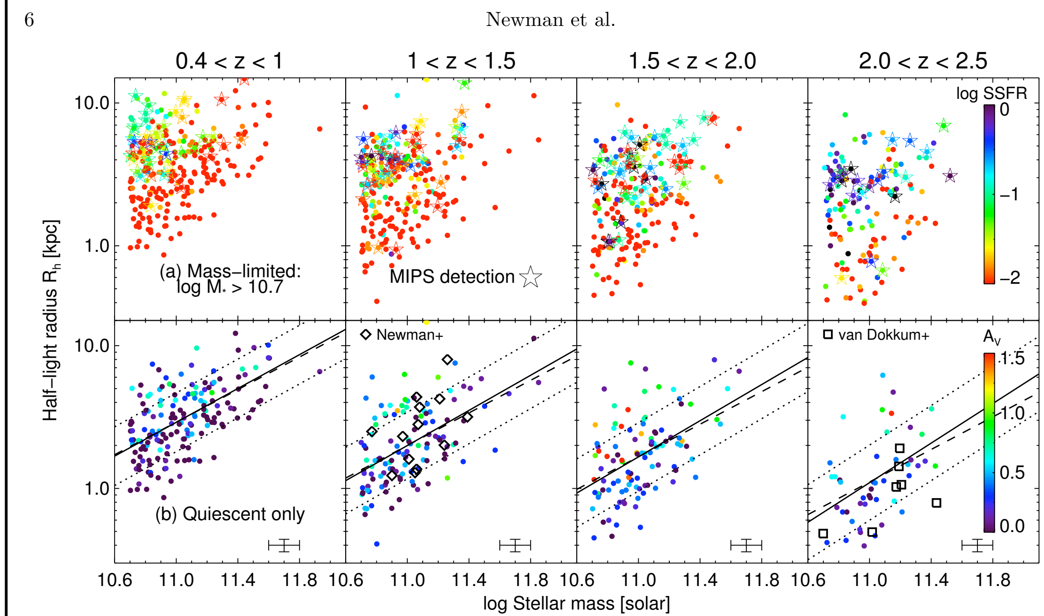

6
Newman et al.
0.4 < z < 1
1 < z < 1.5
1.5 < z < 2.0
2.0 < z < 2.5
log SSFR
(a) Mass-limited: log M. > 10.7
MIPS detection
(b) Quiescent only
Newman+
van Dokkum+
A_V
Half-light radius R_h [kpc]
log Stellar mass [solar]

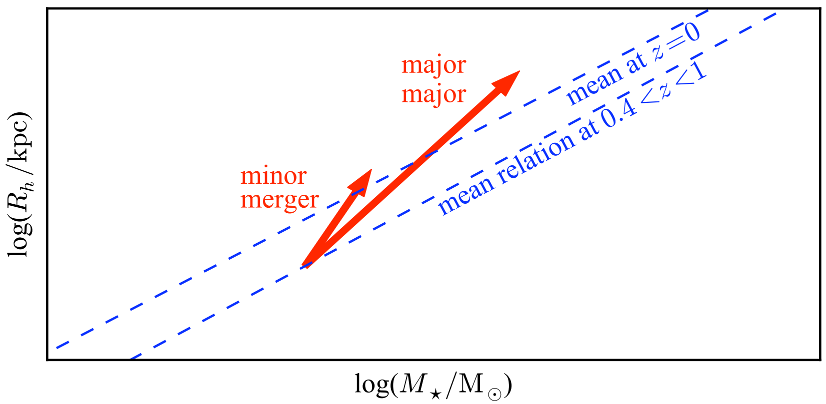

6 Newman et al.

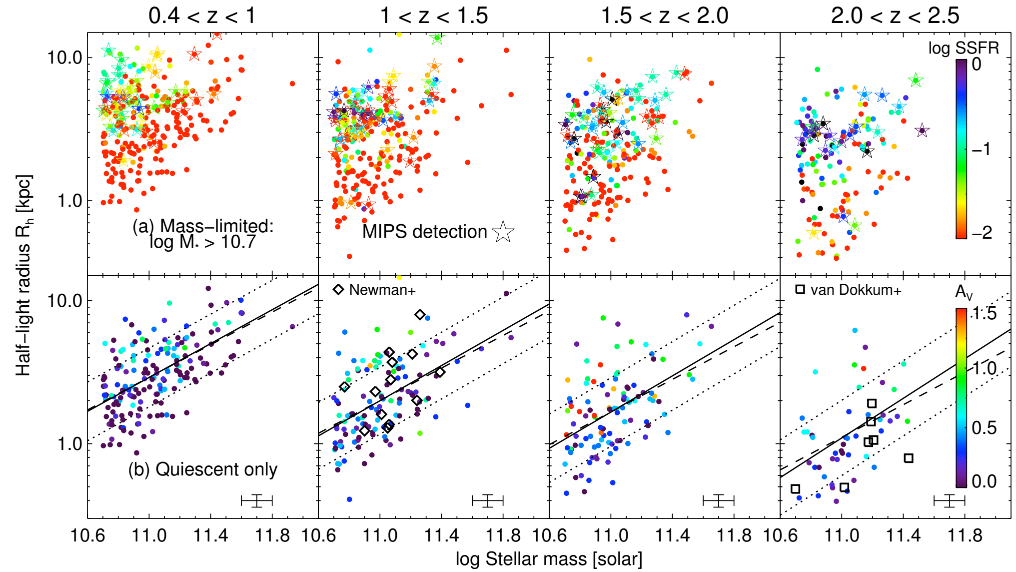

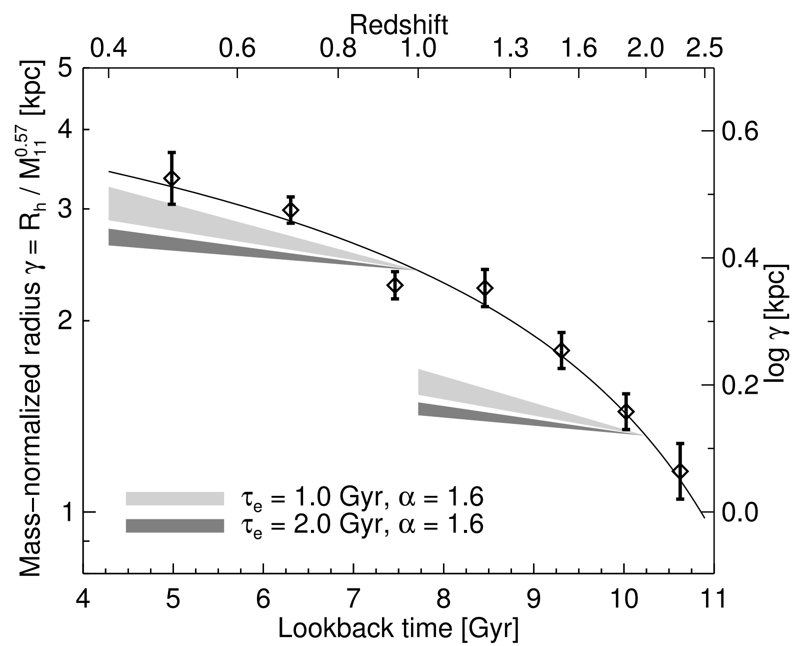

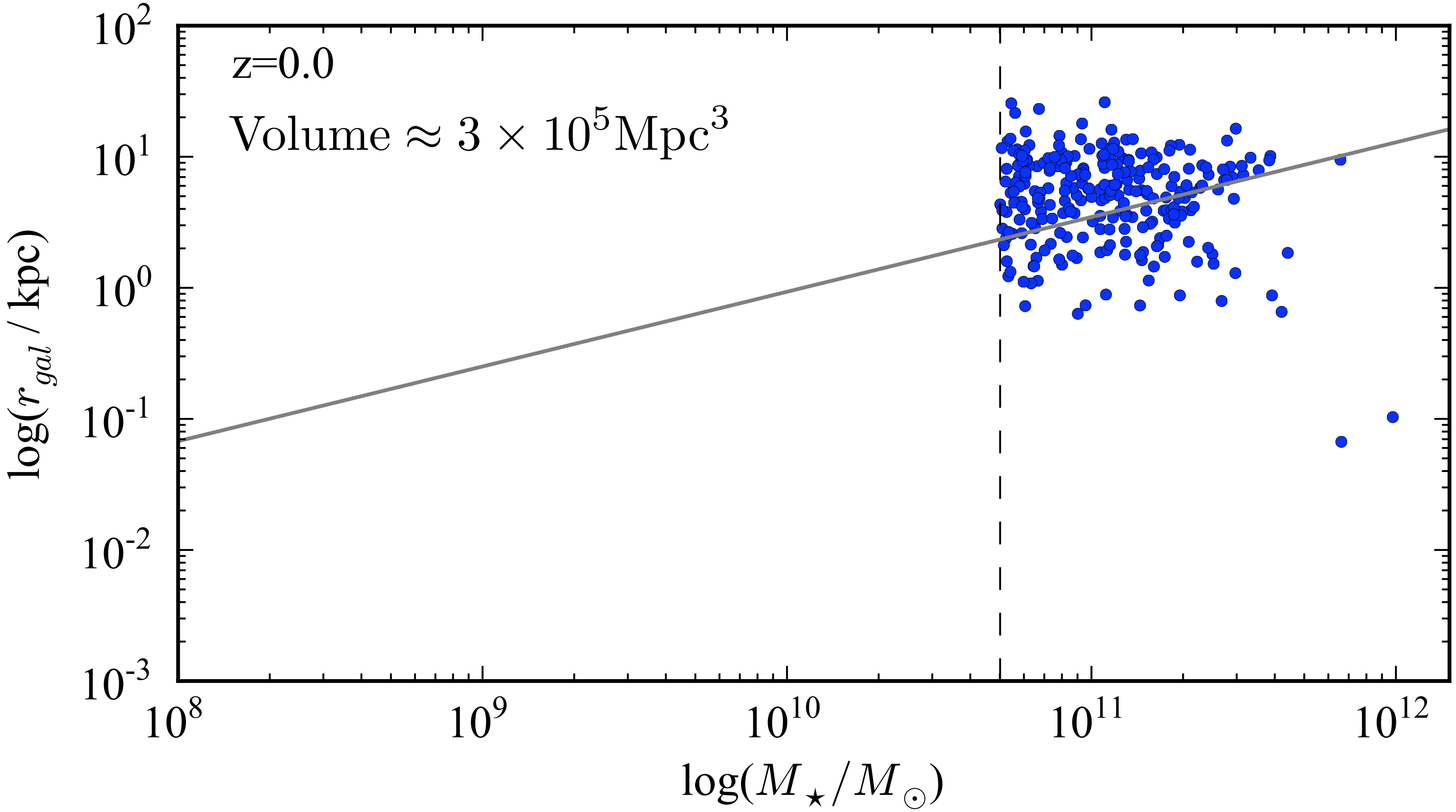
z=0.0
Volume $\approx 3 \times 10^5 \mathrm{Mpc}^3$
$\log(r_{gal}$ / kpc)
$\log(M_\star/M_\odot)$
10^{-3}
10^{-2}
10^{-1}
10^{0}
10^{1}
10^{2}
10^{8}
10^{9}
10^{10}
10^{11}
10^{12}

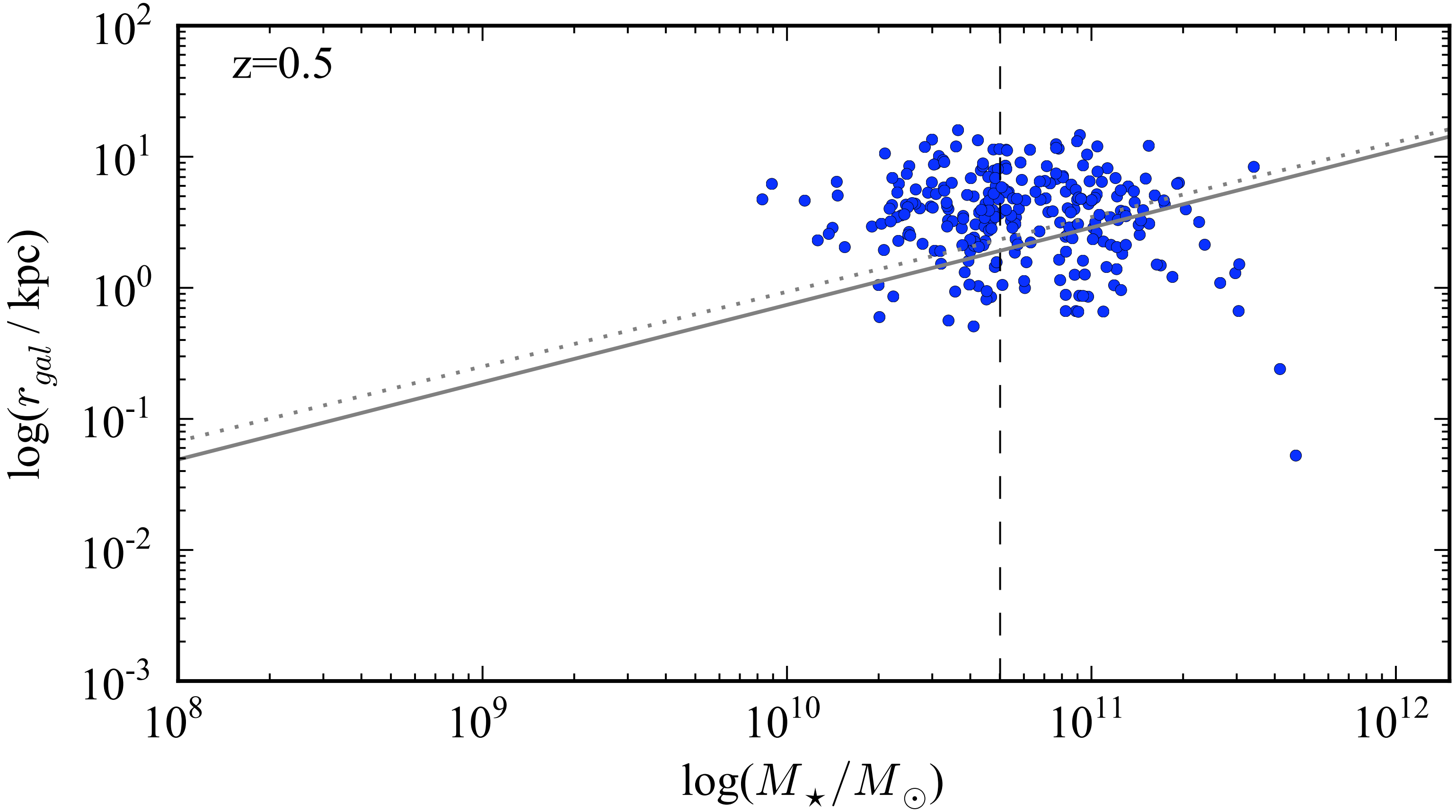

Martin Stringer l'Observatoire de Paris LERMA

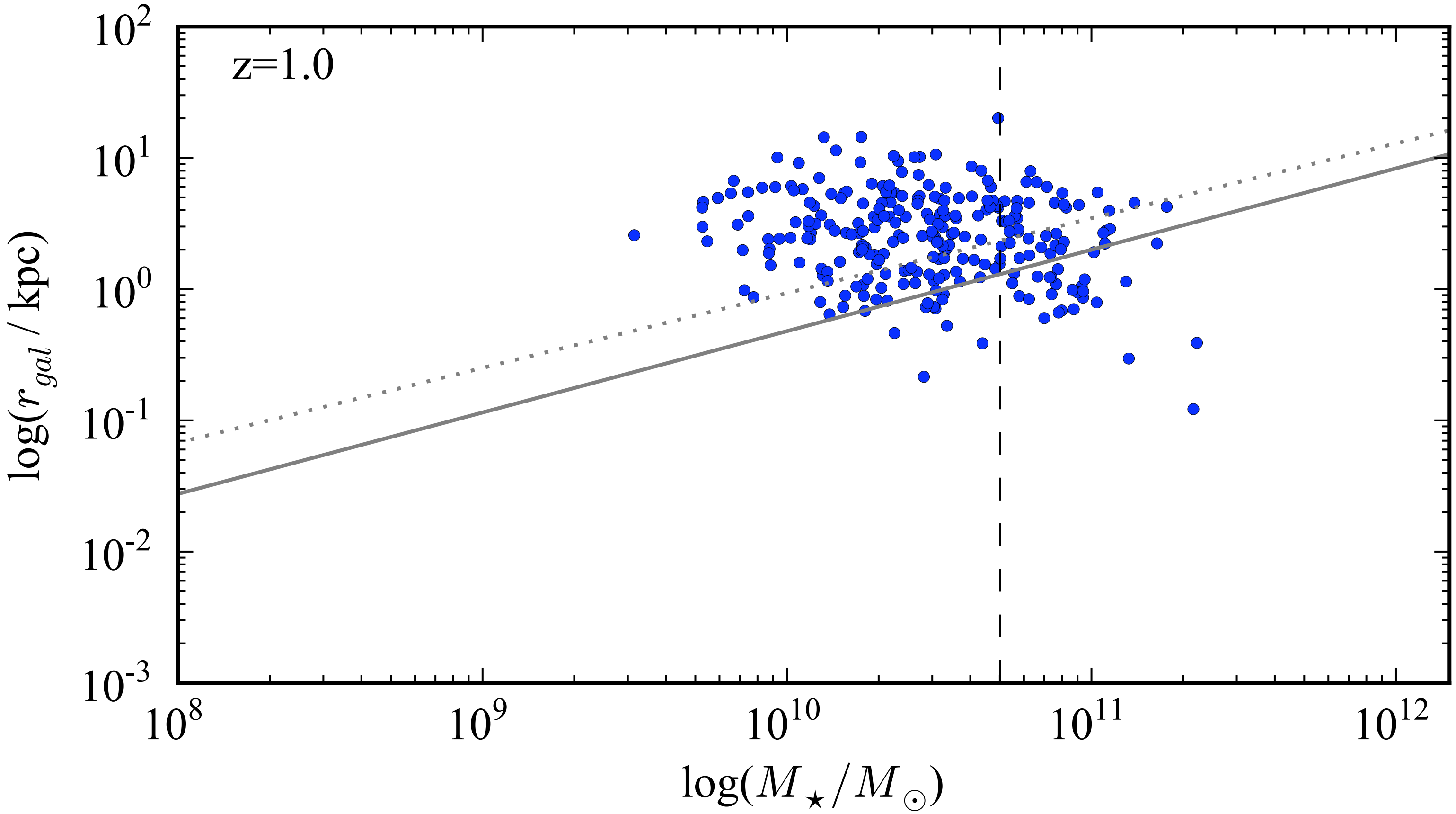

z=1.0
10^{2}
10^{1}
10^{0}
10^{-1}
10^{-2}
10^{-3}
$\log(r_{gal}$ / kpc)
10^{8}
10^{9}
10^{10}
10^{11}
10^{12}
$\log(M_\star/M_\odot)$

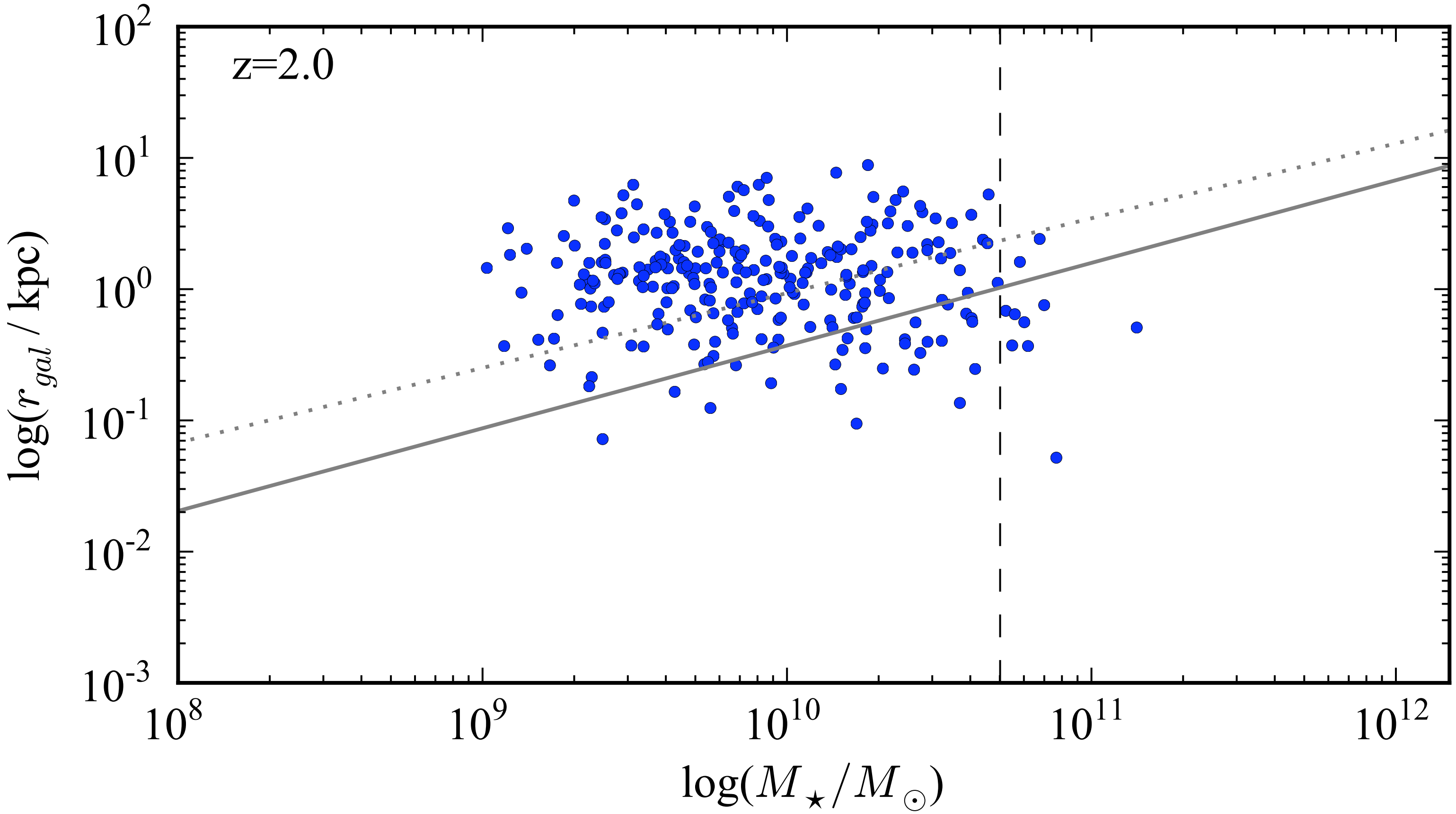

z=2.0
10^2
10^1
10^0
10^{-1}
10^{-2}
10^{-3}
10^8
10^9
10^{10}
10^{11}
10^{12}
$\log(r_{gal}$ / kpc)
$\log(M_\star/M_\odot)$

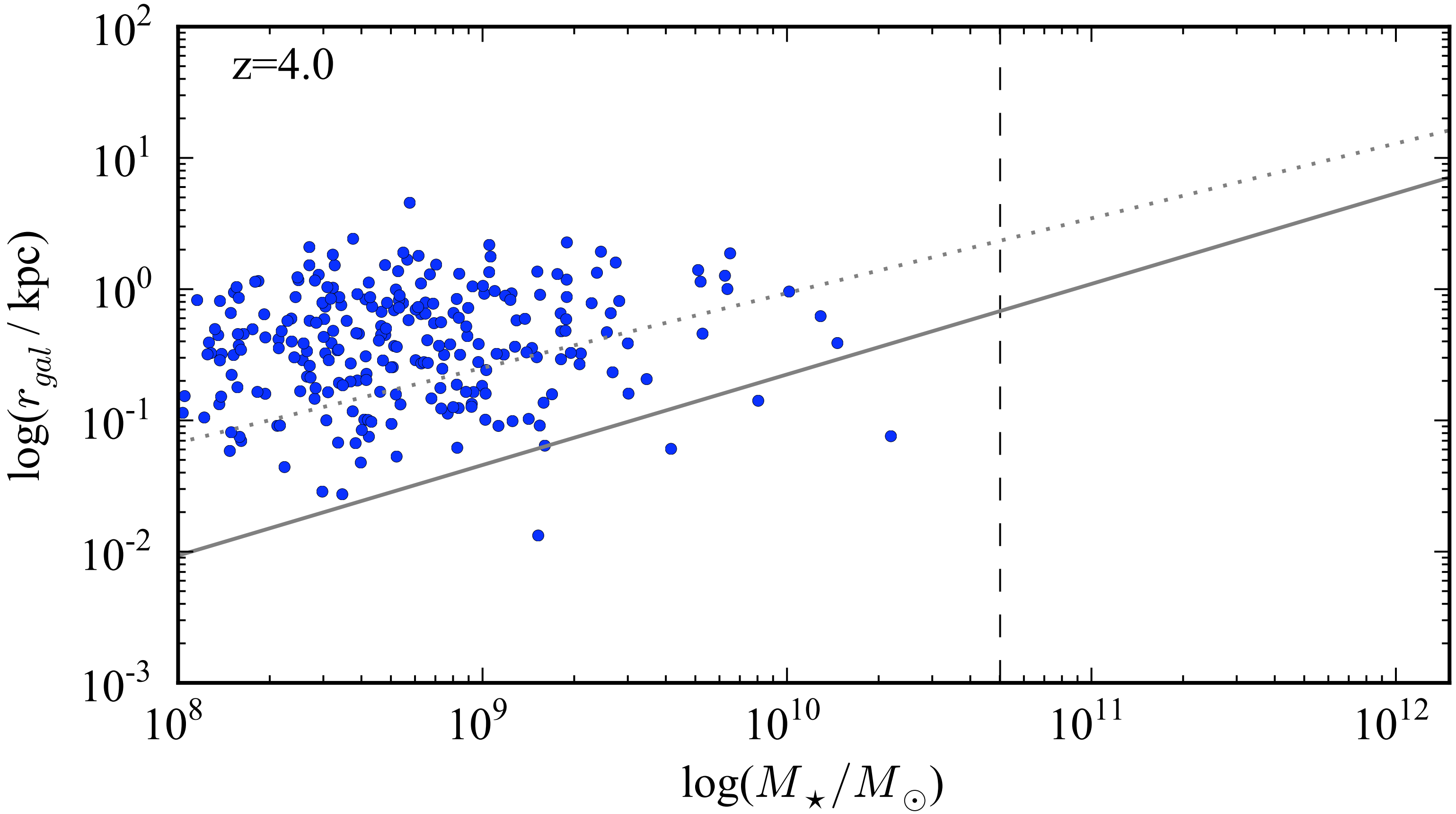

Martin Stringer l'Observatoire de Paris LERMA

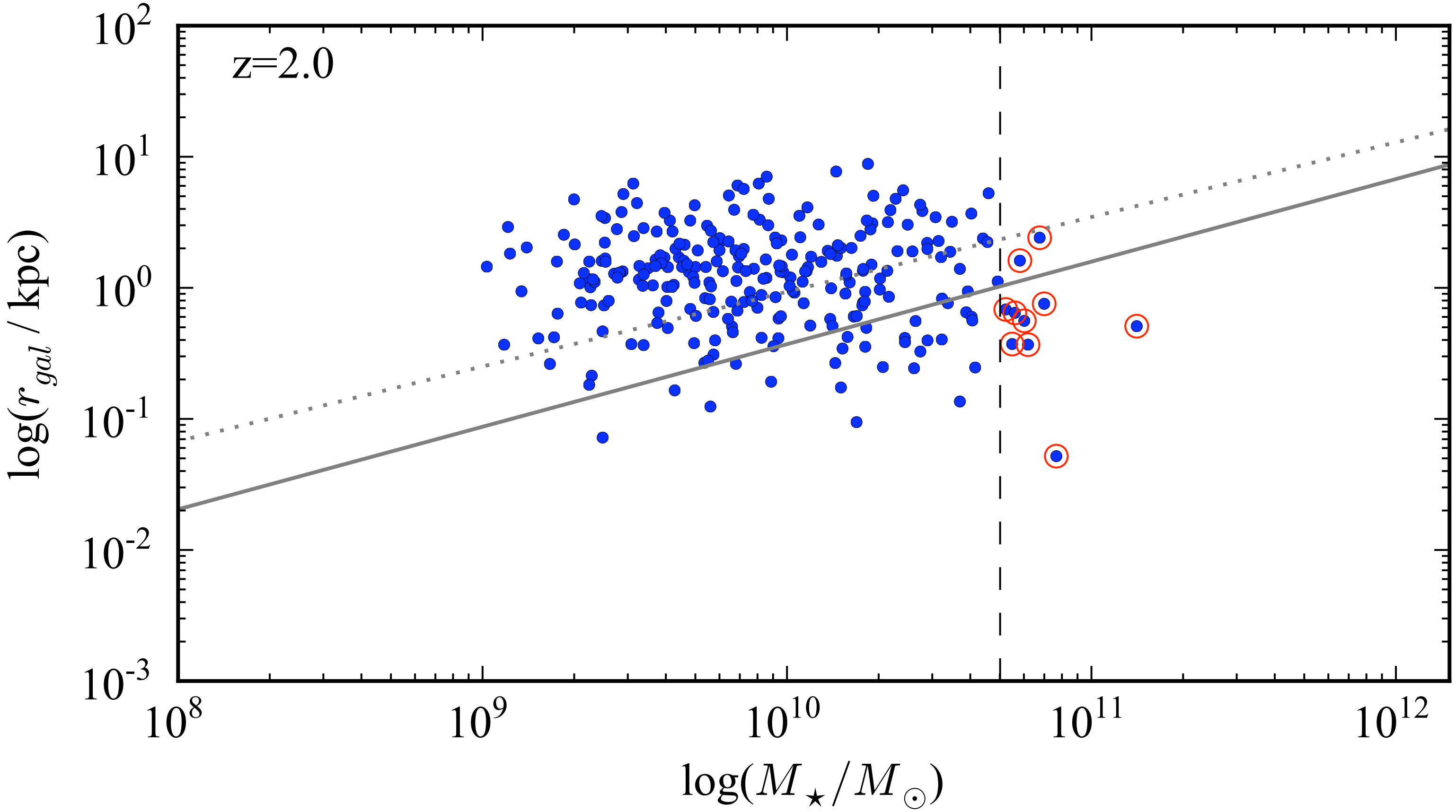

Martin Stringer l'Observatoire de Paris LERMA

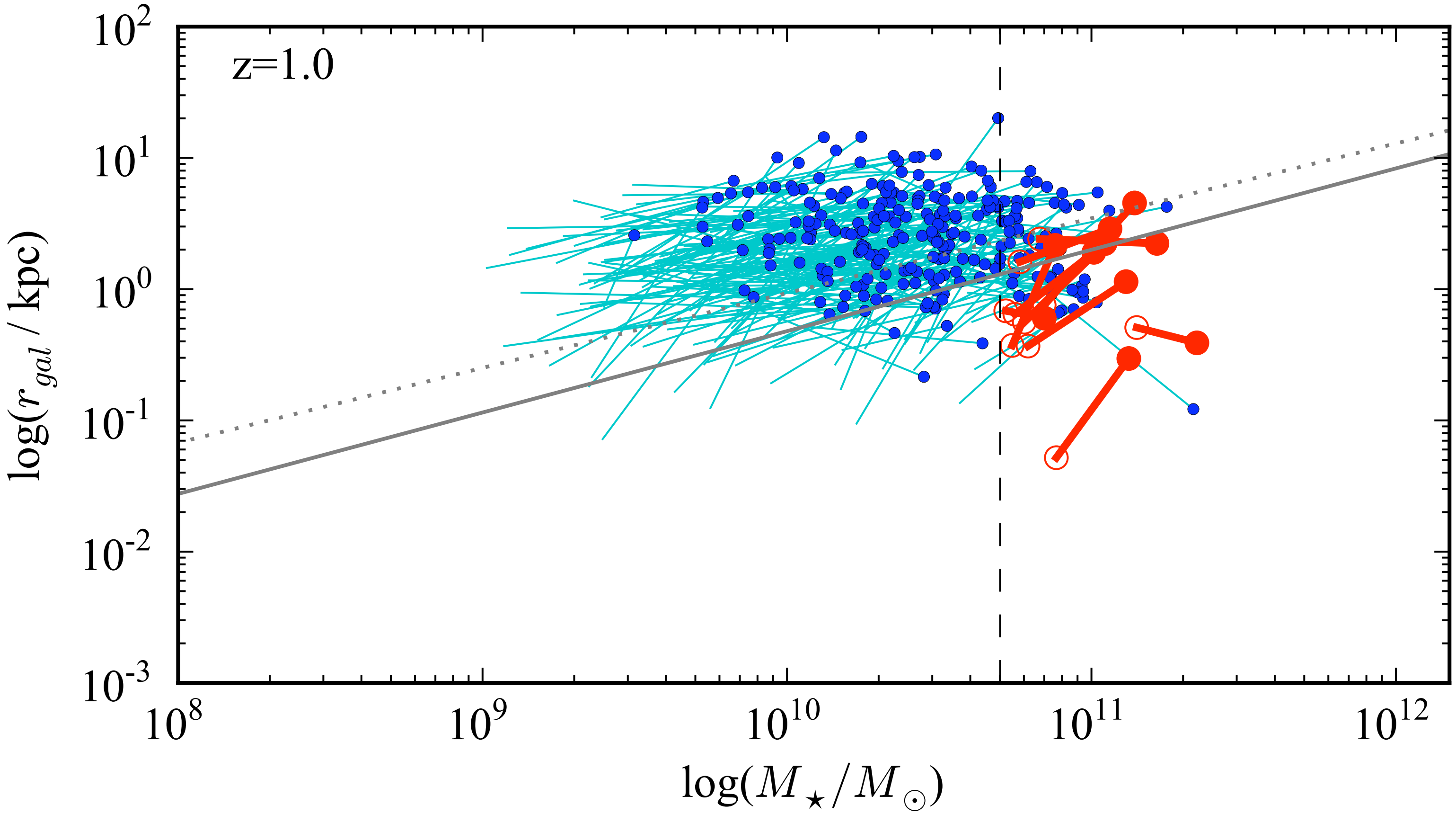

Martin Stringer l'Observatoire de Paris LERMA

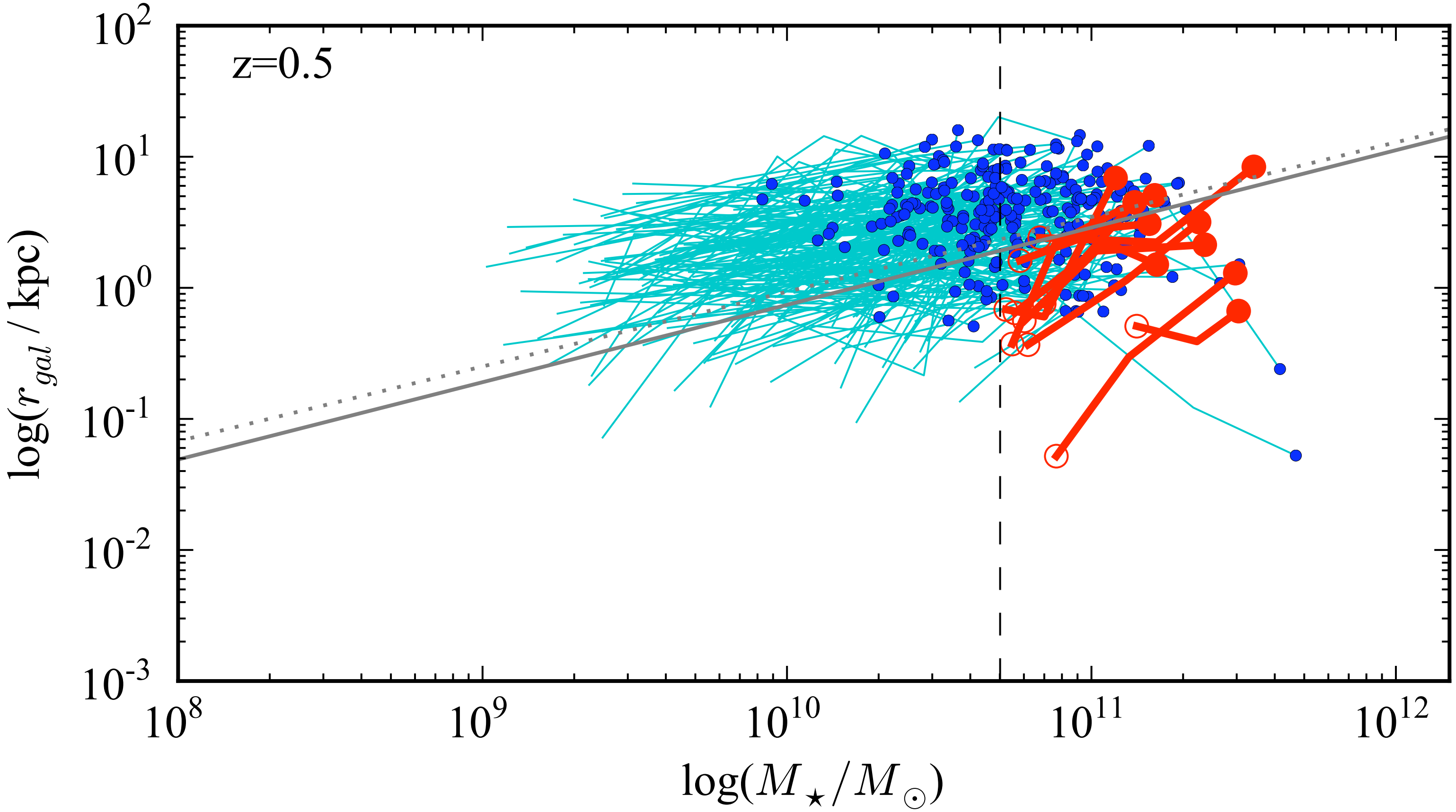
z=0.5
log(r_{gal} / kpc)
log($M_\star/M_\odot$)
10^2
10^1
10^0
10^-1
10^-2
10^-3
10^8
10^9
10^10
10^11
10^12

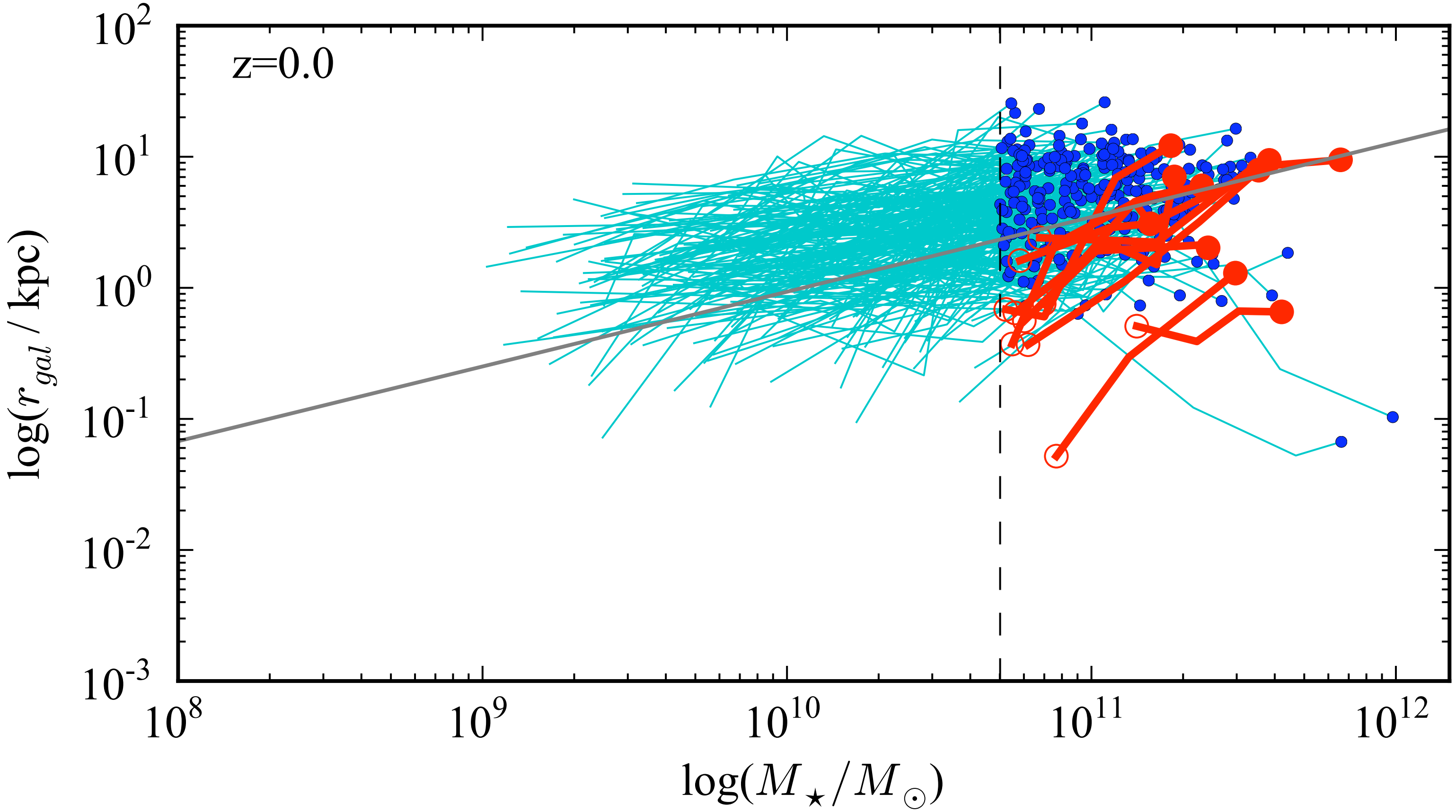

Martin Stringer l'Observatoire de Paris LERMA

Massive Galaxies at High Redshift:

Rare, but...

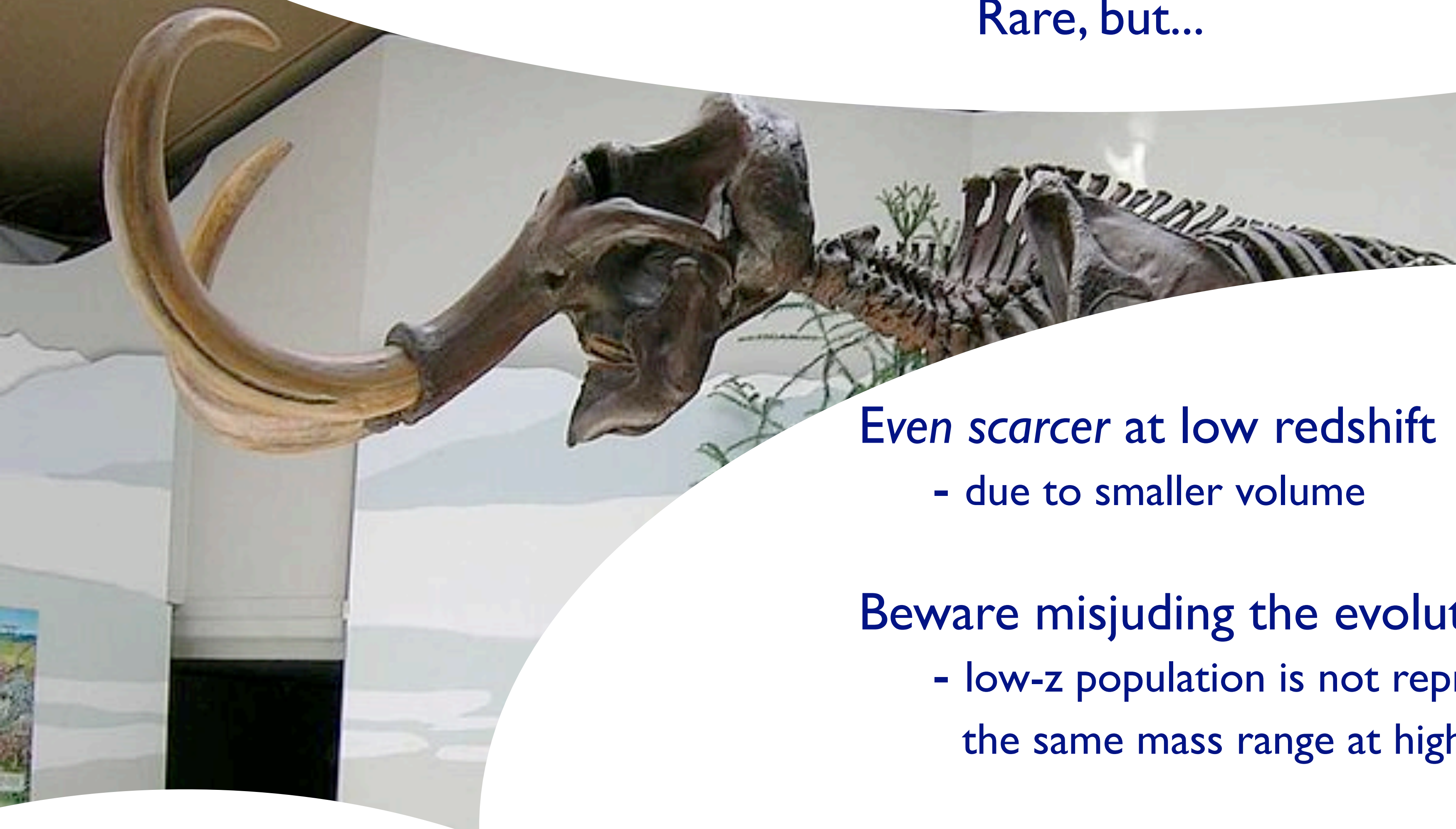

Even *scarcer* at low redshift

- due to smaller volume

Beware misjuding the evolution

- low-z population is not representative of the same mass range at high z

Stellar fraction in BCG naturally limited

- Hierarchical assembly crucial to understand cooling history
- final gas reservoir *does* cool, but only onto central at late times

Martin Stringer

l'Observatoire de Paris

LERMA

Laboratoire d'Étude du Rayonnement et de la Matière en Astrophysique